Aus dem Lehrstuhl für Physiologische Genomik im Biomedizinischen Centrum (BMC)
Institut der Universität München
Vorstand: Prof. Dr. Magdalena Götz

Adaptive Cellular Response within Neural Stem Cell Niches in the Adult Murine Brain Following Spinal Cord Injury

Dissertation zum Erwerb des Doktorgrades der Medizin
an der Medizinischen Fakultät der
Ludwig-Maximilians-Universität München

vorgelegt von

Melanie Yiqing Li
aus München

2023

Mit Genehmigung der Medizinischen Fakultät
der Universität München

Berichterstatterin:	PD Dr. rer. nat. Swetlana Sirko
MitberichterstatterInnen:	PD Dr. Roman Schniepp
	PD Dr. Florence Bareyre
Dekan:	Prof. Dr. med. Thomas Gudermann
Tag der mündlichen Prüfung:	16. Februar 2023

Für meine Familie

Table of Contents

1. Introduction

1.1 Background and Overview

Spinal cord injuries (SCI) are among the most common causes for long-term disability in neurologic patients and are associated with devastating consequences comprising physical, behavioral, mental, and psychosocial factors (Ahuja et al., 2017). Although severity and localization of the initial tissue trauma are primary determinants of SCI-related disability (Norenberg et al., 2004), an increasing body of evidence suggests that several processes attributed to the so-called secondary injury may significantly influence functional recovery and neurological outcome upon spinal cord damage as well (Ahuja et al., 2016, Nardone et al., 2013, Pereira et al., 2019). Therefore, new experimental treatment paradigms increasingly focus on targeting these processes. However, it remains to be understood how irreversible cell damage following SCI contributes to subsequent changes occurring not only at the injury site but also in central nervous system (CNS) regions proximal to the primary lesion.

Of particular interest in this context are a variety of changes in distinct brain regions that can be triggered by pathophysiological events taking place after SCI (Chen et al., 2002, Felix et al., 2012, Freund et al., 2013, Humanes-Valera et al., 2016, Jure et al., 2017, Orr and Gensel, 2018). As shown by electrophysiological studies and functional neuroimaging in animals and humans suffering from SCI, these changes include the modification of neuronal activity and state of networks within motor and sensorimotor cortical areas (Chen et al., 2002, Humanes-Valera et al., 2016), as well as structural reorganization, which highly correlates with clinical outcome and post-injury recovery (Freund et al., 2013, Seif et al., 2018, Nardone et al., 2018, Solstrand Dahlberg et al., 2018). Presently, mechanisms underlying these changes are still poorly understood. Although glial cells constitute the majority of cells in the CNS and are fundamentally involved in various processes (Gotz et al., 2015, Dimou and Gotz, 2014), to date, only little is known about their involvement in pathophysiological processes in the brain that take place after SCI. Therefore, this hypothesis led us to investigate how different types of glial cells and, in particular, adult neural stem cells (aNSCs) in the brain react to SCI, and to which extent they may contribute to physiological or pathological mechanisms of cerebral reorganization during the acute and subacute phases after SCI.

1.2 Clinical Aspects of Spinal Cord Injury

Clinical aspects of SCI are complex. Beside an anatomic categorization i.e. cervical, thoracic, and lumbar, four major groups of SCI can be distinguished: (a) solid injury, the rarest form of SCI, where the spinal cord appears macroscopically intact but shows clear histological damage, (b) contusion, the most common form, with hemorrhage, necrosis and cavitation, (c) laceration, defined by slice damage to the tissue, and (d) compression, characterized by maceration and pulpification (Norenberg et al., 2004). Each of these groups can be further subdivided into complete or incomplete SCI. Most SCIs are incomplete and located in the cervical spinal cord (Hachem et al., 2017). Although injury mechanisms vary widely, more than 90% are caused traumatically (NSCISC, 2019) and commonly present as an initial impact followed by persistent compression, while transient impact, distraction, laceration, and transection are more seldom (Dumont et al., 2001).

Depending on the injury level and severity, clinical symptoms can range from virtually none, minor sensory or motor impairments, to incomplete or complete paraplegia with impaired function of both legs (Waters et al., 1992). In high cervical SCI, even the diaphragm, and therefore respiration can be impaired (Cregg et al., 2017). Recovery can be long and arduous, but most functional improvement happens within the first three months after injury and usually reaches a plateau around six months later. Small improvements, however, are still possible and seen much later (Fehlings et al., 2013). As symptoms can vary and can be hard to assess in detail, standardized scoring systems are very important for making a proper and complete diagnosis before initiating treatment.

Clinical management is focused on early surgical decompression and spinal stabilization, the most effective treatment to prevent further damage (Wilson et al., 2017, Alizadeh et al., 2019, Ahuja et al., 2017). Methylprednisolone infusion to reduce systemic inflammation is controversially discussed, but recommended in the AOSpine guidelines, ideally administered within 8 hours of injury and for a maximum treatment period of 48h hours to prevent unwanted side effects (Fehlings et al., 2017). After initial stabilization, only very few therapeutic standards are established in the clinical setting. The existing ones focus on hemodynamic management (Karsy and Hawryluk, 2019). Regular exercise and physical therapy are key factors in restoring at least some degree of functionality in SCI patients and were found to cause biochemical and cellular changes supporting neuroregeneration

(Sandrow-Feinberg and Houle, 2015). Furthermore, many non-pharmacological treatment methods such as hypothermia or spinal cord stimulation are increasingly established (Ahuja et al., 2017) and recent experimental approaches aim to modify extracellular matrix molecules secreted by activated astrocytes, inject specially designed biomaterials affecting glial function, deplete invading immune cells, or modulate their intercellular interaction (Orr and Gensel, 2018). Pharmacotherapeutic studies already show promising effects for a variety of agents (Zhang et al., 2015, Bracken et al., 1990, Gensel et al., 2017, Knoller et al., 2005), with further trials coming up.

1.3 Cell Biological Aspects of SCI

SCI is not limited to the primary injury, which mostly determines the severity of the lesion but must be seen as a dynamic process associated with the secondary injury cascade that expands during the subacute and chronic post-injury phases (Fig. 1). In fact, the concept of a primary and secondary injury was first described by Alfred Allen already in 1911 (Allen, 1911).

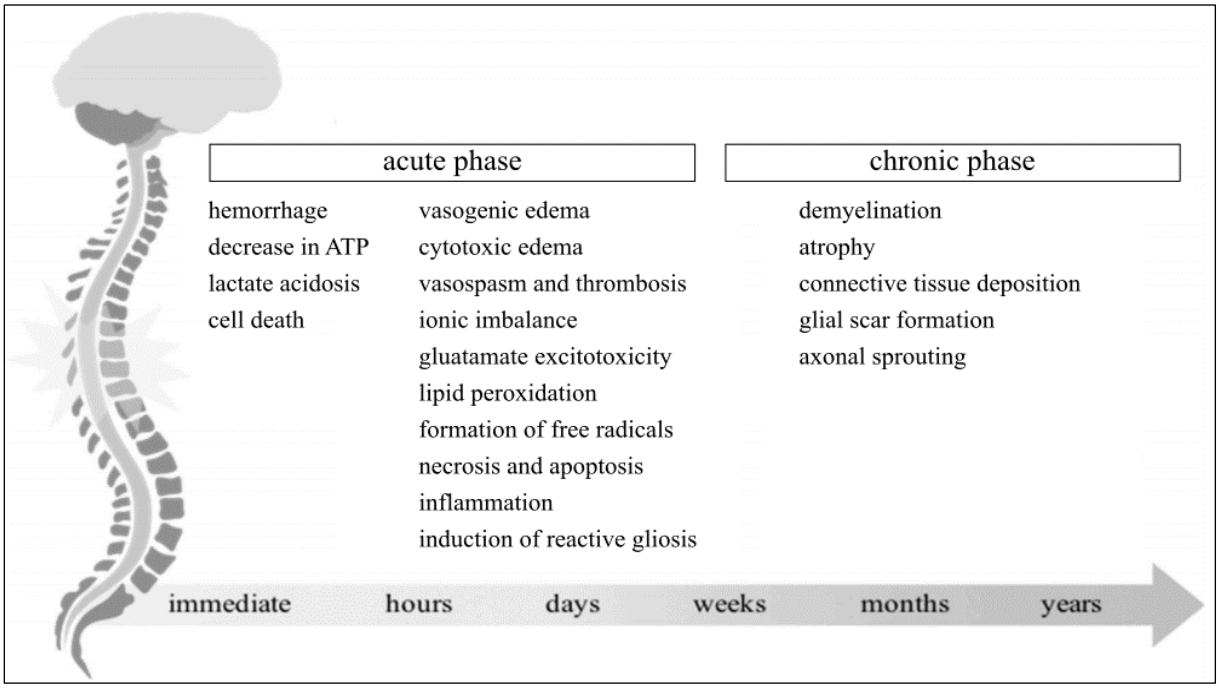

Figure 1. Processes initiated after SCI. The primary injury activates a cascade of pathophysiological processes that embody the so-called secondary injury. Both are determinants of the final extent of damage. The chronic phase may last throughout the patient's whole life. Modified from Ahuja et al. 2016 and Pereira et al. 2019.

The secondary injury is characterized by a complex cascade of immune responses which occur throughout an acute, subacute, and chronic phase (Fig. 2) (Nakamura and Okano, 2013, Alizadeh et al., 2019).

The acute or inflammatory phase starts as early as a few hours post injury with the activation of microglia, astrocytes, and neutrophils (Donnelly and Popovich, 2008, Alizadeh et al., 2019). Astrocytes play a crucial role in releasing cytokines and chemokines, and therefore in expanding the reaction of immune cells (Pineau et al., 2010, Nakamura et al., 2003). Within few days macrophages and monocytes start to invade the lesion site from the peripheral blood and their numbers as well as the number local microglia usually peak less than a week after injury (Donnelly and Popovich, 2008, Sroga et al., 2003). Around 3 days post-injury (dpi), lymphocytes start to invade the injured parenchyma (Donnelly and Popovich, 2008). The subsequent activation of B-lymphocytes is then associated with impaired functional recovery and unfavorable lesion pathology at the spinal cord (Ankeny et al., 2009). This complex immune response also involves a pronounced loss of the oligodendrocyte population which are essential for the insulation of axon through their production of myelin (Jessen, 2004), thereby leading to diffuse demyelination even outside the affected area (Dong et al., 2003). The course of disease can be further complicated by formation of harmful reactive oxygen and nitric oxide species (Dizdaroglu et al., 2002), glutamate derived excitotoxicity (Li and Stys, 2000), compromised tissue perfusion, calcium overload, and lipid and protein oxidation that can finally lead to necrosis, necroptosis, apoptosis, and dysregulated autophagy (Alizadeh et al., 2019).

The subacute phase is characterized by a gradual decrease of neuroinflammation parallel to the onset of tissue remodeling processes (Burda and Sofroniew, 2014). These are mainly characterized by glial scar formation during the chronic phase around 14 dpi (Nakamura and Okano, 2013). Even when our understanding of the secondary injury is still incomplete, extracellular matrix molecules and humoral factors most likely also play a crucial role in pathophysiological processes within and outside the injured parenchyma which is why they have gained increasing insight in recent therapeutic approaches (Orr and Gensel, 2018).

Taken together, the activation of the immune system during the secondary cascade following SCI can lead to further damage through a variety of mechanisms. This process starts as early as hours after the insult, gradually merges into scar formation and remodeling around 14dpi.

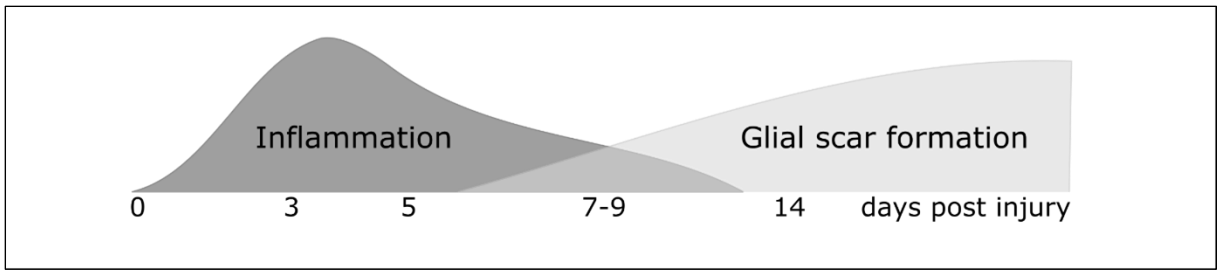

Figure 2. The temporal development of inflammation and tissue reorganization after SCI. The acute phase is marked by an inflammatory response to the lesion that peaks around 3dpi. After the initiation of tissue remodelling processes, the chronic phase sets in approximately 14dpi and characterized by glial scar formation at the lesion site. Modified from Nakamura and Okano, 2013.

However, the secondary cascade also has crucially beneficial and regenerative effects. For instance, both invading macrophages and resident microglia are essential for local regeneration and the promotion of axonal regeneration and enhance precursor differentiation into favorable cells such as oligodendrocytes (David and Kroner, 2011). Indeed, neutrophile depletion is associated with worse recovery results due to downregulation of important neurotrophic agents (Stirling et al., 2009). It is also noteworthy that glial scar formation serves as a barrier by preventing the spread of immune cells into areas with remaining vital tissue (Norenberg et al., 2004, Cregg et al., 2014, Voskuhl et al., 2009). On the other hand, a persisting glial scar acts as an obstacle to axonal sprouting and therefore functional recovery (Yuan and He, 2013) which is why recent research is focused on reducing the size and persistence of injury-induced scarring.

1.4 Symptoms in Patients Suffering from SCI Related to Changes in Brain Regions

The most prominent deficits in SCI patients are motor and sensory loss, functions that are directly attributed to structural spinal cord damage (Alizadeh et al., 2019). However, current clinical evidence shows a wide range of other symptoms suggesting the involvement of extra-spinal parts of the CNS.

Many SCI patients suffer from chronic neuropathic pain (Solstrand Dahlberg et al., 2018, Ziegler et al., 2018), which is likely caused by a dysregulated overshooting activation of pain fibers (Baron et al., 2010). SCI patients are also at higher risk of developing headaches (Sabre et al., 2016), with the prevalence of severe migraine found to be almost five times higher when

compared to healthy controls (Warner et al., 2015). Autonomic, gastrointestinal, sexual and endocrine dysfunction occur more often, suggesting the involvement of the neuroendocrine system and, in particular, the hypothalamus and the hypophysis (Solstrand Dahlberg et al., 2018). Psychological disorders occur at a rate up to three times higher than that of the general population with psychopharmaceutic medication being clinically indicated in more than a third of the patients (Craig et al., 2015). Recently, there has also been evidence of cognitive impairment in the context of SCI, although co-contributing factors might also play an important role, such as concomitant head trauma, and psychological or somatic comorbidities (Sachdeva et al., 2018, Wecht and Bauman, 2013, Faden et al., 2016).

The variety of symptoms in SCI patients suggest structural changes that are not limited to the spinal cord but also affect different brain regions. Sophisticated imaging techniques have granted insight into where these might be located and whether they could cause the clinical features observed: atrophic changes were found in both the grey matter (GM) of many different cortical areas and the white matter (WM) (Freund et al., 2013, Seif et al., 2018). While the GM of the primary motor cortex was especially affected, WM changes were most obvious at the level of the internal capsule and the cerebral peduncles, and both findings were associated with poor recovery (Freund et al., 2013). Interestingly, there seems to be a correlation between the severity of neuropathic pain and the degree of cortical reorganization within the somatosensory cortex (Jutzeler et al., 2015). Accordingly, Diffusion Tensor Imaging (DTI) also exhibited abnormalities in SCI patients which are likely connected to neuropathic pain (Nardone et al., 2018).

However, the question of how these changes in the brain parenchyma could be related to the symptoms of SCI patients still remains open and requires further research effort. Considering the great importance of glial cells in both physiological and pathophysiological processes, they are most likely highly involved in the changes in the brain parenchyma following SCI. Patients suffering from traumatic brain injury (TBI) can experience similar symptoms ranging from chronic pain (Irvine and Clark, 2018), neuroendocrine dysfunction (Li and Sirko, 2018), and permanent cognitive impairment (Hellawell et al., 1999). As TBI can induce reactive changes in both parenchymal astrocytes and neural stem cell niches (Falnikar et al., 2018, Wang et al., 2016), it does seem reasonable to assume similar underlying processes.

1.5 Astroglia and Their Role in Health and Injury

Two cell types mainly form neural tissue, neurons and glial cells. In the CNS, glial cells comprise astrocytes and oligodendrocytes. While oligodendrocytes are mostly responsible for the formation of myelin, a fat-rich substance that ensheathes nerve fibers, serving as an electrical insulation layer for both directed and faster signal transmission, astroglia are fundamental for a broad variety of functions. These include but are not limited to providing structural guidance during neural development, support of neuronal survival, synapse formation and control of synaptic function, and neurotransmitter homeostasis, electrolyte, and water (Jessen, 2004). Strikingly, a subpopulation of astrocytes are indeed aNSCs that are responsible for neurogenesis in the adult murine brain (Doetsch et al., 1999b). As both structural and functional reorganization after SCI involve complex mechanisms that are not only limited to neuronal plasticity, the reaction of glial cells and in particular, aNSCs requires further investigation.

1.5.1 Neurogenesis in Adult Neural Stem Cell Niches

For a long time, the CNS has been regarded as an organ unable to recover from injury. It was first in 1962, when Joseph Altman challenged this view by demonstrating that the adult brain against all opinions does show proliferative activity (Altman, 1962). Electron microscopy later confirmed that these dividing cells in the adult murine brain indeed present a neuronal and not glial morphology (Kaplan and Hinds, 1977) and were capable to proliferate *in vitro* (Richards et al., 1992).

In early mammalian development, radial glia (RG) are the primary type of NSCs that generate all types of neural cells (Taverna et al., 2014, Gotz and Barde, 2005). While most RG undergo differentiation into parenchymal astrocytes by the end of embryonic neurogenesis (Voigt, 1989), a small subset in the subependymal zone (SEZ), a thin layer of cells within the subventricular zone (SVZ) lining the lateral ventricles (LV) (Fischer et al., 2011) (Fig. 3), were later found to be still actively proliferating in the adult brain (Doetsch et al., 1999b, Temple, 1999, Kriegstein and Alvarez-Buylla, 2009). The SEZ is one of the two most important rodent neurogenic niches – defined regions presenting with unique architecture and milieu features

that are capable of spontaneous and exercise-induced neurogenesis (Beckervordersandforth et al., 2010, Doetsch et al., 1999a, Kempermann et al., 2015, van Praag et al., 1999, van Praag et al., 2000). The other niche lies within the dentate gyrus (DG) of the hippocampus (HC) and lies within a thin cell layer beneath the granular zone – the subgranular zone (SGZ) (Kempermann et al., 2015) (Fig. 4). While there is no evidence of adult neurogenesis in the human SEZ, proliferative activity and the generation of neurons was indeed demonstrated in the human hippocampus (Eriksson et al., 1998).

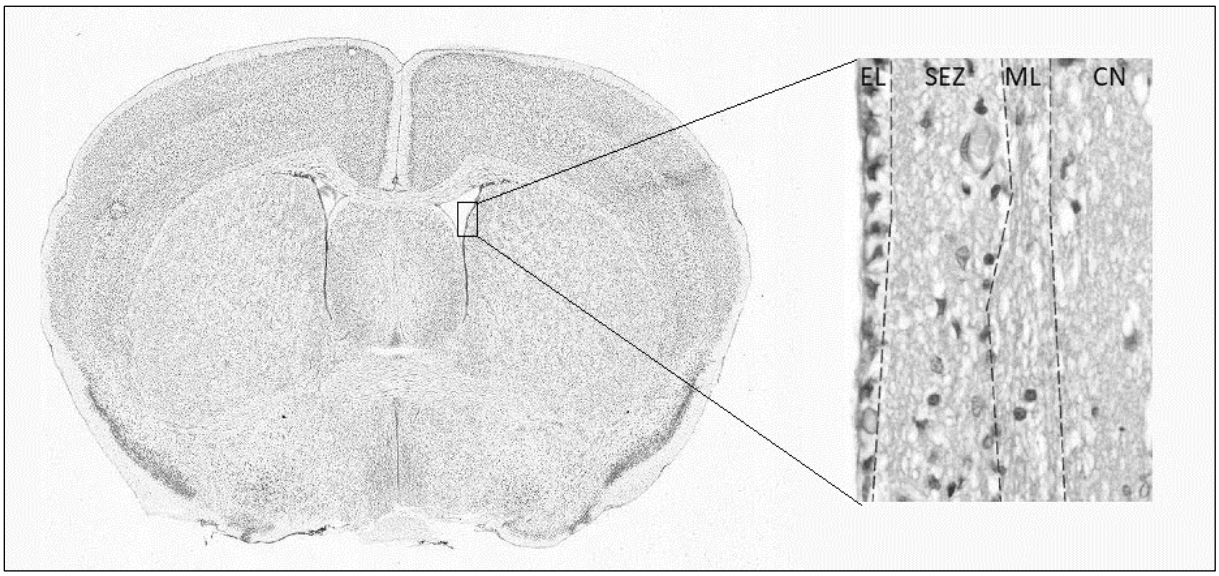

Figure 3. The Subependymal Zone (SEZ). The SEZ is a thin layer of cells between the ependymal layer (EL) consisting of ependymal cells lining the lateral ventricles and the myelin layer (ML) which separates the SEZ from the caudate nucleus (CN) of the striatum. Figure modified from The Allen Mouse Brain Reference Atlas (https://mouse.brain-map.org/static/atlas) and Curtis et al. 2005.

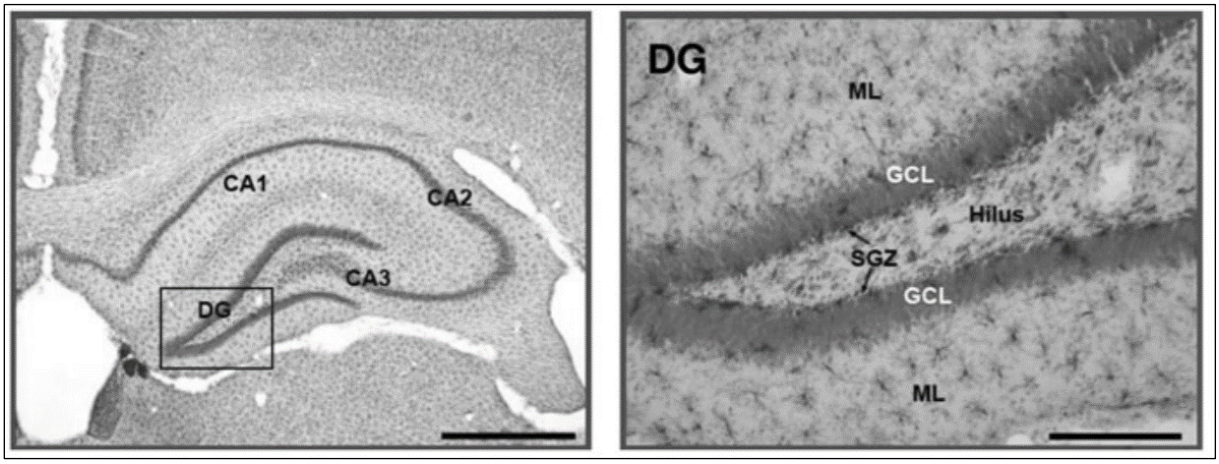

Figure 4. Morphological features of the hippocampus. Dentate gyrus (DG), layers of the cornu ammonis (CA 1-3), granular cell layer (GCL), molecular layer (ML). The subgranular zone (SGZ) is a thin cell layer on the inside of the GCL of the DG. Modified from Liaury et al. 2012.

The SEZ (Fig. 5A) harbors neural stem cells that express a variety of astroglial markers such as Glial Fibrillary Acidic Protein (GFAP) and Glutamate Aspartate Transporter (GLAST), also known as Excitatory Amino Acid Transporter 1 (EAAT1) and encoded by the gene SLC1A3 (Zhou and Danbolt, 2013), as well as stem cell markers (Colak et al., 2008, Doetsch et al., 1997). Morphologically, they show RG-like characterstics such as a long apical primary cilium reaching into the ventricle from the subependymal layer in which the cell body resides (Mirzadeh et al., 2008). Indeed, they are a subset of SEZ astrocytes (Beckervordersandforth et al., 2010) which are mostly quiescent (qNSCs) (Type B cells) but can become activated and generate proliferating progenitors, so-called transit amplifying progenitors (TAPs) (Type C cells) (Doetsch et al., 1999b), which in turn generate immature neuroblasts (Type A cells). These then migrate to the olfactory bulb (OB) through the rostral migratory stream (RMS), where they mature into neurons and integrate into neuronal networks (Doetsch et al., 1999b). All these cells, together with postmitotic niche astrocytes, create a specialized microenvironment within the neurogenic niche (Andreotti et al., 2019). Moreover, the SEZ is lined with and penetrated by blood vessels (Fischer et al., 2011).

Postnatal neurogenesis in the hippocampus was demonstrated as early as in 1965 (Alman and Das, 1965). Ever since, the underlying cellular structures have been extensively investigated and described (Kempermann et al., 2015) (Fig. 5B). The DG contains precursor cells, their progeny, glial cells and neuroblasts, but also abundant blood vessels and immune cells such as microglia. So-called type 1 precursor cells represent the origin of adult hippocampal neurogenesis and give rise to type 2 cells or transiently amplifying cells. Through an intermediary stage (type 3 cells), these later generate neuroblasts that show increased synaptic plasticity and growing axons and dendrites, respectively. If these are successfully integrated into the neuronal network, they finally mature into granule neurons. Interestingly, type 1 cells also exhibit morphologic and molecular similarities to both RG and astroglia. They posses a long apical process extending into the molecular layer from their cell body that is located in the SGZ (Breunig 2008, Kriegstein and Alvarez-Buylla 2009), and exhibit both GFAP and stem cell markers (Filippov et al., 2003). Type 1 cells retain typical stem cell attributes including self-renewal and multipotency, but in contrast do show some limitations and therefore faster exhaustion (Calzolari et al., 2015, Encinas et al., 2011).

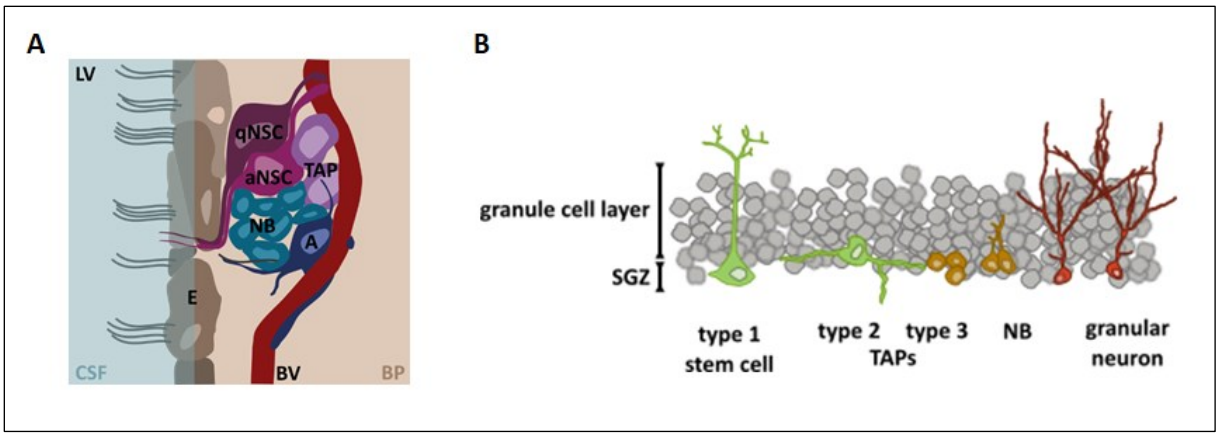

Figure 5. Cellular structure of adult neural stem cell niches. (A) The SEZ mainly consists of five cell types: quiescent (qNSC) and active (aNSC) neural stem cells, neuroblasts (NB), transit-amplifying progenitors (TAPs) and niche astrocytes (A). Lateral ventricle (LV), cerebrospinal fluid (CSF), ependymal cells (E) with cilia, blood vessel (BV), brain parenchyma (BP). (B) In the SGZ, type 1 cells are equal to stem cells, type 2 and 3 cells belong to the group of transit-amplifying progenitors. Immature neurons are called neuroblasts (NB) that later transform into mature granular neurons. Figures created based on Fischer et al. 2011, and Kempermann et al. 2015.

1.5.2 Identification and Characteristics of Adult Neural Stem Cells

There are several molecular markers that were established to facilitate the process of identifying aNSCs. Some are typically expressed by aNSCs, e.g. GFAP and Sox2 (Sex Determining Region Y Box 2) (Dimou and Gotz, 2014, Beckervordersandforth et al., 2010, Ellis et al., 2004), while others indicate proliferative activity, e.g., Marker of Proliferation Ki-67 (Ki67) (Sirko et al., 2013, Gotz et al., 2015, Scholzen and Gerdes, 2000). Ki67 was first described in 1983 as an antigen associated with cell proliferation (Gerdes et al., 1983) and is expressed during the mitotic phase in the cell cycle and but not in resting cells (Gerdes et al., 1984). Ever since, Ki67 has been established in many fields as a marker of proliferative activity (Scholzen and Gerdes, 2000). Doublecortin (DCX) has been established as a marker of immature neurons and is expressed as well in adult neurogenesis (Couillard-Despres et al., 2005, Kempermann et al., 2015). Today, a combination of aforementioned markers is often used to detect both aNSCs and neuroblasts (Zhang and Jiao, 2015).

In 1992, the foundation for an important method to isolate and assess NSCs *in vitro* was laid (Reynolds and Weiss, 1992): by enzymatically dissociating striatal tissue containing the SEZ into a single cell suspension and plating it under nonadherent conditions in serum-free medium containing epidermal growth factor (EGF), a small fraction soon started to form free-floating colonies termed neurospheres. To meet the definition of stem cell capacity, self-

renewal and multipotency are required as general hallmarks (Gotz et al., 2016) which can be assessed *in vitro*. Self-renewal can be observed after repetitive passaging, i.e. enzymatic dissociation and single-cell plating of neurospheres (Fischer et al., 2011). Some of the neurosphere-forming cells have the capability to form into both neurons and glial cells when plated under adherent, differentiation-enhancing cell culture conditions and are therefore considered multipotent (Sirko et al., 2007). The neurosphere assay has been improved markedly and constitutes a widely accepted method to identify NSCs and their proliferation and differentiation characteristics *in vitro* (Dimou and Gotz, 2014, Pastrana et al., 2011, Campos, 2004).

1.5.3 Reactive Astrogliosis

CNS injury can induce a process called reactive gliosis already shortly after the insult. During early stages, microglia – CNS-resident macrophages – are activated and initiate an immune response leading to an inflammatory cascade (Hughes et al., 2013, Nimmerjahn et al., 2005). Astrocytes undergo a reactive transformation, acquiring a characteristic phenotype characterized by cellular hypertrophy and the upregulation of GFAP (Pekny et al., 2014). This process is known as 'reactive astrogliosis' or 'astrocyte reactivity' and involves many more complex changes including those of their molecular profile and cellular functions (Escartin et al., 2021). Astrocyte reactivity can range from subtle to moderate and very pronounced stages, culminating in glial scarring (Sofroniew, 2005) (Fig. 6). The upregulation of GFAP is often proportional to the production and release of cytokines (Escartin et al., 2019) that are responsible for the expansion of the reactive response and the involvement of peripheral immune cells and fibroblasts (Robel et al., 2011, Burda and Sofroniew, 2014). However, the glial scar also serves as a protective barrier for vial tissue, "secur[ing] the survival […] through the acute post-traumatic phase, and allow[ing] a measure of repair even though this comes at the price of a restricted regenerative capacity and hence limited functional recovery" as this scar acts as an obstacle to axonal sprouting (Pekny et al., 2014).

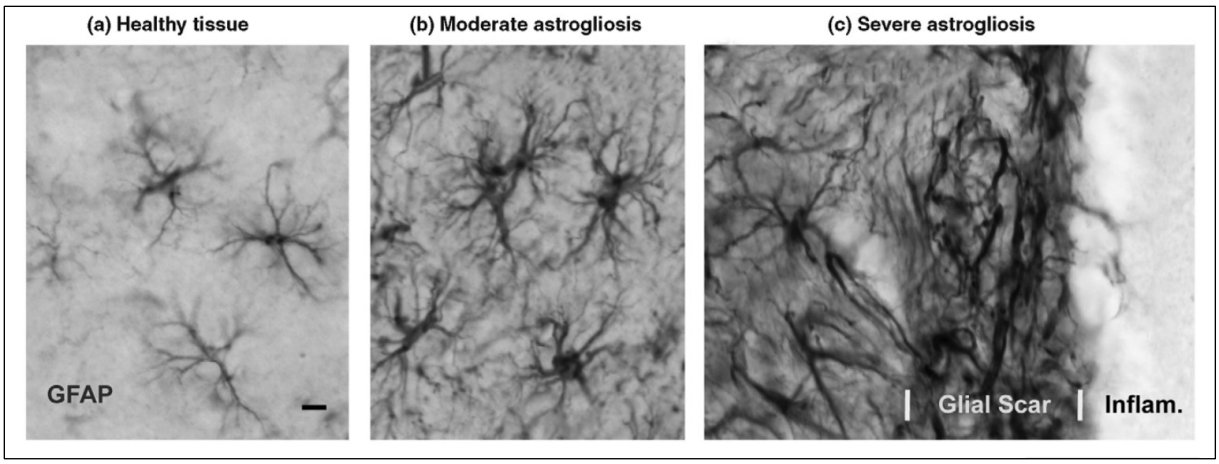

Figure 6. Reactive astrogliosis. Immunohistochemical staining of the adult murine cerebral cortex using GFAP demonstrates typical characteristics of reactive astrocytes (b, c) compared to astrocytes in the brain of healthy mice (a): increase in GFAP-expression, cellular hypertrophy and overlapping of astrocytic processes. Scale Bar 8 µm. Modified from Sofroniew, 2009.

Interestingly, a subset of reactive parenchymal astrocytes in the brain of mice that underwent TBI exhibit stem cell properties including proliferative activity and multipotency *in vitro* (Sirko et al., 2013, Sirko et al., 2015). The specific function of these changes is still subject to research. However, it does seem reasonable to assume that they represent an attempt of CNS plasticity and functional improvement. These characteristics make astrocytes key regulators in the process of post-injury reorganization and repair, and therefore, many scientists have put their research focus on trying to understand how exactly this role is played.

1.6 Aims

This project aims to investigate cellular and molecular changes in adult neural stem cell niches of mice following traumatic SCI. In particular, the proliferative activity of adult neural stem cell niches was analyzed quantitatively and qualitatively in order to draw conclusions regarding the extent of proliferation and the distribution of different cell types involved. In doing so, the focus will not only lie on regional differences between the SEZ and the SGZ but also on the evolution of the observed changes in a time-specific and region-specific manner. For this, immunohistochemical analyses will be performed in naïve adult mice at different time points after surgically induced SCI. An additional group will undergo sham surgery (without damage to the spinal cord parenchyma), which will allow the identification of possible differences between invasive CNS trauma and non-invasive spinal trauma. At the timepoint with the maximum effect size *in vivo*, *in vitro* studies on cells obtained from both adult neural stem cell niches will focus on potential changes in their self-renewing capacity as well as their multipotency. Then, alterations in the expression levels of important proliferative and reactive regulators will be analyzed to assess molecular changes in parenchymal astrocytes residing in CNS regions distant to the spinal cord. To gain insights into potential underlying molecular processes that underly the injury-type related changes within the neurogenic niches, proteome analysis of cerebrospinal fluid (CSF) will be performed. All findings will be then critically discussed and compared to recent research to identify possible underlying pathophysiological mechanisms that can be tested in future studies. Finally, the results will be put into context with clinical aspects of SCI and future perspectives in SCI treatment paradigms.

2. Materials and Methods

2.1 Equipment

Calculator	Casio (Tokyo, JPN)
Centrifuge 54150	Eppendorf (Hamburg, D)
Centrifuge Megafuge Heraeus 8R	Thermo Scientific (Waltham, MA, USA)
Centrifuge Minispin	Eppendorf (Hamburg, D)
Centrifuge Perfect Spin	Peqlab (Erlangen, D)
Centrifuge Qualitron® Microcentrifuges	Krackeler Scientific (Albany, NY, USA)
Centrifuge Sorvall Evolution RC	Thermo Scientific (Waltham, MA, USA)
Centrifuge Universal 320R	Hettich (Tuttlingen, D)
Counting chamber Neubauer Improved	Heinz Herenz Medizinalb. (Hamburg, D)
Forceps	Fine Science Tools (Heidelberg, D)
Freezer (-20°C)	AEG (Frankfurt am Main, D)
Freezer (-20°C)	Liebherr (Bulle, CH)
Freezer (-80°C)	Liebherr (Bulle, CH)
Ice machine MF46	Scotsman (Vernon Hills, IL, USA)
Incubator	Memmert (Schwabach, D)
Incubator	Binder (Bohemia, NY, USA)
Incubator Galaxy 170R and 170S	New Brunswick (Enfield, CT, USA)
Laboratory balances	Mettler Toledo (Giessen, D)
Laminar flow (B-MaxPro2)	Berner (Elmshorn, D)
Light Cycler 480 II (27773)	Roche (Basel, CH)
Magnetic stirrer	IKA Jahnke und Kunkel (Staufen, D)
Microscope Axiovert 40CFL	Zeiss (Oberkochen, D)
Light source HXP-120	Visitron Systems (Puchheim, D)
Microscope Fluo BX61	Olympus (Tokyo, JPN)
Microscope Leica DFC 3000G	Leica (Wetzlar, D)
Microscope Leica MZ125 und MZ6	Leica (Wetzlar, D)
Microscope LSM 710	Zeiss (Oberkochen, D)
Microwave	Severin (Sundern, D)

Mouse cages	Techniplast (Buguggiate, IT)
pH-meter pH720	WTW inoLab (Weilheim, D)
Pipette controller accu-jet® pro	Brand (Wertheim, D)
Pipettes (10µl, 20µl, 100µl, 200µl, 1000µl)	Eppendorf (Hamburg, D)
Pipettes (10µl, 20µl, 100µl, 200µl, 1000µl)	Gilson (Middleton, WI, USA)
Proflex PCR System	Life Technologies (Carlsbad, CA, USA)
Refrigerator	Privileg (Stuttgart, D)
Refrigerator	Liebherr (Bulle, CH)
Shaker Duomax 1030	Heidolph (Schwabach, D)
Shaker IKA-Vibrax VXR	IKA Jahnke und Kunkel (Staufen, D)
Shaker Thermoshake	C. Gerhardt (Königswinter, D)
Spectrophotometer Nano-Drop ND-1000	Thermo Scientific (Waltham, MA, USA)
Spectrophotometer Prim Advanced	Secomam (Alès, FR)
Stereotactic mouse adaptor	Stoelting (Wood Dale, IL, USA)
Thermomixer comfort	Eppendorf (Hamburg, D)
Tissue grinder	Wheaton (Millville, NJ, USA)
Vibratom VT1000S	Leica (Wetzlar, D)
Vortex-Genie 2	Bender & Hobein (Bruchsal, D)
Water bath	Memmert (Schwabach, D)
Fiber Optic Light Source KL 1500 LCD	Leica (Wetzlar, D)
Fiber Optic Light Source KL 1500 LCD	Schott (Mainz, D)
Water Sterilizer Milli-Q	Merck (Darmstadt, D)

2.2 Consumables

Anti-ACSA-2 MicroBead Kit for MACS®	Miltenyi Biotec (Bergisch Gladbach, D)
Cell culture flasks CELLSTAR® (T25, T75)	Greiner Bio-One (Kremsmünster, AT)
Cell strainer	BD Biosciences (Franklin Lakes, NJ, USA)
Coverslips	Carl Roth (Karlsruhe, D)
Disposal Boxes Euromatic Multisafe	Sarstedt (Nürnbrecht, D)
Eye and nose ointment	Bepanthen (Leverkusen, D)

Filaments (Vicryl)	Ethicon (Norderstedt, D)
Filter paper	BIO-RAD (Hercules, CA, USA)
Filter tips Biosphere	Sarstedt (Nürnbrecht, D)
Glass bottles	Schott (Mainz, D)
Glass slides	Thermo Scientific (Waltham, MA, USA)
Gloves	Meditrade (Kiefersfelden, D)
Insulin needles (U-100, 1 ml)	BD Biosc. (Franklin Lakes, NJ, USA)
Light Cycler P480 Probes Master	Roche (Basel, CH)
Maxima First Strand cDNA Synthesis Kit for RT-qPCR with dsDNA (LOT 00460459)	Thermo Scientific (Waltham, MA, USA)
Microscope slides	Carl Roth (Karlsruhe, D)
Microscope slides	Thermo Scientific (Waltham, MA, USA)
Pasteur pipettes	VWR International (Darmstadt, D)
Parafilm	Peckiney Plastic P. (Chicago, IL, USA)
PCR micropipets (5-000-1001-x10)	Drummond (Broomall, PA, USA)
PVDF membrane	Merck (Darmstadt, D)
Reaction tubes (0,5 ml, 1 ml, 2 ml)	Brand (Wertheim, D)
Reaction tubes safelock (1,5 ml)	Eppendorf (Hamburg, D)
Reaction tubes (15 ml, 50 ml)	Greiner Bio-One (Kremsmünster, A)
Scalpel blades	Fine Science Tools (Heidelberg, D)
Serological pipettes (5 ml, 10 ml, 25 ml)	Sarstedt (Nürnbrecht, D)
Syringes (1 ml, 2 ml, 5 ml)	B. Braun (Melsungen, D)
4-well petri dishes	Greiner Bio-One (Kremsmünster, AT)
24-well plates	Sarstedt (Nürnbrecht, D)
Wipes	Kimtech (Irving, TX, USA)

2.3 Chemicals

Acetone	Carl Roth (Karlsruhe, D)
Agarose	Serva (Heidelberg, D)
Aqua	B. Braun (Melsungen, D)
B27 Supplement	Life Technologies (Carlsbad, CA, USA)

Basic fibroblast growth factor (FGF)	Life Technologies (Carlsbad, CA, USA)
Bovine serum albumin (BSA)	Sigma-Aldrich (St. Louis, MO, USA)
Calcium chloride ($CaCl_2$)	Sigma-Aldrich (St. Louis, MO, USA)
D-Glucose	Sigma-Aldrich (St. Louis, MO, USA)
4',6-diamidino-2-phenylindole dilactate (DAPI)	Life Technologies (Carlsbad, CA, USA)
Di-Sodium hydrogen phosphate (Na_2HPO_4)	Sigma-Aldrich (St. Louis, MO, USA)
Di-Sodium hydrogen phosphate dihydrate ($Na_2HPO_4 * 2 H_2O$)	Merck (Darmstadt, D)
DMEM/F12 21331	Life Technologies (Carlsbad, CA, USA)
DNAse I	Roche (Basel, CH)
Ethanol 99,8%	Carl Roth (Karlsruhe, D)
Ethanol 70%	Carl Roth (Karlsruhe, D)
Ethylenediamine-tetraacetic acid (EDTA)	Sigma-Aldrich (St. Louis, MO, USA)
Ethylene glycol	Sigma-Aldrich (St. Louis, MO, USA)
Fentanyl	Hexal (Holzkirchen, D)
Fetal calf serum (FCS)	Life Technologies (Carlsbad, CA, USA)
Glycerol	Sigma-Aldrich (St. Louis, MO, USA)
Glycine	Sigma-Aldrich (St. Louis, MO, USA)
Human epidermal growth factor (EGF)	Sigma-Aldrich (St. Louis, MO, USA)
Hyaluronidase	Sigma-Aldrich (St. Louis, MO, USA)
Hydrogen chloride (HCl)	Sigma-Aldrich (St. Louis, MO, USA)
4-(2-hydroxyethyl)-1-piperazineethanesulfonic acid (HEPES) (1M)	Life Technologies (Carlsbad, CA, USA)
Isopropanol	Carl Roth (Karlsruhe, D)
Ketaminhydrochlorid (Ketavet® 100 mg/ml)	Pfizer (New York City, NY, USA)
L-15 Medium	Sigma-Aldrich (St. Louis, MO, USA)
L-Glutamin	Life Technologies (Carlsbad, CA, USA)
Laminin	Roche (Basel, CH)
Magnesium sulfate ($MgSO_4$)	Merck (Darmstadt, D)
Medetomidine	Pfizer (New York City, NY, USA)
Methanol	Merck (Darmstadt, D)
Midazolam	Ratiopharm (Ulm, D)

Monopotassium dihydrogen phosphate (KH_2PO_4)	Merck (Darmstadt, D)
Monopotassium sulfate (KH_2PO_4)	Sigma-Aldrich (St. Louis, MO, USA)
Mounting solution (Aqua Polymount®)	Polysciences (Warrington, PA, USA)
NaCl 0,9 % solution (Saline)	B. Braun (Melsungen, D)
Normal Goat Serum (NGS)	Life Technologies (Carlsbad, CA, USA)
Paraformaldehyd (PFA)	Sigma-Aldrich (St. Louis, MO, USA)
Penicillin (100 U/ml) /Streptomycin (100 mg/ml)	Life Technologies (Carlsbad, CA, USA)
Poly-D-Lysine (PDL)	Sigma-Aldrich (St. Louis, MO, USA)
Poly-L-ornithine (PLO)	Sigma-Aldrich (St. Louis, MO, USA)
Potassium chloride (KCl)	Sigma-Aldrich (St. Louis, MO, USA)
2-Propanol	Carl Roth (Karlsruhe, D)
Sodium chloride (NaCl)	Sigma-Aldrich (St. Louis, MO, USA)
Sodium dihydrogen phosphate (NaH_2PO_4)	Merck (Darmstadt, D)
Sodium hydroxide (NaOH)	Sigma-Aldrich (St. Louis, MO, USA)
Sucrose	Merck (Darmstadt, D)
Triton X-100	Sigma-Aldrich (St. Louis, MO, USA)
Trypsin	Sigma-Aldrich (St. Louis, MO, USA)
Trypsin/EDTA (0,05%)	Life Technologies (Carlsbad, CA, USA)
Trypsin Inhibitor	Sigma-Aldrich (St. Louis, MO, USA)
Xylazine hydrochloride (Rompun® 100 mg/ml)	Bayer (Leverkusen, D)
Yeast extract	BD (Franklin Lakes, NJ, USA)

2.4 Buffers and Solutions

Blocking solution for brain sections	1 ml NGS ad 9 ml 0,5% Triton X-100
Blocking solution for cells	0,1 g BSA 0,1 ml Triton X-100 ad 100 ml PBS 1x
cDNA mix	1 µl cDNA 4 µl H2Odd

Ketamin/Xylazine	2,5 ml Saline 1 ml Ketavet 0,25 ml Rompun
Krebs-Ringer-Hepes-Buffer (KRH)	3,65 g NaCl (125mM) 0,18 g KCl (4,8mM) 0,095 g $CaCl_2$*$2H_2O$ (1,3mM) 0,15 g $MgSO_4$*$7H_2O$ (1,2mM) 0,08 g KH_2PO_4 (1,2mM) 0,55g D-Glucose (5,6mM) 3,25 g HEPES (25mM) ad 500 ml H2Odd pH 7,40
KRH with 0,1% BSA (KRH/A)	0,1 g BSA ad 100 ml KRH
Midazolam/Medetomidine/Fentanyl (MMF)	5/0,5/0,05 mg/kg MMF 1:3 NaCl 0,9%
Neurosphere medium	500 µl Penicillin/Streptomycin 1 ml B27 500 µl L-Glutamin ad 50ml DMEM/F12 add 50 µl EGF and 50 µl FGF right before usage
Ovomucoid	1 mg Trypsin Inhibitor 50 µg BSA 40 µg DNase I In 1 ml L-15 Medium

Paraformaldehyd stock (PFA 20%)	134 g Na_2HPO_4 * 2 H_2O in 800 ml H2Odd 400 g PFA 10 ml NaOH passed through paper filters pH 7,40
Paraformaldehyd (PFA 4%)	100 ml PFA 20 % 400 ml H2Odd
Phosphate buffer saline (PBS 10x)	58,75 g Na_2HPO_4 10 g KH_2PO_4 400 g NaCl 10 g KCl ad 5 l H2Odd pH 7,40
Phosphate buffer saline (PBS 1x)	100 ml PBS 10x ad 900 ml H2Odd
PO4-buffer (10x)	65 g NaH2PO4 15 g NaOH 2 ml HCl ad 400 ml H2Odd pH 7,40
Poly-L-ornithine solution (PLO solution)	750µL PLO ad 50mL H_2O
Probe mix	0.3 µl Probe (Roche) 10 µl PCR mix (Roche) 1 µl primer forward (PF) 1 µl primer reverse (PR) 2.7 µl H2Odd

Storing solution for free floating brain sections	150 ml H2Odd 150 ml Ethylene glycol 150 ml Glycerol 50 ml PO4-buffer (10x)
Sucrose solution (30%)	15 g Sucrose ad 50 ml PBS 1x
Triton X-100 0,5% (0,5% Tx)	1 ml Triton X-100 ad 200 ml PBS 1x

2.5 Animals and Surgical Procedures

Adult 2-3 months old female C57BL/6J mice (Charles River Laboratories, Sulzfeld, Germany) were used for all experiments performed. All animals were kept under standard conditions (12h/12h light/dark cycle and access to food and water *ad libitum)*. Allocation to the different experimental groups was randomized. All animal experience and handling adhered to German and European Union guidelines and were approved by the State of Upper Bavaria. Maximum efforts were made minimizing animal suffering and the lowest possible number of animals was used for all experiments.

All surgical procedures were performed by Dr. Kristina Loy (Department of Clinical Neuroimmunology, LMU Munich, head Prof. Dr. Martin Kerschensteiner). An intraperitoneal injection of MMF (Midazolam/Medetomidine/Fentanyl at dosage of 5/0,5/0,05 mg per kg body weight) was used to anesthetize mice. In the Hemisection (Hemi) group, a laminectomy at mid-thoracic level (T8) and a dorsal hemisection of the spinal cord using fine iridectomy scissors as described previously (Lang et al., 2012) was performed. This lesion maintains the integrity of the minor ventral corticospinal tract components. After complete hemostasis, the wound was closed using Glover Bulldog clamps. In the Sham Surgery group (Sham), all steps listed above were exerted likewise but lacking the spinal cord lesion. In the naïve control group, skin incision and closure only were performed (Fig. 7). After surgery, animals were treated with analgesics and observed frequently in order to prevent wound infection. All experimental procedures were performed in accordance with and approved by the animal welfare policies of the Upper State of Bavaria.

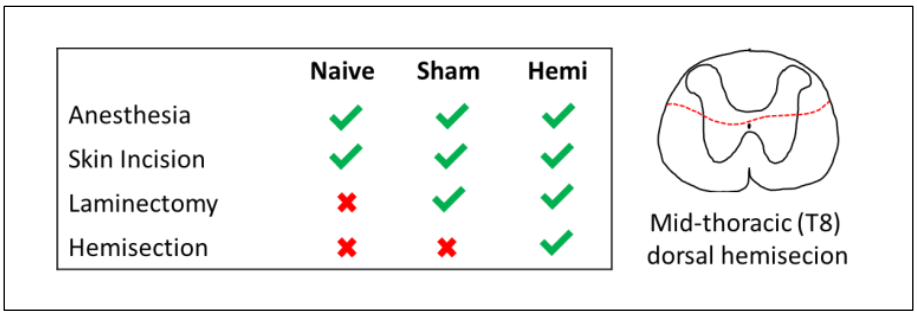

Figure 7. Experimental groups and surgical procedures. Hemisection animals underwent all steps including a mid-thoracic dorsal hemisection (see scheme), Sham animals did not undergo hemisection of the spinal cord, naïve controls only underwent superficial skin incision.

2.6 Immunohistochemical Analysis

To distinguish between the acute, subacute, and chronic phase after SCI, animals were sacrificed with an overdose injection of 5µl Ketamin/Xylazine solution per g body weight intraperitoneally at 5, 7, and 14 dpi. Animals were perfused transcardially with phosphate-buffered saline (PBS 1x) (pH 7.40) and afterwards with 4% paraformaldehyde diluted with PBS 1x (4% PFA) until blood was cleared out. Brains and spinal cords were dissected, post-fixed overnight in 4% PFA at 4°C, cryoprotected by saturation in 30% sucrose and embedded in 4% Agarose for processing. Coronal sections of the brains of 50 µm thickness were cut on a vibratome. Those were selected for further analysis which exhibited specific cytoarchitectonic features which were determined using The Allen Reference Mouse Brain Atlas (http://mouse.brainmap.org/static/atlas). For the neurogenic stem cell niches within the hippocampus (HC), position 273/image 69 to position 293/image 74 were chosen as templates. The subependymal or subventricular zone (SVZ) (Fischer et al., 2011, Kempermann et al., 2015, Doetsch et al., 1999a) could be seen in position 181/image 46 to position 201/image 51, respectively.

The following primary antibodies diluted in blocking solution were used for free floating immunohistochemistry:

anti-Ki67 (rabbit; 1:100)	Life Technologies (Carlsbad, CA, USA)
anti-GFAP (mouse IgG1; 1:400)	Sigma-Aldrich (St. Louis, MO, USA)
anti-DCX (guinea pig; 1:1000)	Sigma-Aldrich (St. Louis, MO, USA)

After incubation with the primary antibodies overnight at 4°C on a shaker and extensive washing in PBS, the following subclass-specific secondary antibodies coupled with fluorescents diluted in blocking solution were used to detect marked epitopes:

Alexa Fluor 488 (guinea pig; 1:500)	Dianova (Hamburg, D)
Cy3 (rabbit; 1:500)	Dianova (Hamburg, D)
Alexa Fluor 647 (mouse IgG; 1:500)	Dianova (Hamburg, D)

After incubation for 1h and 50 minutes in the dark at room temperature on a shaker, DAPI (1:1000) (Sigma-Aldrich, St. Louis, MO, USA) was added for another 10 minutes. Finally, after extensive washing in PBS, sections were carefully positioned onto glass slides and coverslips were mounted with a mounting medium. All slides were stored dry and dark until analyses. Confocal laser scanning microscopy (Zeiss LSM5) was used to quantify immunopositive cells in *in vivo* sections. For each count, at least three animals were examined based on the analysis of a minimum of three sections. Regions of interest were marked using the Zeiss ZEN 2 blue edition software, labelled cells were counted per section and normalized using the area of the marked region and the depth in the z-axis to obtain absolute numbers per mm^3. Mean values for each individual animal were formed and plotted into the GraphPad Prism 5.0 database. Fold changes compared to naïve controls were calculated by dividing absolute numbers per mm^3 by the mean value of corresponding slices of naïve controls, then again mean fold changes for each individual animal were formed and plotted into the GraphPad Prism 5.0 database. Statistical analyses were performed using the GraphPad Prism 5.0 software, testing for normal distribution and significance between experimental groups by accordingly chosen testing methods (Mann-Whitney-U-Test or unpaired t-test for comparison between two groups, Kruskal-Wallis-Test with Dunn's post-test and one-way analysis of variance (ANOVA) with Tukey's post-test for comparison of three or more groups, respectively). All values were plotted as mean ± standard error of the mean (SEM), unless otherwise stated. Significance is indicated as *($p < 0.05$), **($p < 0.01$), and ***($p < 0.001$).

2.7 Neurosphere Culture

2.7.1 Preparation of Cell Cultures

Animals were sacrificed by cervical dislocation at 5, 7, and 14 days post injury. Brains were removed immediately and put into 15 ml Falcon tube filled with ice-cold neurosphere medium lacking growth factors. Meninges and white matter were removed, regions of interest were dissected according to established protocols (Fig. 8). Samples from the SEZ and the HC were transferred into 15 ml Falcon tubes filled with 1 ml of neurosphere medium lacking growth factors. Tissue dissociation was initiated by manually trituration and completed by adding Trypsin to a final concentration of 0,05% and incubation for 25 minutes at 37°C in a water bath. After the enzymatic process was stopped by adding 1 ml Ovomucoid, cells were centrifuged at 1500 rpm for 5 minutes, resuspended, and plated in 24-wells cell culture plates at a density of 5 cells per µl determined using a Neubauer cell counting chamber. Finally, the wells were filled up to 1 ml neurosphere medium, and FGF and EGF were added to a concentration of 10 ng/ml, respectively.

Statistical analyses were performed using the GraphPad Prism 5.0 software, testing for normal distribution and significance between experimental groups by accordingly chosen testing methods (Mann-Whitney-U-Test or unpaired t-test for comparison between two groups, Kruskal-Wallis-Test and Dunn's post-test or one-way ANOVA and Tukey's post-test for comparison of three or more groups, respectively).

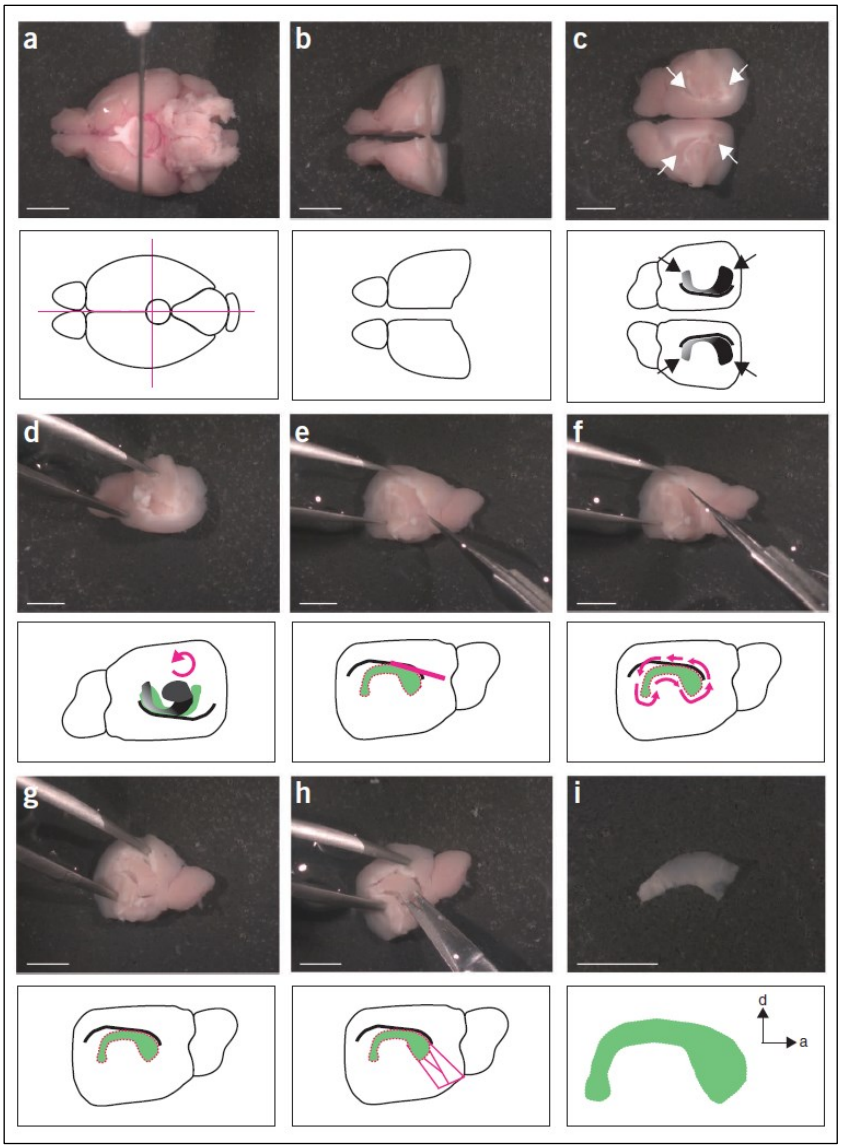

Figure 8. Dissection of the lateral ventricular wall and the hippocampus. Two cuts are made at the level of the optic chiasm and along the midline to isolate the hemispheres (a, b). Medial view on hemispheres, arrows pointing at the ends of the hippocampus (c). Removal of the hippocampus (d). Dissection of the SEZ from white matter and the striatum (e-h). Image of the dissected SEZ. Scale bar 5 mm. Modified from Fischer et al. 2011.

2.7.2 Analysis of Self-Renewing Capacity

Cells were kept in an incubator at stable standard conditions for 14 days *in vitro* until further analysis. When quantifying the number of spheres per well, only those were considered that were greater than 50 µm in diameter with a nice and healthy morphology (clear borders, round vital cells, yellowish color). The cell suspension from each sample was distributed between 4 wells, and mean values were generated to reduce errors caused by manual

discrepancies. The data was finally normalized and plotted as number of neurospheres per 10,000 plated cells. After quantification, the cell suspension was centrifuged at 1500 rpm for 5 minutes and resuspended in 1 ml neurosphere medium lacking growth factors. Trypsin was added until a final concentration of 0,025% was reached, and after gentle mechanical dissociation with a pipette, the tubes were incubated at 37°C for 15 minutes. All other steps as in the first passage were repeated, and the remaining cell suspension was kept in cell culture flasks.

2.7.3 Analysis of Differentiation Potency

After passaging the neurospheres for three times, individual spheres from the third and fourth passage were assessed and spheres from at least four wells per animal were picked for differentiation. As NSCs are thought to give rise to bigger spheres (Pastrana et al., 2011), only those were chosen for differentiation with a diameter greater than 100 µm. For this purpose, glass cover slips were prepared by PLO solution coating and incubation at 37°C overnight. After extensive washing with H_2O, Laminin was applied, and the slides were incubated for another 2h. Spheres were then transferred onto the coverslips and incubated for 6-7 days at 37°C in neurosphere medium containing 1% fetal calf serum and lacking growth factors. The following primary antibodies were used for immunohistochemistry:

anti-GFAP (rabbit; 1:500)	Dako (Hamburg, D)
anti-O4 (mouse IgM; 1:50)	Millipore (Burlington, MA, USA)
anti-ßIII Tubulin (mouse IgG2b; 1:250)	Promega (Madison, WI, USA)

Anti-O4 was diluted in KRH solution containing 0,1% BSA for alive staining, incubated for 20 minutes at room temperature and only after this, cells were fixated with 4% PFA for 5 minutes. After washing in PBS, the cells were again incubated at room temperature for 20 minutes with the remaining antibodies diluted in blocking solution. Finally, after multiple washings in PBS, nuclei were marked with DAPI (dilution 1:10 000) and the following subclass specific secondary antibodies coupled to fluorescents were used to detect marked epitopes:

Alexa Fluor 488 (mouse IgM; 1:500)	Dianova (Hamburg, D)
Cy3 (mouse IgG; 1:500)	Dianova (Hamburg, D)
Alexa Fluor 647 (rabbit; 1:500)	Dianova (Hamburg, D)

Again, the coverslips were washed extensively in PBS and mounted onto microscopy slides using mounting medium. All samples were stored dry and dark until further analysis.

2.8 RNA Extraction from MACS-sorted Astrocytes and RT-qPCR

For purposes of real-time quantitative polymerase chain reaction (RT-qPCR), magnetic-activated cell sorting (MACS) (Anti-ACSA-2 microbead kit, Miltenyi Biotec) was used to isolate astrocytes from punched samples from the cortex according to protocols established in our lab from naïve animals, as well as from the 5dpi Hemi and Sham group (performed by Dr. Judith Fischer-Sternjak and Tatiana Simon-Ebert). RNA was extracted from these cells using the PicoPure RNA isolation kit (Thermo Scientific) adhering to the manufacturer's instructions (performed by Dr. Giacomo Masserdotti).

For retrotranscription into complementary deoxyribonucleic acid (cDNA), the Maxima First Strand cDNA Synthesis Kit for RT-qPCR with dsDNase (Thermo Scientific) containing the Maxima Reverse Transcriptase and oligo(dT)18 such as random primers were used according to the manufacturer's instructions. cDNA was then diluted 1:1 to ensure a sufficient amount of fluid. All samples were further processed and prepared (Probe mix and cDNA mix) for RT-qPCR using the LightCycler Probe Master Kit (Roche) following the manufacturer's instructions. Three technical replicates per biological replicate were included in the analysis, while one biological replicate consists of MACS-sorted astrocytes of individual animals. On the LightCycler480 II (Roche), approximately 55 cycles were run using the program Monocolor Hydrolysis Probe. For statistical analyses, transcript levels were normalized by the level of the housekeeping gene of hypoxanthineguanine phosphoribosyltransferase (HPRT1) so that the ΔΔCt method (Livak and Schmittgen, 2001) could be applied. The GraphPad Prism 5.0 software was used for statistical analyses (one-way ANOVA, Tukey's post-test). All probes were

purchased from Roche (Basel, CH) and are listed in Tab. 1 along with the primers designed by Metabion (Planegg, D) using the *Universal ProbeLibrary* by Roche.

Symbol	Name	Probe	Sequence
CCND1	Cyclin D1	67	PF: GAGATTGTGCCATCCATGC PR: CTCCTCTTCGCACTTCTGCT
GLI1	GLI family zinc finger 1	84	PF: CTGACTGTGCCCGAGAGTG PR: CGCTGCTGCAAGAGGACT
HPRT1	Hypoxanthine phosphoribosyltransferase 1	95	PF: TCCTCCTCAGACCGCTTTT PR: CCTGGTTCATCATCGCTAATC
MKI67	Marker of proliferation Ki-67	88	PF: AGGGTAACTCGTGGAACCAA PR: TCTTAACTTCTTGGTGCATACAATG
STAT3	Signal transducer and activator of transcription 3	18	PF: GGAAATAACGGTGAAGGTGCT PR: CATGTCAAACGTGAGCGACT

Table 1. List of primers and sequences.

2.9 Collection of CSF Samples and Proteome Analysis

For proteome analysis, samples of cerebrospinal fluid (CSF) were collected from the cisterna magna by use of fine glass microcapillaries (Drummond, Broomall, PA, USA) (performed by Dr. Swetlana Sirko). The obtained CSF samples (5-10 µl per animal) were stored in 1,5 ml Safelock Eppendorf® tubes on dry ice for transport. Label-free mass spectrometry analysis of the collected samples was performed (performed by Dr. Fabian Metzger) at the Research Unit Protein Science of the Helmholtz Center Munich (head Dr. Stefanie Hauck) according to previously established protocols (Stoop et al., 2010, Hauck et al., 2010). Proteins were identified with ≥2 unique peptides and filtered at a false discovery rate (FDR) of 0.01. The overlap between the detected proteins and existing mouse proteomics datasets was analyzed using the Proteomics DB database (https://www.proteomicsdb.org/). Proteins which met the statistical criteria (fold change >1.5 and p-value <0.05) were used for functional association analysis according to Gene Ontology (GO) terms (http://geneontology.org/) using the the STRING database (https://string-db.org/). Graphs and diagrams were created by Dr. Swetlana Sirko using the GraphPad Prism 9.0 software.

3. Results

Parts of the results of this project are currently under submission for publication and are planned to appear under the title “Region-specific reaction of glial cells in the brain parenchyma of adult mice following spinal cord injury”.

3.1 Induction of Cell Proliferation in Adult Neural Stem Cell Niches After SCI

To assess whether SCI induces a proliferative response in adult neural stem cell niches, the SEZ and DG were analyzed using immunohistochemical labelling. A marked increase in Ki67+ cells around 5-7 days after hemisection could be noted compared to controls (Fig. 9).

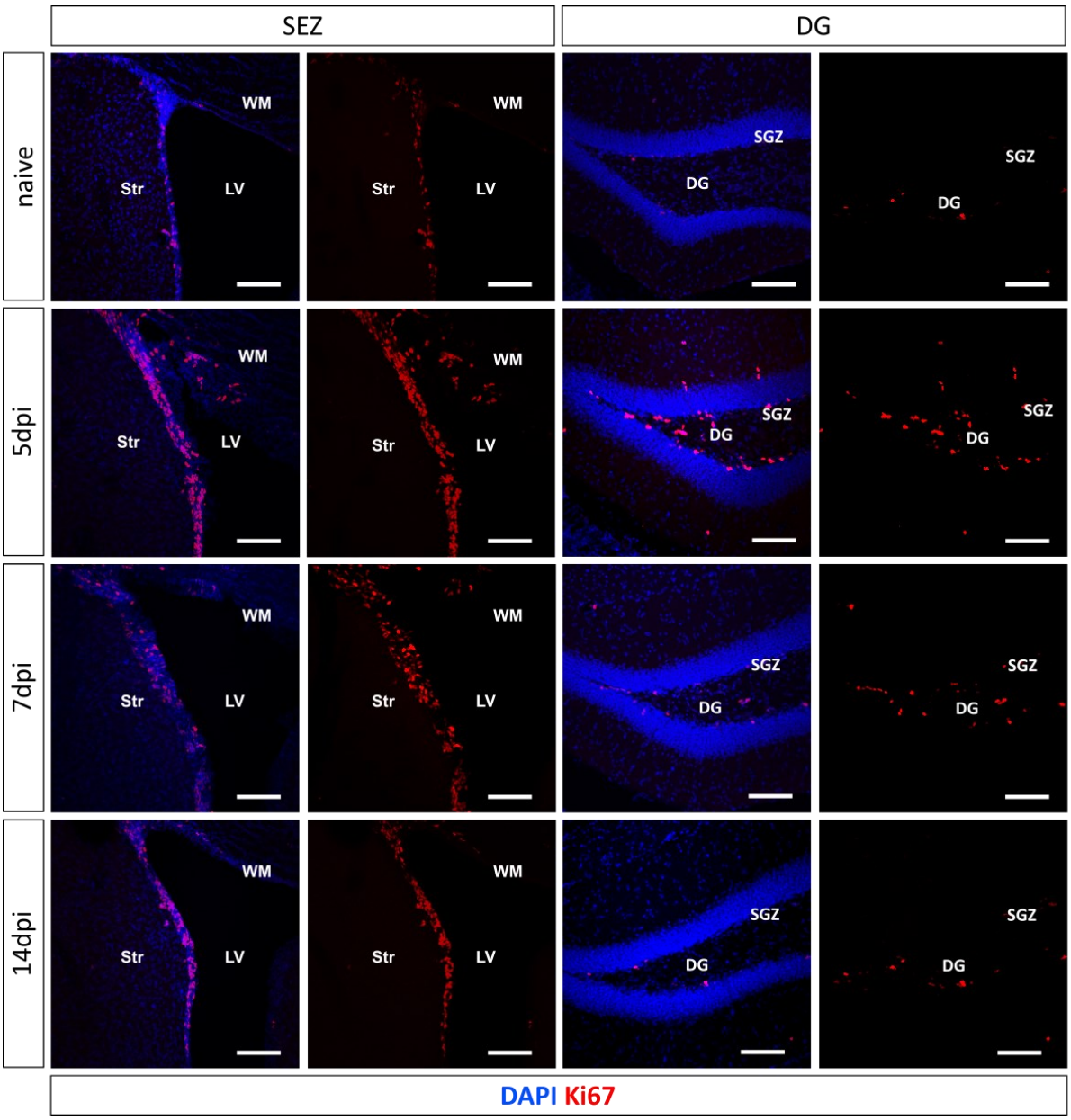

Figure 9. **SCI induces cell proliferation in adult murine stem cell niches.** Striatum (Str), white matter (WM), lateral ventricle (LV), dentate gyrus (DG), subgranular zone (SGZ). Scale bars 100µm.

The number of Ki67+ cells was significantly increased at 5dpi in the SEZ (p=0.0095) and up to almost three times higher compared to naïve controls (fold change 2.68). At 14dpi, no significant difference could be found, suggesting that at this time point cell cycle activity has slowly returned to physiological levels (Fig. 10A). Similarly, in the DG, the number of Ki67+ cells was also significantly increased 5dpi compared to naïve controls (p=0.0238) with a mean fold change of 2.67, while at later time points a slow return to baseline levels was noted (Fig. 10B).

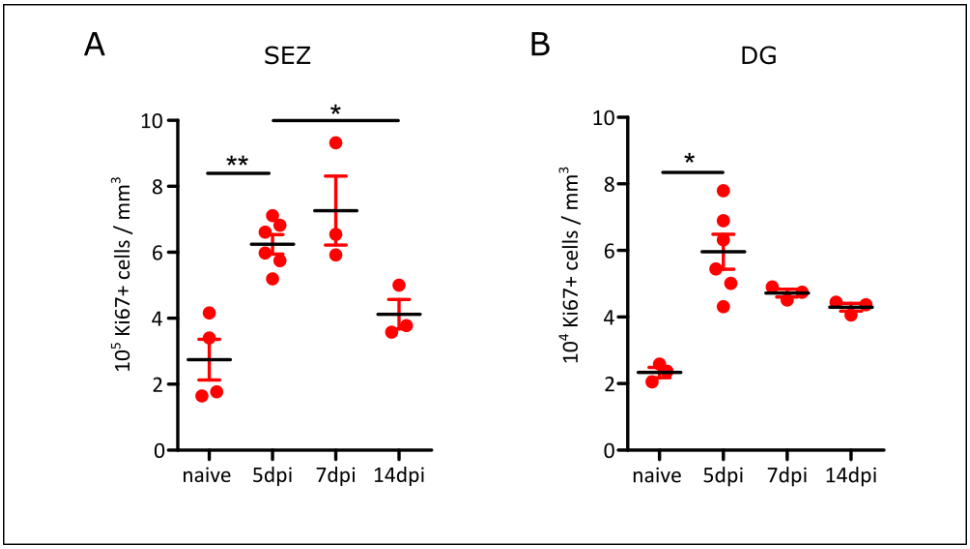

Figure 10. SCI induces cell proliferation in adult murine stem cell niches. (A) Quantification of Ki67+ cells in the SEZ showed a significantly higher number of proliferating cells at 5 dpi compared to naïve controls, with numbers normalizing around 14 dpi (**p=0.0095; *p=0.0238). Naïve n=4; 5dpi n=6; 7dpi n=3; 14dpi n=3. Kruskal-Wallis-test and Dunn's post-test; Mann-Whitney-U-test for comparison of two groups. (B) Quantification of Ki67+ cells in the DG showed a significantly higher number of proliferating cells at 5 dpi compared to naïve controls (*p=0.0238). Naïve n=3; 5dpi n=6; 7dpi n=3; 14dpi n=3. Kruskal-Wallis-test and Dunn's post-test; Mann-Whitney-U-test for comparison of two groups.

3.2 SCI-Induced Expansion of Proliferating Neuronal Progenitors within Adult Neural Stem Cell Niches

The peak of SCI-induced proliferation in adult neural stem cell niches occurred around 5dpi. To assess whether an increase of the number of actual aNSCs is responsible, samples from both stem cell niches were co-stained for GFAP. As aNSCs are indeed a subset of GFAP expressing astrocytes, which are able to proliferative even outside of any pathological context (Gotz et al., 2016), the use of co-staining with a marker of proliferation such as Ki67 allows for their identification. Exemplary co-staining with Sox2, another marker expressed in aNSCs (Dimou and Gotz, 2014), to increase certainty of identifying aNSCs showed that all Ki67+/GFAP+ double positive cells indeed express Sox2 (Fig. 11).

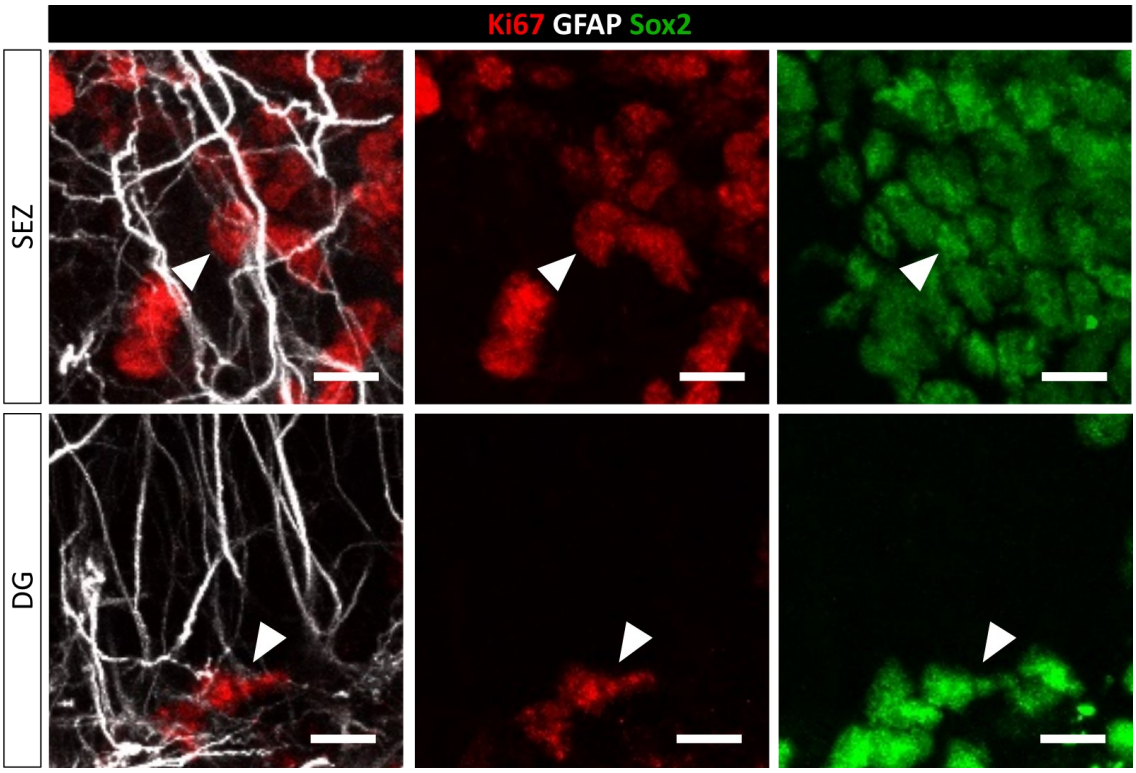

Figure 11. Immunostaining of aNSCs. Co-staining using Ki67, GFAP and Sox2 reveal that all Ki67+/GFAP+ double positive cells also stain positive for Sox2, increasing the certainty that Ki67+/GFAP+ double positive cells within the adult neural stem cell niches are indeed aNSCs.

Immunostaining demonstrated a marked increase in GFAP+ signal at 5dpi (Fig. 12A). However, quantification showed no statistically significant increase of Ki67+/GFAP+ cells at 5dpi (p=0.2571) or at any other time after SCI compared to naïve controls. On the contrary, the pool of Ki67+/GFAP+ cells was 40% lower at 14dpi when compared to baseline levels of naïve animals (Fig. 12B).

To identify neuroblasts undergoing cell division, DCX was used in combination with Ki67 for immunohistochemical staining of brain sections. The number of Ki67+/DCX+ cells within the SEZ was clearly increased at 5dpi compared to naïve controls. In fact, quantification showed a fold change of 3.74. Statistical analyses revealed no statistical significance (p=0.0571), but marked and visible changes could be found in representative images (Fig. 12A). At 7 and 14dpi, the number of immunopositive cells remained at a higher level but did show a trend of slow return towards baseline (Fig. 12C).

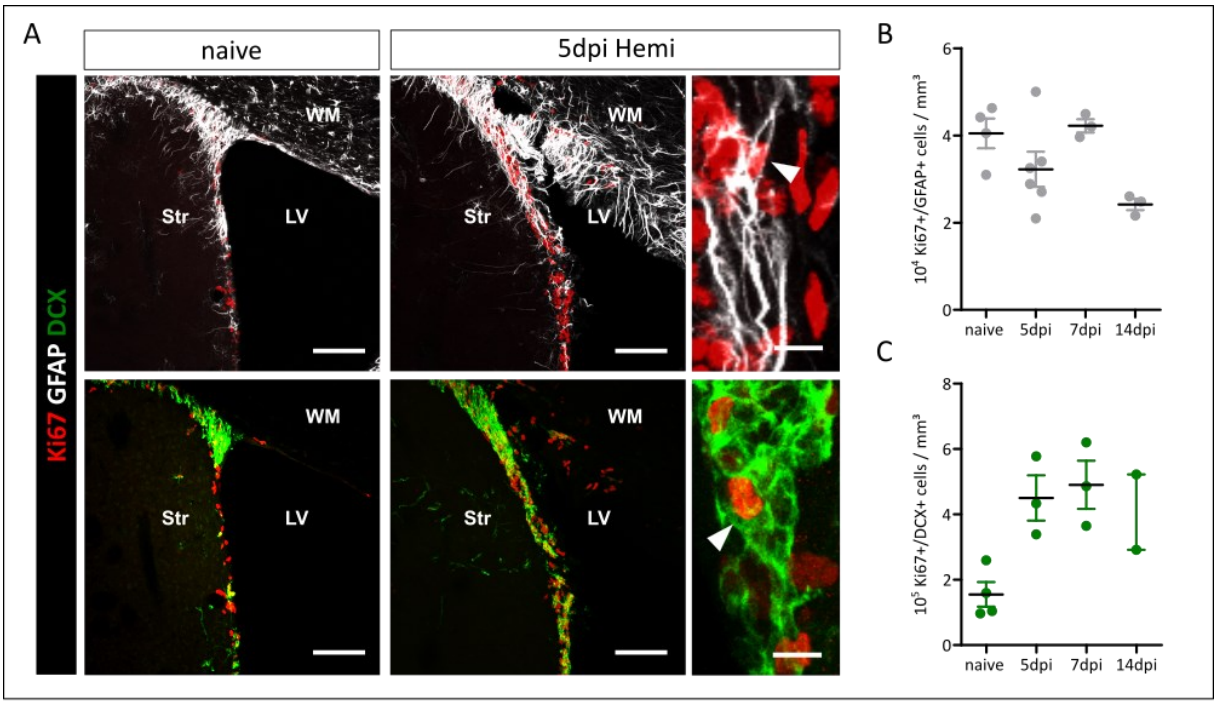

Figure 12. SCI induces neuroblast proliferation in the SEZ. (A) Immunostaining with GFAP and DCX demonstrated an increase in both Ki67+/GFAP+ and Ki67+/DCX+ cells at 5dpi. Normalized quantification, however, revealed no remarkable increase in Ki67+/GFAP+ cells (p=0.2571) (B) but in Ki67+/DCX+ cells (p=0.0571) (C) at 5dpi. At 14dpi, Ki67+/GFAP+ cells seemed to have decreased compared to naïve controls (B), while the number of Ki67+/DCX+ cells remained relatively stable. Striatum (Str), white matter (WM), lateral ventricle (LV). Naïve n=4; 5dpi n=3; 7dpi n=3; 14dpi n=2. Mann-Whitney-U-test. Note that Ki67+/DCX+ numbers at 14dpi were exemplarily counted based on one brain slice per animal (7dpi), and two animals per group (14dpi), respectively, to outline a trend. Therefore, no statistical analysis was performed on those datasets. Scale bars 100 µm, 10 µm in magnifications.

In contrast to the SEZ, analysis of the DG using markers of proliferating astroglia and neuronal progenitors did reveal increased numbers of immunopositive cells following SCI (Fig. 13A). Thereby, the maximum effect could be observed at 5dpi, with almost twice as many Ki67+/GFAP+ cells (p=0.0476) (Fig. 13B) and a similar increase in Ki67+/DCX+ cells (p=0.1000) (Fig. 13C) compared to naïve animals. Around 14dpi, Ki67+/GFAP+ showed a tendency towards physiological levels but the changes in the number of Ki67+/DCX+ labelled cells remained at a high level without a clear trend towards baseline (Fig. 13B, C).

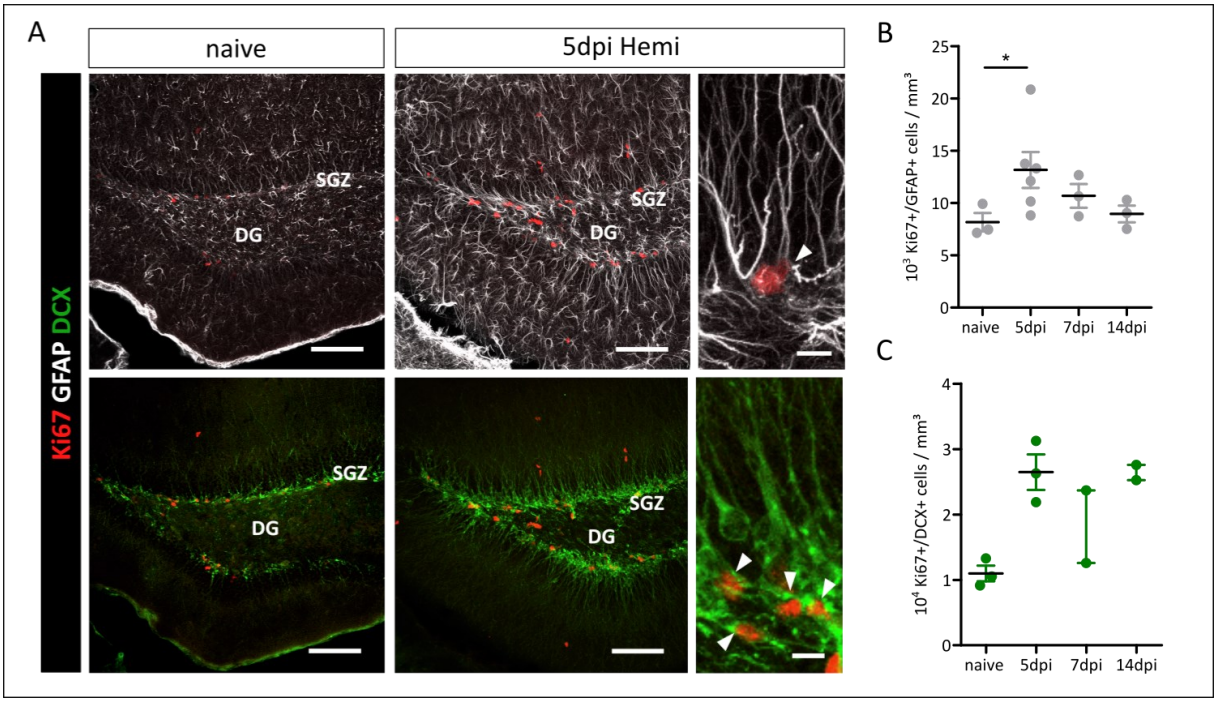

Figure 13. SCI increases proliferation of neuroblasts and aNSCs in the DG. (A) Immunostaining with GFAP and DCX demonstrated an increase in both Ki67+/GFAP+ and Ki67+/DCX+ cells at 5dpi. Quantification revealed a significant increase in Ki67+/GFAP+ cells (*p=0.0476) (B) but not in Ki67+/DCX+ cells (p=0.1000) (C) at 5dpi. At 14dpi, Ki67+/GFAP+ seemed to slowly return to normal levels (B) while the number of Ki67+/DCX+ cells remained relatively stable (C). Dentate gyrus (DG), subgranular zone (SGZ). (B) Naïve n=3; 5dpi n=6; 7dpi n=3; 14dpi n=3. Mann-Whitney-U-test. (C) Naïve n=3; 5dpi n=3; 7dpi n=2; 14dpi n=2. Mann-Whitney-U-test. Note that Ki67+/DCX+ numbers at 7 and 14dpi were exemplarily counted from two animals per group to outline a trend, therefore, no statistical analysis was performed on those datasets. Scale bars 100 µm, 10 µm in magnifications.

3.3 Consequences of Spinal Sham Surgery on Adult Neural Stem Cell Niches

Analogous to the SCI group, the pool of proliferating cells within both stem cell niches was analyzed after sham surgery by immunolabelling for Ki67. In the SEZ, there was a marked expansion of the Ki67+ cell pool (Fig. 14A). A significantly higher number of immunopositive cells, approximately 3 times compared to naïve animals, could be found at 5dpi ($p=0.0251$). While there was an overall trend of decreasing numbers at more chronic time points, Ki67+ cells remained at a higher level compared to baseline (Fig. 14B). Very similar effects of sham surgery were also observed in the DG, where the number of Ki67+ cells was approximately 2.5 times higher at 5dpi compared to naïve controls ($p=0.02216$) (Fig. 14C).

Given that sham surgery induces proliferation within adult neural stem cell niches, the pool of proliferating cells was further analyzed by co-labelling Ki67 with GFAP and DCX (Fig. 15A). In the SEZ, Ki67+/GFAP+ cell numbers did not show any obvious changes at 5dpi. However, at 14dpi, there was a clear decrease with fold changes as low as 0.61 compared to naïve controls. In contrast, the population of proliferating DCX+ cells behaved differently. Starting at 5dpi, their number expanded during the first two weeks after sham surgery, reaching a level that remained relatively stable at almost 4 times compared naïve controls (Fig. 15B).

In contrast, in the DG, sham surgery induced a strong proliferative response in both subgroups. At 5dpi, there were significantly more proliferating GFAP+ cells ($p=0.0077$) compared to naïve controls. Also, there was an increase in the population of Ki67+/DCX+ cells at 5dpi with numbers twice as high, which remained relatively stable during the course of two weeks post sham surgery (Fig. 15C).

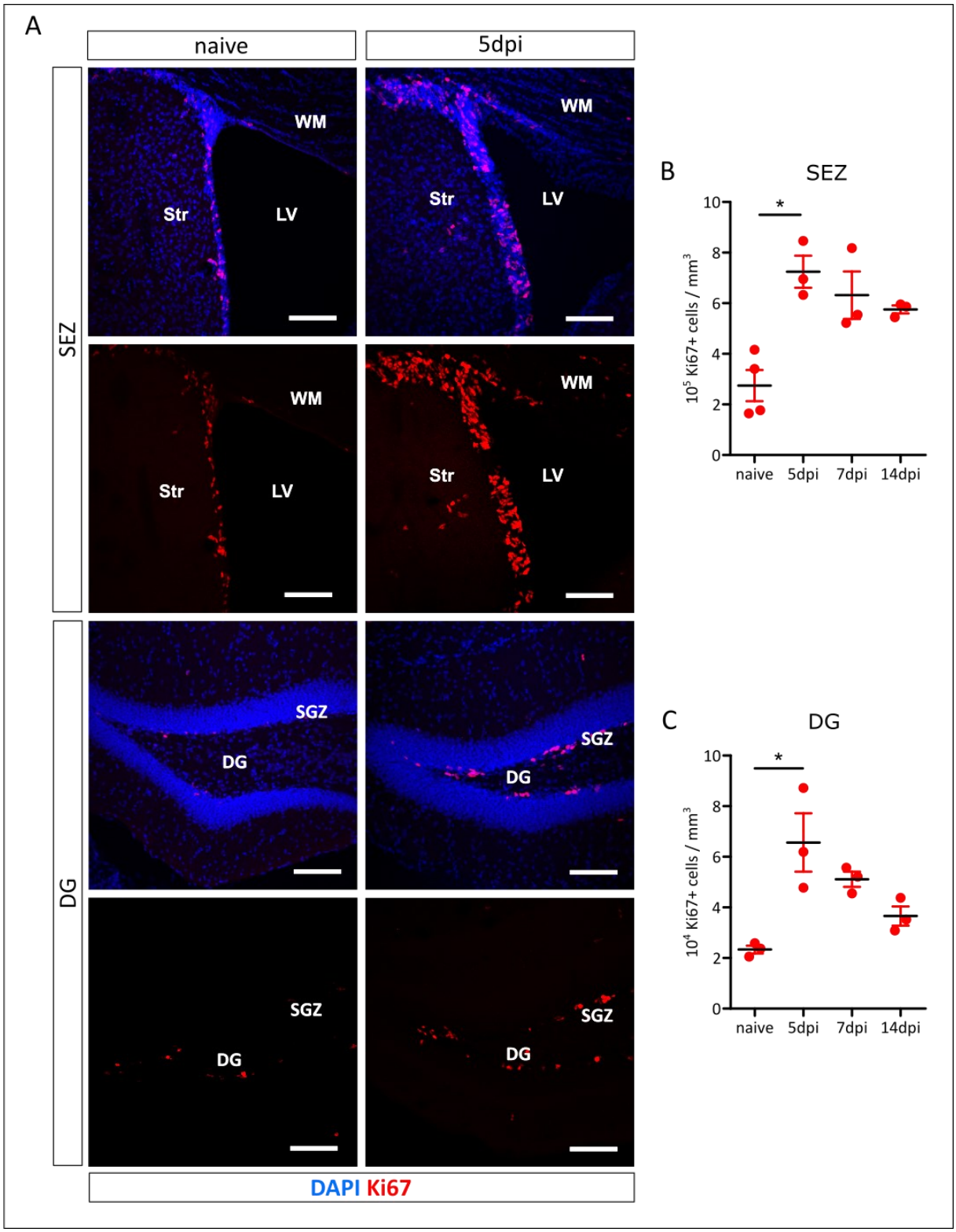

Figure 14. Sham surgery induces cell proliferation in stem cell niches. (A) Immunostaining with Ki67. (B) Quantification of Ki67+ cells in the SEZ showed a significantly higher number of proliferating cells at 5 days after sham surgery compared to naïve controls (*p=0.0251), with numbers decreasing but remaining relatively high at 14 days after sham surgery. Naïve n=4; 5dpi n=3; 7dpi n=3; 14dpi n=3. (C) Quantification of Ki67+ cells in the DG showed significantly more proliferating cells at 5 days after sham surgery compared to naïve controls (*p=0.02216), with numbers normalizing around 14 days after sham surgery. Naïve n=4; 5dpi n=3; 7dpi n=3; 14dpi n=3. Kruskal-Wallis-test and Dunn's post-test; Mann-Whitney-U-test for comparison of two groups. Striatum (Str), white matter (WM), lateral ventricle (LV), dentate gyrus (DG), subgranular zone (SGZ). Scale bars 100µm.

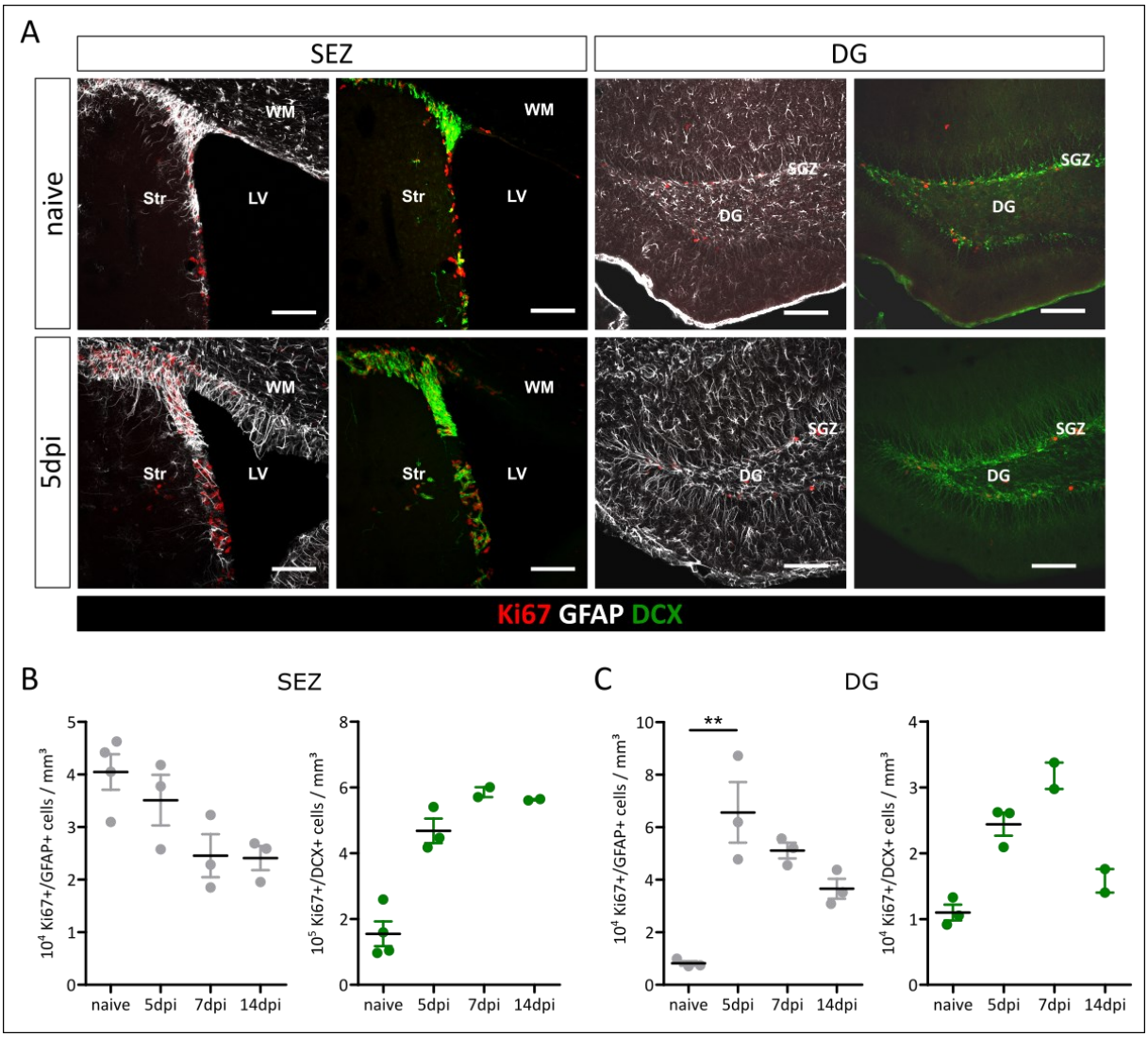

Figure 15. Sham surgery increases proliferation of neuroblasts and of DG aNSCs. (A) Immunostaining with GFAP and DCX. Quantification of Ki67+/GFAP+ cells revealed no increase within the SEZ at 5dpi but a slight decrease towards later timepoints (B), and a significant increase in the DG (**p=0.0077) (C). Quantification of Ki67+/DCX+ cells showed an increase in both the SEZ and the DG at 5dpi (B, C). While numbers of Ki67+/DCX+ cells remained relatively stable and high within the SEZ at later timepoints (B), a decrease in the DG could be observed around 14dpi (C). Striatum (Str), white matter (WM), lateral ventricle (LV), dentate gyrus (DG), subgranular zone (SGZ). Ki67/GFAP (B): naïve n=4; 5dpi n=3; 7dpi n=3; 14dpi n=3. Ki67/GFAP (C): naïve n=3; 5dpi n=3; 7dpi n=3; 14dpi n=3. Ki67/DCX (B): naïve n=4; 5dpi n=3; 7dpi n=2; 14dpi n=2. Ki67/DCX (C): naïve n=3; 5dpi n=3; 7dpi n=2; 14dpi n=2. Kruskal-Wallis-test and Dunn's post-test; Mann-Whitney-U-test or unpaired t-test for comparison of two groups. Note that Ki67/DCX numbers at 7 and 14dpi were exemplarily counted from two animals per group to outline a trend, therefore, no statistical analysis was performed on those datasets. Scale bars 100 µm.

3.4 Injury Type-specific Proliferative Response in Adult Neural Stem Cell Niches

To assess the differences in the proliferative response between sham surgery and spinal cord hemisection, the number of Ki67+ cells and Ki67+/GFAP+ of both neural stem cell niches were further compared. The number of Ki67+/DCX+ was further compared specifically at 5dpi, the timepoint of maximum effect. In the SEZ, the data showed no significant differences for the number of Ki67+ cells (Fig. 16A), Ki67+/GFAP+ cells (Fig. 16B), and Ki67+/DCX+ cells (Fig. 16C) at all timepoints of analysis.

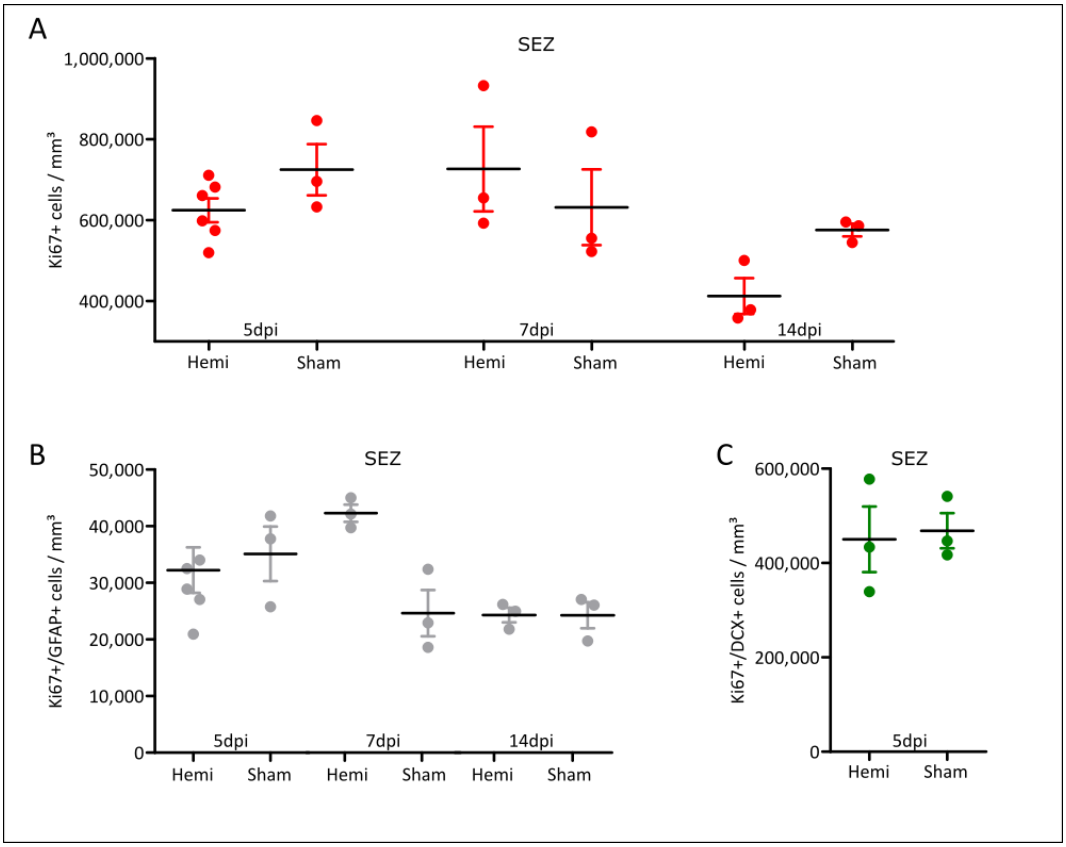

Figure 16. Quantification of immunopositive cells within the SEZ following SCI versus sham surgery. No significant differences in the number of Ki67+ cells (A), Ki67+/GFAP+ cells (B), and Ki67+/DCX+ cells (C) were found between the Hemi and the Sham groups at all timepoints of analysis. 5dpi Hemi n=6 (n=3 for Ki67+/DCX+); 5dpi Sham n=3; 7dpi Hemi n=3; 7dpi Sham n=3; 14dpi Hemi n=3; 14dpi Sham n=3. Mann-Whitney-U test.

In the DG, there were also no significant differences for the number of Ki67+ cells (Fig. 17A), and Ki67+/DCX+ cells (Fig. 17C) at all timepoints of analysis. However, there were generally more Ki67+/GFAP+ cells in the Sham groups compared to the Hemi groups and at 5dpi, the difference was also statistically significant (p=0.0238) (Fig. 17B).

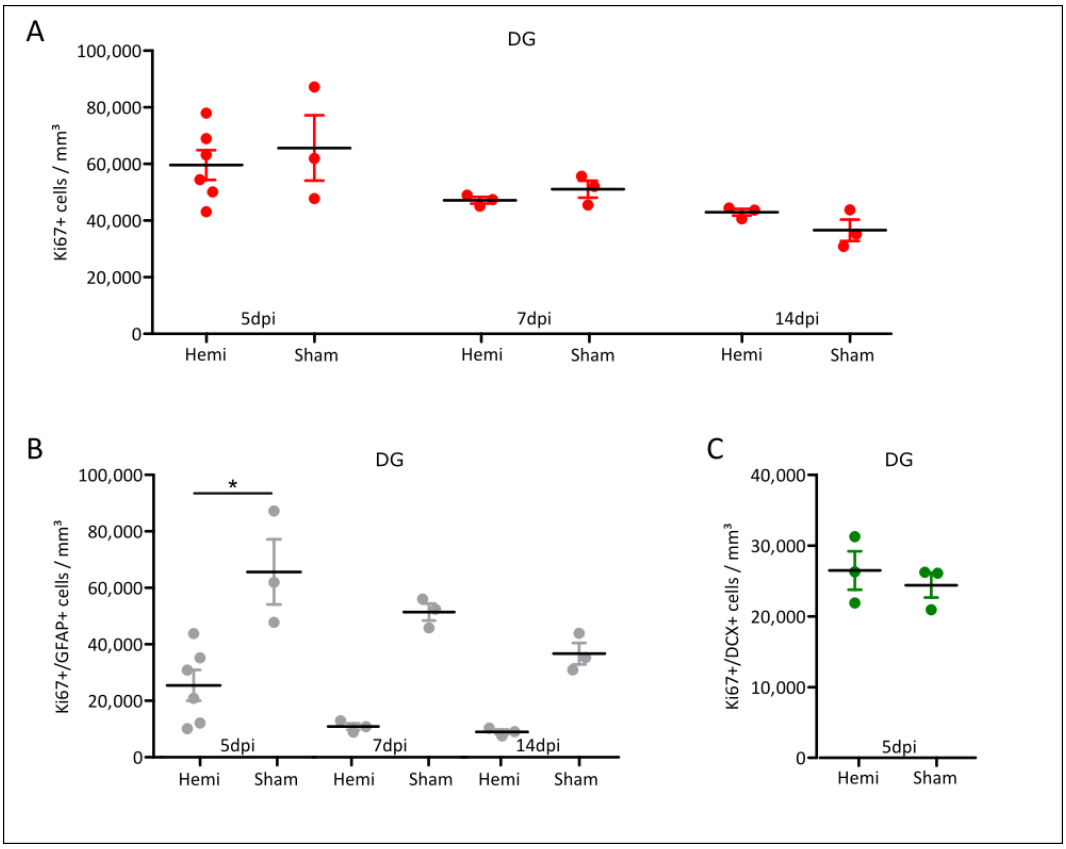

Figure 17. Quantification of immunopositive cells within the DG following SCI versus sham surgery. No significant differences in the number of Ki67+ cells (A) and Ki67+/DCX+ cells (C) were found between the Hemi and the Sham groups at all timepoints of analysis. (B) Significantly more Ki67+/GFAP+ cells could be found at 5dpi in the Sham group compared to the Hemi group (*p=0.0238), but not at 7 and 14dpi. 5dpi Hemi n=6 (n=3 for Ki67+/DCX+); 5dpi Sham n=3; 7dpi Hemi n=3; 7dpi Sham n=3; 14dpi Hemi n=3; 14dpi Sham n=3. Mann-Whitney-U test.

In regard to the subpopulations of Ki67+ cells in the SEZ, there was a clear decrease of the Ki67+/GFAP+ fraction in favor of the Ki67+/DCX+ group in the 5dpi Hemi group compared to naïve controls, while the Ki67+/GFAP-/DCX- fraction stayed more or less stable (Fig. 18A). In the DG, there was a more subtle reduction of the Ki67+/GFAP+ fraction in the 5dpi Hemi group, while the Ki67+/GFAP-/DCX- fraction showed an increase compared to naïve controls. Similarly, the percentage of Ki67+/DCX+ cells stayed relatively stable (Fig. 18B). The distribution of Ki67+ cell subtypes neither remarkably differed between the Hemi and the Sham group within the SEZ, nor within the DG. However, a slightly stronger increase in the Ki67+/DCX+ fraction could be observed in the Sham group compared to the Hemi group (Fig. 18A, B).

The temporal development of the proliferative response was very similar over all cell subpopulations in both neural stem cell niches. After hemisection, the peak proliferative

response could be found at acute time points with a slow return to baseline at 14dpi in both the SEZ (Fig. 18C) and the DG (Fig. 18D), after both invasive and non-invasive injury. All subgroups roughly followed the overall trend except for two populations: the number of proliferating GFAP+ cells in the SEZ underwent a moderate reduction at 5dpi, followed by a progressive decline to only 40% compared to baseline at 14dpi after both injury types (Fig. 18C, grey lines). Also the Ki67+/DCX+ fraction in the DG behaved differently, responding to hemisection with an increase at 14dpi after an initial decrease (Fig. 18D, green dashed line).

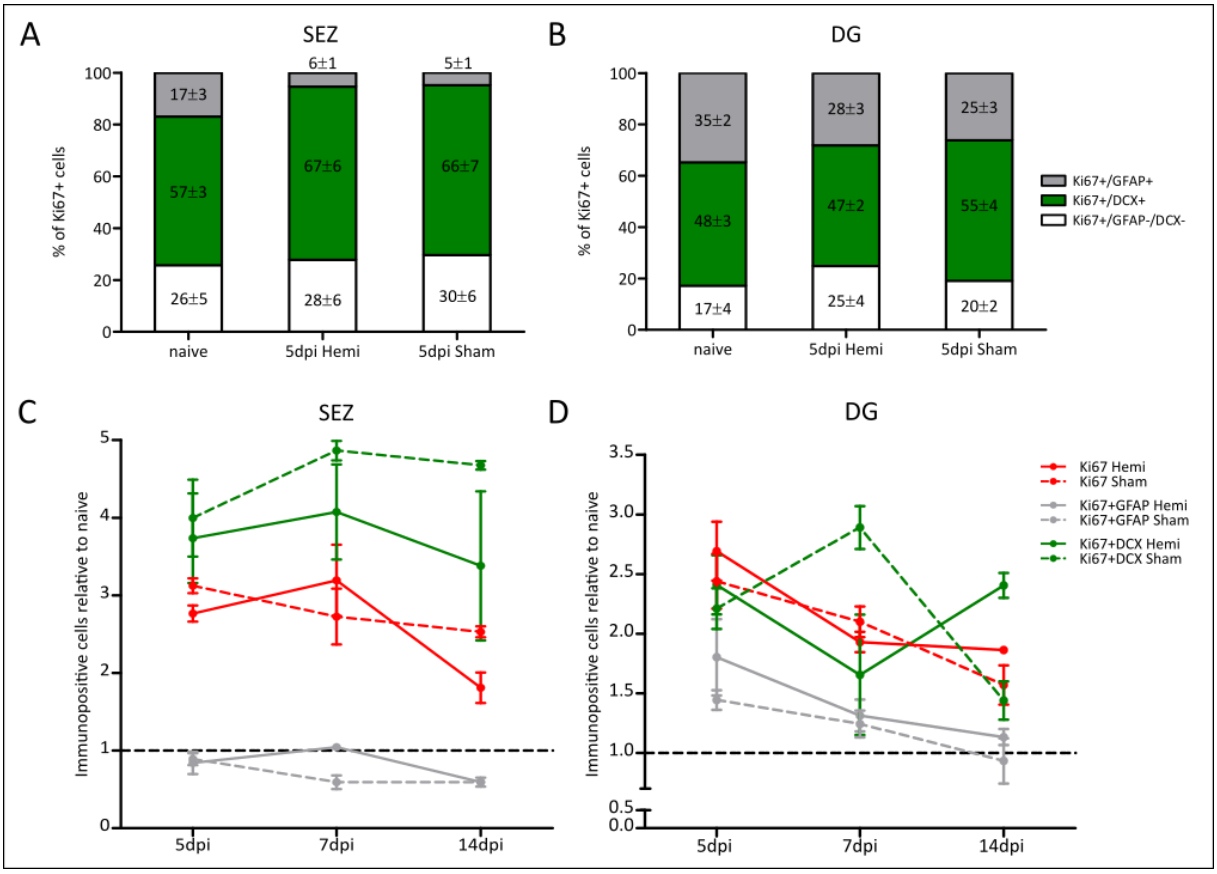

Figure 18. Comparison of changes in the distribution of Ki67+ cells in adult neural stem cell niches following SCI versus sham surgery and their temporal development. (A) Distribution of Ki67+ cell subtypes in the SEZ at 5dpi showed a decrease of the Ki67+/GFAP+ fraction in favor of the Ki67+/DCX+ fraction. Mean ± SEM. (B) Distribution of Ki67+ cell subtypes in the DG at 5dpi showed a mild decrease of the Ki67+/GFAP+ fraction in favor of the Ki67+/DCX+ fraction and an increase in the Ki67+/GFAP-/DCX- fraction in the Hemi group. Mean ± SEM. Temporal development of Ki67+ cell subtypes in the SEZ (C) and the DG (C) plotted as fold changes compared to naïve controls. Note that connection lines in between timepoints were added for purposes of visual demonstration and do not depict continuous quantification. 5dpi Hemi n=6 (n=3 for Ki67+/DCX+); 5dpi Sham n=3; 7dpi Hemi n=3; 7dpi Sham n=3; 14dpi Hemi n=3; 14dpi Sham n=3.

3.5 Injury Type-specific Effects on Self-renewal and Multipotency of Adult Neural Stem and Progenitor Cells *in vitro*

Given the increase in cell proliferation within both adult neural stem cell niches *in vivo* with a peak at 5dpi, we decided to investigate whether these changes are also associated with alterations in aNSC behavior *in vitro*. Therefore, we prepared neurosphere cultures dissected from the SEZ and DG according to established protocols (see 2.7.1) (Fig. 20A).

First, we focused on changes of the number of spheres over passaging. Passaging serves as a stepwise purification and isolates more and more self-renewing cells each passage. Indeed, samples from the SEZ showed significantly more spheres in the second and third passage compared to the first passage in all groups (naïve controls: first passage vs. second passage p=0.0288, first passage vs. third passage p=0.0018; 5dpi Hemi: first passage vs. second passage p=0.0013, first passage vs. third passage p=0.0055; 5dpi Sham: first passage vs. second passage p=0.0004 and first passage vs. third passage p=0.0014) (Fig. 19A). By contrast, cells dissected from the DG did not show significant increases in sphere formation over passaging with exception for the 5dpi Sham group, that generated significantly more spheres in the second passage (p=0.0019) (Fig. 19C)

When comparing the number of spheres from the SEZ between the three groups, a slight tendency towards higher numbers in the injury groups could be observed, however, without statistical significance (Fig. 19B). Plotted as fold changes relative to naïve controls, the data suggested that both SCI and sham surgery enhanced neurosphere formation especially in later passages (Fig. 20B).

By contrast, the number of secondary spheres in the DG showed a marked decline after SCI, although not statistically significant. While levels of tertiary spheres of the 5dpi Hemi group remained low, those cultured from animals 5 days after sham surgery showed an increase back to levels that were higher than in naïve animals (Fig. 19D). Plotted as fold changes relative to naïve controls, the data suggested that sham surgery generally increases neurosphere formation while SCI is rather associated with long term suppression (Fig. 20C).

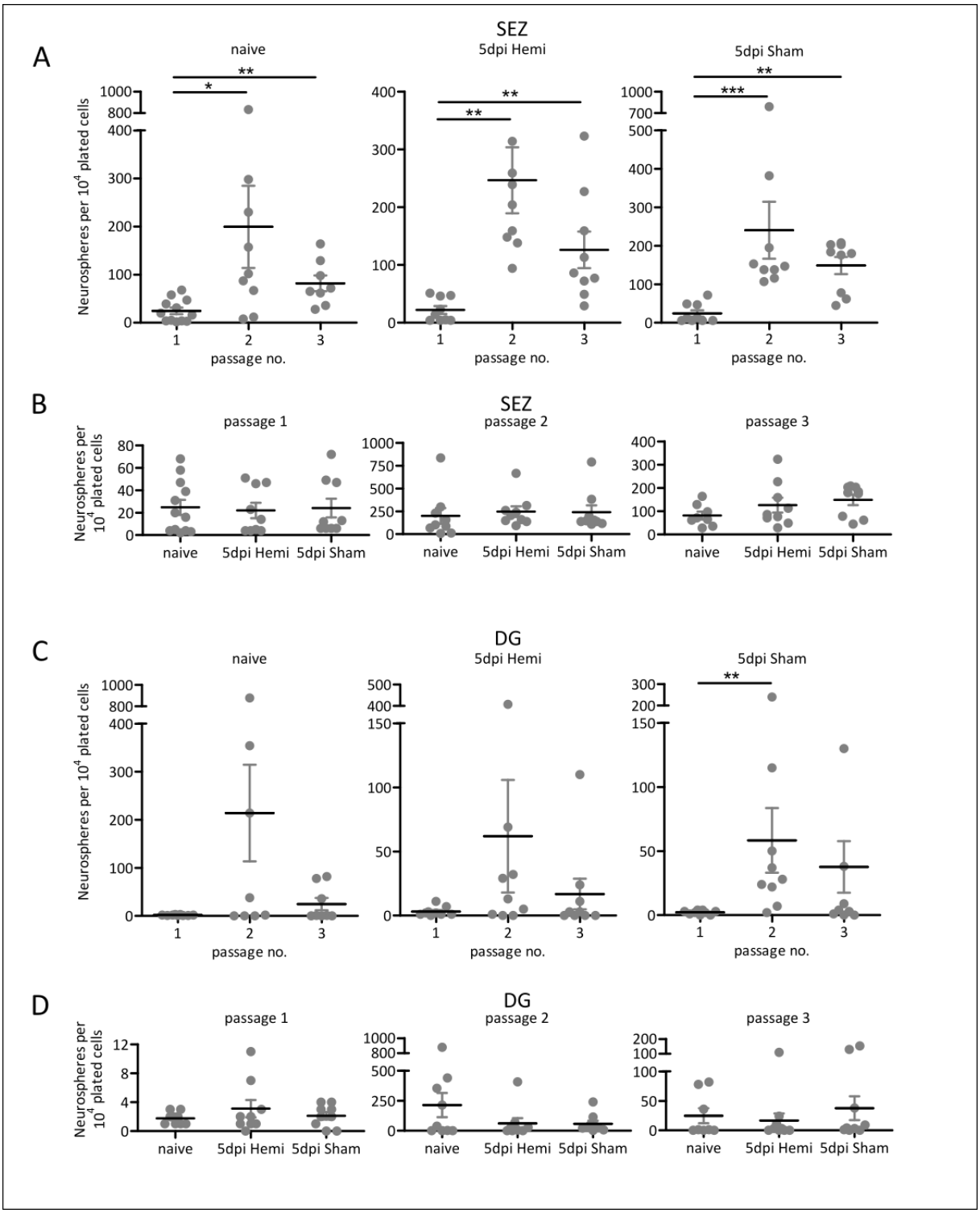

Figure 19. Quantitative analysis of SCI/sham surgery impact on neurosphere assay. (A) Quantification of SEZ-derived neurospheres (naïve: passage 1 vs. 2 *p=0.0288, passage 1 vs. 3 **p=0.0018; 5dpi Hemi: passage 1 vs. 2 **p=0.0013, passage 1 vs. 3 **p=0.0055; 5dpi Sham: passage 1 vs. 2 ***p=0.0004, passage 1 vs. 3 **p=0.0014). Student's t-test and Mann-Whitney-U test. Passage 1: naïve n=12; Hemi n=9; Sham n=9. Passage 2 all groups n=9. Passage 3: naïve n=8; Hemi n=9; Sham n=9. (B) Comparison of passaged SEZ-derived neurospheres between experimental groups. One-way ANOVA and Kruskal-Wallis test. (C) Quantification of DG-derived neurospheres (5dpi Sham: passage 1 vs. 2 **p=0.0019). Student's t-test and Mann-Whitney-U test. Passage 1: all groups n=9. Passage 2: all groups n=9. Passage: naïve n=8; Hemi n=9; Sham n=9. (D) Comparison of passaged DG-derived neurospheres between experimental groups. One-way ANOVA and Kruskal-Wallis test. It is to note that there are several confounding factors that could have had an impact on the results, such as experimenter- and motion-

induced aggregation, fusion, intrinsic locomotion, aggregation (Pastrana et al., 2011), which possibly explain occasional fluctuations.

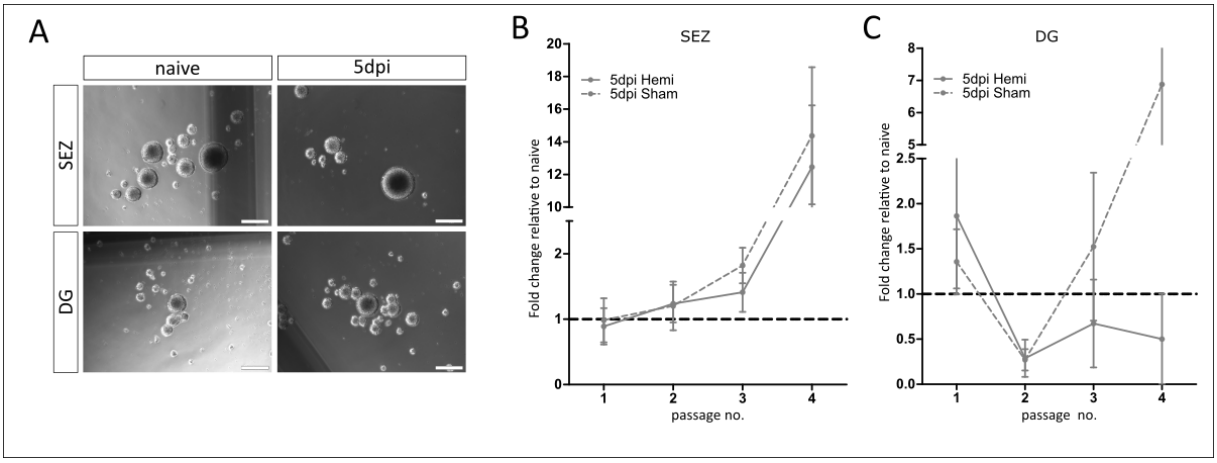

Figure 20. Quantitative analysis of SCI/sham surgery impact on neurosphere assay. (A) Exemplary neurospheres. Scale bar 200µm. Quantification of primary, secondary, tertiary and quaternary SEZ (B) and DG (C) neurospheres as fold changes compared to naïve controls. Note that connection lines in between timepoints were added for purposes of visual clarification and do not depict continuous quantification. N=4 for all groups in passage 4 due to loss of cultures.

To assess whether SCI affects the multipotency of neurospheres, a differentiation assay (Fig. 21A) as described in 2.9.3 was performed. Neurospheres from later passages were used that have fulfilled the criteria of self-renewal through multiple, e.g. three or more passages. Immunostaining using GFAP to identify astrocytes, O4 for oligodendrocytes and ß-III-Tubulin for immature neurons allowed for differentiation between three ranges of potency (Fig. 21D): unipotent (only GFAP+ cells), bipotent (GFAP+ and O4+ cells) and tripotent (GFAP+, O4+ and ßIII-Tubulin+ cells).

Neurospheres from the SEZ in all experimental groups were either bipotent or tripotent. Notably, the Hemi group generated a smaller fraction of tripotent spheres (76.92%) compared to naïve controls (90.91%). Complementary, we observed more bipotent spheres after SCI (23.08%) compared to naïve (9.09%). Sham surgery led to a very similar effect, but to a lesser extent (84.62% tripotent and 15.38% bipotent) (Fig. 21B).

In the DG, many of the neurospheres generated astrocytes and oligodendrocytes (46.15%), some were only unipotent (30.77%) and only few (23.08%) also gave rise to neurons. In animals that underwent hemisection, the proportions shifted drastically in favor of the unipotent fraction (77.78%) while bipotent spheres could not be found at all. The percentage

of tripotent spheres remained relatively stable (22.22%). Also here, the effect of sham surgery was very similar, but less pronounced (55,56% unipotent and 44,44% tripotent) (Fig. 21C).

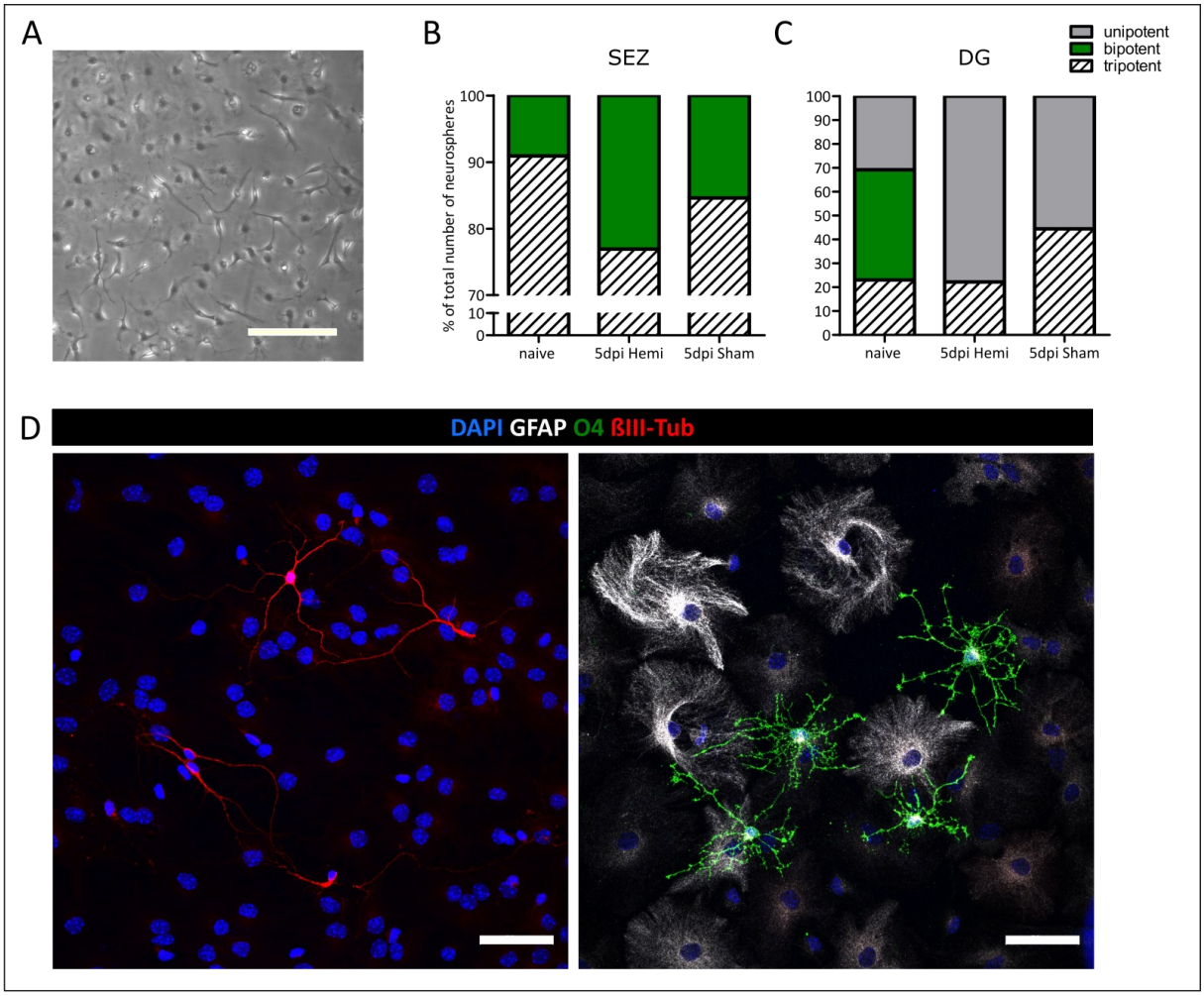

Figure 21. Neurosphere differentiation assay. (A) Exemplary neurosphere during differentiation at 6 days *in vitro*, light microscopy. Scale bar 200 µm. (B) Fractions of unipotent, bipotent and tripotent neurospheres from the SEZ. Naïve spheres are 90.91% tripotent and 9.09% bipotent. 5dpi Hemi show 76.92% tripotent and 23.08% bipotent spheres. 5dpi Sham spheres are 84.62% tripotent and 15.38% bipotent. Naïve n=11; Hemi n=13; Sham n=13. (C) Fractions of unipotent, bipotent and tripotent neurospheres from the DG. Naïve spheres were 23.08% tripotent, 46.15% bipotent and 30.77% unipotent. 5dpi Hemi showed 77.78% unipotent and 22.22% tripotent spheres. 5dpi Sham spheres were 55.56% unipotent and 44.44% tripotent. Naïve n=13; Hemi n=9; Sham n=9. (D) Exemplary confocal microscopy images from immunostainings of differentiated neurospheres using GFAP for astrocytes, O4 for oligodendrocytes and ßIII-Tubulin for neurons. Scale bars 50 µm.

3.6 Injury-Type Specific Changes in Expression Levels of Proliferation Regulators in Cerebral Cortex Astrocytes

To answer the question whether these changes are corroborated at the molecular level and if so, transregionally throughout the CNS, RT-qPCR was performed on MACS-isolated astrocytes of punched samples from the cerebral cortex. The messenger RNA (mRNA) level was analyzed for Cyclin D1 (CCND1), a regulator of the G1-S transition during cell cycle (Xiong et al., 1991), GLI family zinc finger 1 (GLI1), an effector and transcriptional activator of the Shh pathway that also controls cell proliferation (Rowitch et al., 1999), and signal transducer and activator of transcription 3 (STAT3), which amongst many other functions acts as a key regulator in the induction of reactive astrogliosis (Herrmann et al., 2008, Okada et al., 2006, O'Callaghan et al., 2014). Indeed, astrocytes isolated from animals that underwent hemisection 5 days ago showed higher levels expression of all three genes compared to naïve controls (Fig. 22). In the 5dpi sham surgery group, only GLI1 was upregulated, but to a lesser extent than in the Hemi group (Fig. 22B), while levels of CCND1 and STAT3 remained comparable or even slightly lower than those of the control group (Fig. 22A, C).

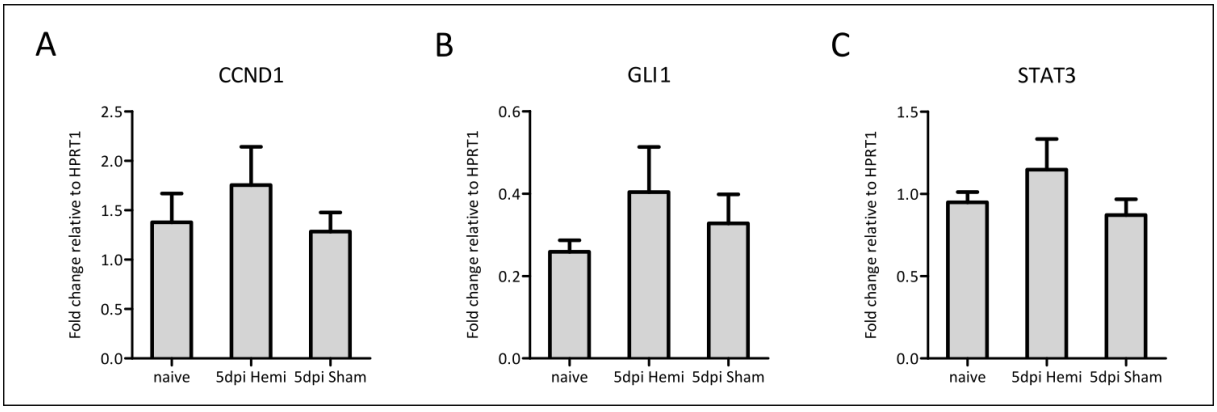

Figure 22. Level of mRNA expression in cortical astrocytes determined using RT-qPCR. Data shows an upregulation of proliferative (A, B) and reactive (C) genes of cortical astrocytes compared to baseline levels in naïve controls at 5dpi. Effects are more accentuated after hemisection compared to sham surgery. Naïve n=3; Hemi n=5; Sham n=4. Mean ± SEM. One-way ANOVA and Tukey's post-test.

3.7 Injury-Type Specific Changes in Proteome Signature of CSF

Proteome analysis was performed to identify similarities and differences in the CSF protein profiles following SCI and sham surgery. Although samples with macroscopically relevant blood contamination were excluded from analysis, hemoglobins (Hb) and albumin which indicate blood contamination (You et al., 2005) and are usually some of the most abundant proteins in CSF (Smith et al., 2014) could be found in all of our samples. However, there were no statistically significant differences in the expression levels of these proteins between the experimental groups (Fig. 23).

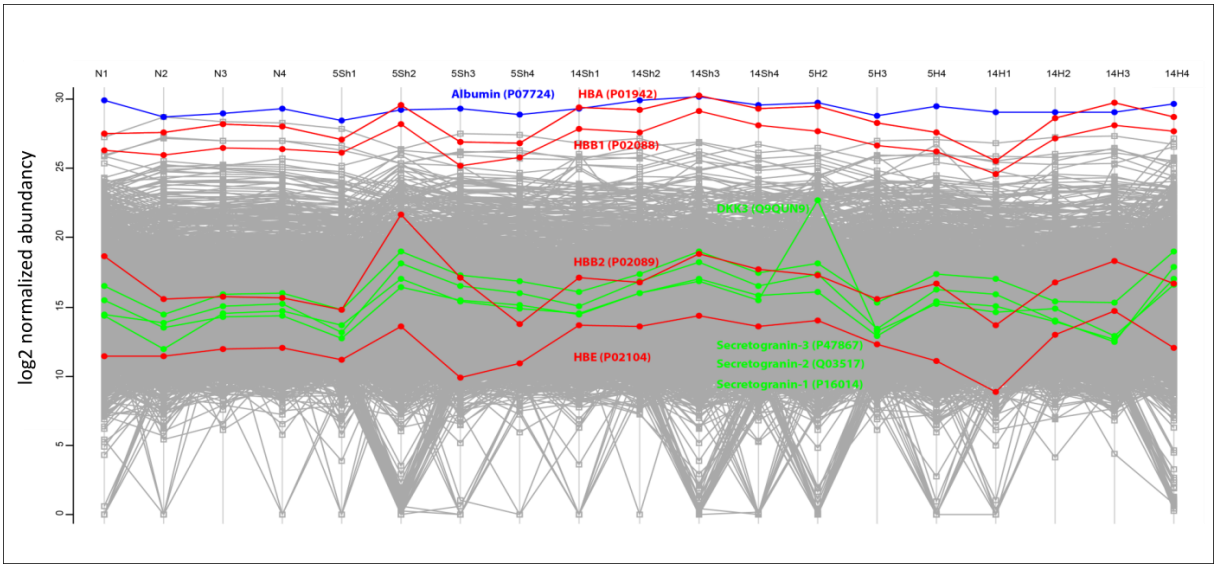

Figure 23. Normalized protein abundancy of murine CSF (Metzger, unpublished data). CSF proteome from naïve controls (N) and mice after spinal cord hemisection (H) or sham surgery (Sh) was analyzed using label-free mass spectrometry. Overview of normalized protein abundancy (shown in log2) reveals that the expression levels of highly abundant blood-related proteins, like albumin (P07724), hemoglobin A (HBA; P01942), and hemoglobin B1 (HBB1; P02088) were comparable between the different experimental groups.

A core proteome with 1486 proteins of ≥2 unique peptides (excluding albumin) was identified at a false discovery rate (FDR) of 0.01. Unbiased fingerprint analysis using the Proteomics DB database revealed close relationships to various CNS tissue proteome profiles (Fig. 24A). Given that changes of the abundancy of certain proteins rather than their presence in CSF would vary depending on the specific pathological context (Aasebo et al., 2014), there were marked differences in the CSF protein signature upon SCI as well as sham surgery (Fig. 24B). Indeed,

compared to CSF from naïve animals, the expression of 114 proteins was significantly downregulated and the expression of 89 proteins significantly upregulated 5 days following hemisection (Fig. 24C). At 5 days after sham surgery, 153 were down- and 121 upregulated, respectively (Fig. 24D).

Functional and enrichment analysis using the STRING database showed that the top ten enriched Reactome Pathways at 5dpi following SCI were platelet degranulation, platelet activation/signaling/aggregation, regulation of complement cascade, hemostasis, innate immune system, post-translational protein phosphorylation, regulation of Insulin-like Growth Factor (IGF) transport and uptake by IGF binding proteins (IGFBPs), retinoid metabolism and transport, plasma lipoprotein assembly, and initial triggering of complement (Fig. 24E). At 5dpi following sham surgery, they were platelet degranulation, platelet activation/signaling/aggregation, innate immune system, neutrotrophil degranulation, immune system, hemostasis, regulation of complement cascade, degradation of the extracellular matrix, extracellular matrix organization, and retinoid metabolism and transport,respectively (Fig. 24F).

Among the strongest upregulated proteins at 5dpi following both procedures, we identified Epidermal Growth Factor Receptor (Egfr), Aldehyde Dehydrogenase 1 Family Member A2 (Aldh1a2), and Dynein Cytoplasmic 1 Heavy Chain 1 (Dync1h1) (Fig. 24G). Interestingly, proteins such as Dickkopf 3 (Dkk3) and Galectin-3 binding protein (Lgals3bp) were also significantly upregulated at 14dpi following SCI or sham surgery (Fig. 24G). Complement C1q subcomponent A (C1qa) and B (C1qb), Complement C3 (C3), and Apolipoproteins C3 (Apoc3) were significantly higher expressed at 5 and 14 days after sham surgery and at 5dpi after SCI, whereas Apolipoprotein E (Apoe) was only significantly upregulated 14 days after sham surgery (Fig. 24H).

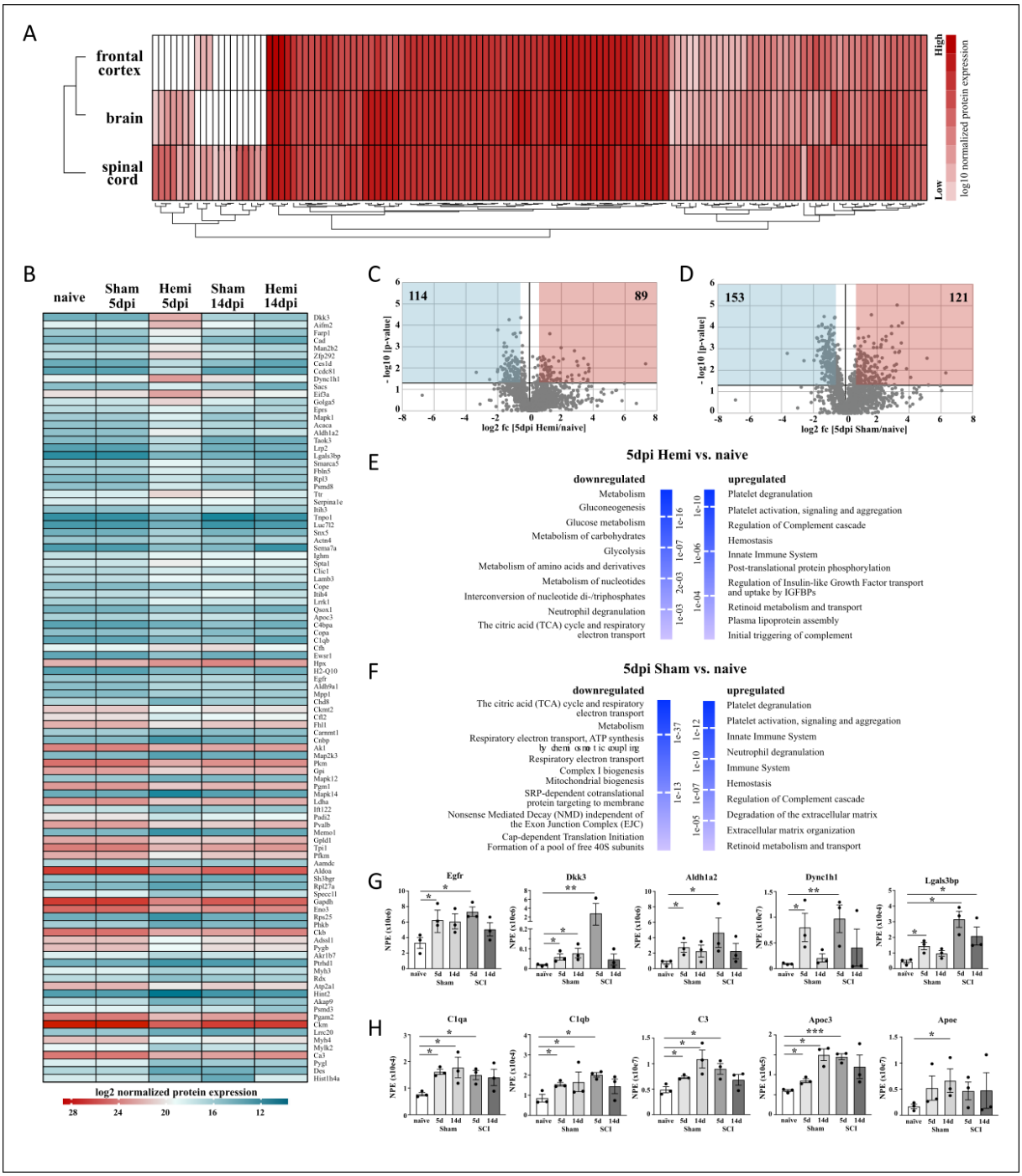

Figure 24. Quantitative proteomics and pathway enrichment analysis of murine CSF (Sirko, unpublished data). (A) Expression heatmap generated from ProteomicsDB (https://www.ProteomicsDB.org) shows that the list of proteins identified in our proteome CSF analysis closely aligns with existing 'pooled footprints' of neural tissue. (B) Heatmap based on log2 normalized protein expression demonstrates most significantly regulated proteins in CSF samples obtained at 5 days after SCI compared to naïve controls or sham injured animals. (C, D) Volcano plots showing mean log2 fold change (fc) with corresponding -log10 p-value comparing the expression of proteins in CSF from naïve controls to CSF obtained 5 days after SCI (Hemi) (C) or sham surgery (Sham) (D) (upregulated proteins are indicated red and downregulated proteins in blue, FDR <0.01 and ≥1.5 fold change). (E, F) Reactome Pathways associated with significantly upregulated or downregulated proteins in CSF at 5 days after SCI (Hemi) (E) or sham surgery (Sham) (F) compared with CSF from naïve controls. Top 10 pathways are ordered by ascending FDR in a colored scale to indicate the corrected probability obtained from over-representation analysis using STRING database (https://string-db.org/). (G, H) Column diagrams displaying changes in normalized expression of selected proteins between different experimental groups/time points of analysis (two-tailed t-test, statistical significance indicated as * p <0.05; ** p <0.01; *** p <0.001).

4. Discussion

4.1 Overview of Results

In this study, we investigated whether SCI had an effect on glial cells in adult neural stem cell niches of the murine brain. The aim was to describe potential cellular changes in a region-, time-, and injury type-specific manner while finding possible mechanisms that could explain those. Our analyses showed that both invasive and non-invasive SCI led to an upregulation of Ki67-labelled cell proliferation *in vivo* within both neural stem cell niches of the mouse brain during the acute to subacute post-injury phase. The maximum effect could be found 5 days after injury, with an overall trend towards normal levels at later timepoints. An expansion of the neuroblast cell pool could be detected, while also aNSCs in the DG but not in the SEZ were involved, a key difference between the SEZ and the DG.

These findings led to further *in vitro* analyses, which showed that the SEZ in both intervention groups harbors more sphere-forming cells displaying a more pronounced self-renewal ability compared to naïve controls. In contrast, SCI but not sham surgery strongly limited self-renewal capacity of neurosphere-generating cells residing in the DG. Moreover, both invasive and non-invasive SCI were found to shift differentiation towards a more glial lineage, creating fewer neurons *in vitro*.

Notably, molecular changes could be observed even outside of adult neural stem cell niches. As shown by RT-qPCR of mRNA isolated from cerebral cortex GM astrocytes, SCI induced a transcriptional upregulation of proteins required for maintenance of proliferation and stem cell-like characteristics, as found in reactive astrocytes. Future investigations are still required to unravel the exact underlying processes, but these results already allow some speculations on possible mechanisms, which will be discussed in the following sections.

In summary, this study showed that both penetrating SCI and non-penetrating spinal injury leads to changes in the proliferative activity of cells within adult neural stem cell niches *in vivo* and *in vitro*, and that these changes occur in a time-specific manner but vary between the neurogenic niches.

4.2 Changes of Glial Proliferative Activity in the Context of Different Types of CNS Injury

The question of how glial cells react to CNS injury has markedly gained interest after the demonstration of their capability to actively proliferate was demonstrated in the adult CNS as a response (Bareyre, 2008, Sirko et al., 2013, Gao and Chen, 2013). A subtype of reactive glia at the lesion site can further exhibit stem cell properties (Sirko et al., 2013, Gotz et al., 2015). Nowadays, a variety of different injury models are giving us insight into possible underlying mechanisms.

After SCI, an upregulation of proliferation could be noted in many astrocytes in close proximity to the lesion with a peak reaction around 3-5dpi and near-normal levels around 14dpi, a temporal development that is very similar to our study. Interestingly, these proliferating astrocytes also showed a change in morphology, presenting with an elongated cell body similar to radial glia or neural progenitor cells, and exhibited several neural stem cell markers including Sox2 and Nestin (Wanner et al., 2013).

Stab wound injury to the cerebral cortex induced under experimental conditions is a well-established animal model for traumatic brain injury that initiates a heterogenous reaction of glial cells. In astrocytes, this includes complex phenotypical and functional changes (Escartin et al., 2021, Bardehle et al., 2013), as well as the acquisition of stem cell properties along with the ability to undergo cell proliferation (Buffo et al., 2008, Sirko et al., 2009, Lange Canhos et al., 2021). When placed under proliferative conditions *in vitro*, these cells are not only able to form self-renewing neurospheres but can additionally acquire multipotency (Sirko et al., 2009, Sirko et al., 2013). Moreover, reactive astrocytes in invasively injured brain parenchyma upregulate their expression of stem cell markers and strikingly, this is paralleled by an increase in generation of neuroblasts at the injury site (Sirko et al., 2009).

In models of stroke, a significant expansion of neurosphere-forming cells isolated from the SEZ was observed (Sirko et al., 2013). An increase in cell proliferation in the SEZ with increased numbers of neural stem cells was described upon transient occlusion of brain-supplying arteries, which was even stronger in mice that overexpress Endothelin-1 (ET-1) (Cheng et al., 2019), a vasoconstricting peptide derived from endothelial cells (Yanagisawa et al., 1988). Higher levels of ET-1-expression were further associated with the differentiation tendency

into astrocytes at the cost of neurons in the SEZ. Interestingly, mice overexpressing ET-1 also showed more severe functional deficits as per neurological score assessment (Cheng et al., 2019). It should further be noted that in contrast to acute CNS injuries, neurodegenerative diseases such as Alzheimer's disease or induced neuronal death are associated with lower rates of cell proliferation and absence of multipotency in cell culture experiments (Sirko et al., 2013).

4.3 Injury-type Specific Changes of Proliferative Activity within Adult Neural Stem Cell Niches after Invasive and Non-Invasive SCI

In this study, we showed that SCI significantly increased the pool of Ki67-labelled cells in both adult neural stem cell niches of the mouse brain. Thereby, DCX+ neuroblasts in both niches were found to make up the majority of proliferating cells. The overall peak of reaction was found during the acute post-injury phase at 5dpi with a trend towards normalization at 14dpi. This finding stands in contrast to a previously reported increase of of 5-bromo-2'-deoxyuridine (BrdU) incorporation observed in the DG even at 14dpi after complete spinal cord transection (Dehler et al., 2018). BrdU is a thymidine analogue that incorporates into DNA and is commonly used to assess proliferative activity in the CNS (Miller and Nowakowski, 1988). However, recent studies have shown that BrdU incorporation in cells within the brain parenchyma occurs not only during the S-phase of the cell cycle in actively proliferating cells but also in dying cells (Kuan et al., 2004). It is thus not possible to distinguish how many BrdU positive cells are indeed mitotically active at the given timepoint of investigation (for review see Breunig et al., 2007). Furthermore, taken under consideration that injury-associated effects on astroglia strongly correlate with the severity of tissue damage (Escartin et al., 2021), it is not surprising that a complete spinal transection has a more pronounced and long-lasting effect on phenotypical changes in residing astrocytes than after spinal cord hemisection.

The results of this study further suggest that the proliferative response of GFAP+ aNSCs to SCI is different in the two neurogenic niches. In the SEZ, no remarkable increase of proliferation could be found at all timepoints of analysis. Moreover, at 14dpi, the number of Ki67+ aNSCs in the SEZ was relatively decreased compared to the physiological state. This corresponds well with previously published data that showed a decrease in DCX+ neuroblasts migrating from the SEZ to the olfactory bulb 15 days after cervical spinal cord hemisection (Felix et al., 2012).

The authors found this as a consequence of decreased cell proliferation and not an induction of cell death within the SEZ. Notably, even at 90dpi, the degree of neurogenic activity did not return to physiological levels. Our results further showed that the DG contained significantly more Ki67+ proliferating aNSCs following SCI at 5dpi than in naïve control animals. Interestingly, the proliferative activity at 14dpi within this neurogenic niche was comparable to the homeostatic baseline. By contrast, data from other groups using BrdU-labelling showed higher numbers of proliferating cells even at 14 days after hemisection as well as more BrdU+/DCX+ neuroblasts (Dehler et al., 2018). Again, given the differences between BrdU and Ki67-based labelling, this does not necessarily contradict our findings. These changes might be related to elevated levels of pleotrophic factors, such as brain-derived neurotrophic factor (BDNF), which reaches a peak during the acute post-injury phase with a rapid decline afterwards (Felix et al., 2012), or Sonic Hedgehog (Shh) (Sirko et al., 2013). This further supports the observations of this study showing a decrease of proliferative activity in the DG after 5dpi, which would most likely normalize at later timepoints, as it has been previously shown at 42 days after thoracic spinal contusion injury in rats (Franz et al., 2014). Taken together, our findings suggest that there are differences in the proliferative response to SCI between the two adult neural stem cell niches.

Surprisingly and in contrast to previous findings (Dehler et al., 2018), immunostainings of brain sections from sham-injured animals also showed obvious changes compared to naïve controls. In fact, the pool of proliferating cells and, in particular, proliferating DCX+ neuroblasts, was clearly increased at 5dpi in both niches. When comparing the number of proliferating cells between the hemisection and the sham group, no significant differences were found with the exception of GFAP+ cells in the DG. Interestingly, there were significantly more proliferating aNSCs 5 days after sham surgery than after hemisection. This may indicate that the invasiveness of injuries is associated with a long-term suppression of neurogenesis in the DG, as previously shown by lower numbers of BrdU+ proliferating cells in the DG of rats 14 days after cervical SCI (Felix et al., 2012), possibly reflecting an exhaustion of the progenitor cell pool after initial upregulation of proliferation within this neurogenic niche.

Of particular interest are also the results of our *in vitro* analyses of self-renewing capacity and differentiation potential of neurosphere-forming cells obtained from both neurogenic niches after SCI. In cultures derived from the SEZ, both experimental groups tended to generate more

spheres compared to naïve controls after the first passage, with numbers going up every passage. Interestingly, when adding 0,5% plasma from mice that underwent traumatic brain injury (TBI) to SEZ neurosphere cultures, a significant increase in the number of generated spheres was noted (Falnikar et al., 2018). In contrast, DG spheres from the Sham group showed an overall increase in the number of spheres, while the number of spheres in the Hemi group underwent a suppression after the first passage. This again is consistent with the decrease of hippocampal neurogenesis at subacute and chronic timepoints after cervical hemisection *in vivo*, as mentioned above (Felix et al., 2012). When examining the differentiation potential of neurosphere-forming cells after the third and fourth passage, i.e. those that have shown their ability of long-term self-renewal, SCI was found to limit the neurogenic in favor of a more gliogenic capacity. This could be due to the activation of molecular pathways that promote neuronal progenitor cell proliferation and differentiation into astrocytes that are also activated after stroke (Cheng et al., 2019). Strikingly, sham surgery led to almost the same effects but at a lesser extent.

Taken together, these findings suggest that both invasive and non-invasive damage to the spinal cord can lead to region-specific changes in the proliferative activity within adult neural stem cell niches *in vivo*, which are reflected by alterations of self-renewing capacity and multipotency of neurosphere-forming cells dissected from those regions *in vitro*.

4.4 Molecular Mechanisms Underlying Glial Cell Reaction to Injury

Interestingly, the reaction of glial cells to SCI was not only limited to the neurogenic niches. Indeed, our lab has shown an activation of astrocytes in different regions of the cerebral cortex. Thereby, some of the activated astrocytes in the cerebral GM acquired a proliferative phenotype during both acute and chronic stages following SCI (Kraska et al., unpublished data). Furthermore, astrocytes isolated from the cerebral cortex of animals 5 days after undergoing SCI revealed an upregulation of proliferative (CCND1, GLI1, STAT3) genes compared to naïve animals. This indicates that the upregulation of these transcriptional factors could be induced even by distal CNS lesions, such as mid-thoracic SCIs.

STAT3 is part of the Janus kinase (JAK)/STAT signaling pathway that conducts information for a variety of cytokines. These include but are not limited to the interferone (IFN), interleukins

(IL), and pro-hematopoietic factors (Kisseleva et al., 2002, Schindler and Strehlow, 2000). Also non-cytokine receptors such as G-protein-coupled receptors, growth factors, including EGF and PDGF (platelet derived growth factor), free radicals, and neurotransmitters are able to activate this signaling pathway (Schindler and Strehlow, 2000, Dziennis and Alkayed, 2008).

In the injured CNS, STAT3 activation plays a major role in the induction of reactive gliosis and glial scar formation (Herrmann et al., 2008, O'Callaghan et al., 2014, Okada et al., 2006, Sofroniew, 2009, Wanner et al., 2013). Glial scar formation then likely serves as a shield that regulates the spreading of immune cells into vital areas, limiting the lesion size and preserving residual functionality (Norenberg et al., 2004, Cregg et al., 2014, Voskuhl et al., 2009, Wanner et al., 2013). Interestingly, STAT3 knockout likely causes a dysregulated pattern of astrocyte activation and improperly aligned gliosis (Herrmann et al., 2008, Wanner et al., 2013). This can lead to impaired migration of astrocytes to the injury site as well as failure to form functional glial scar borders, resulting in widespread inflammation with increased neuronal losses and demyelination, as shown in STAT3 knockout mice (Okada et al., 2006, Wanner et al., 2013). Lately, an activation of the JAK/STAT pathway was also shown in models of ischemic stroke (Wu et al., 2018) and neurodegenerative disease including Alzheimer's (Reichenbach et al., 2019) and Huntington's disease (Ben Haim et al., 2015).

Notably, STAT3 also regulates cell proliferation by targeting cyclin D1 (Leslie et al., 2006). As a promotor of the the G1-S transition during cell cycle (Xiong et al., 1991), cyclin D1 induces cell proliferation via one of the most important cascades, the Cyclin-Retinoblastoma protein (Rb) axis (Kato et al., 1993) (Fig. 25). STAT3-regulated proliferation however is not limited to the STAT3-cyclin D1 axis. In models of stroke, the Notch1-STAT3-Endothelin receptor type B (ETBR) cascade was found involved in astrocyte proliferation (LeComte et al., 2015). Also ET-1 acts as a possible link. Mice with genetically induced overexpression of ET-1 showed increased levels of STAT3 expression, increased overall cell proliferation in the SEZ, including higher number of aNSCs, and decreased number of neuronal descendants in favor of astrocytes in the SEZ upon induced stroke (Cheng et al., 2019). Strikingly, when pretreating these animals with a JAK/STAT inhibitor, a significant reduction of infarct size and improved neurological outcomes were observed.

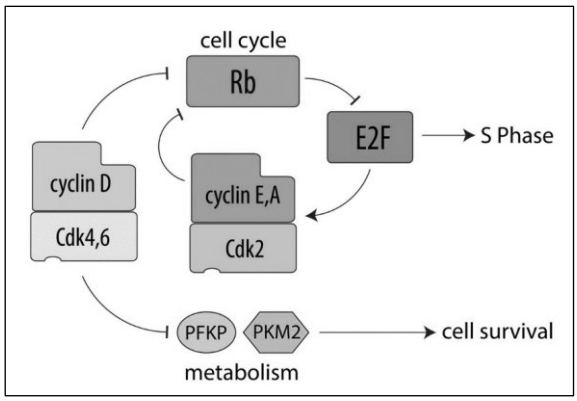

Figure 25. The cyclin-Rb cascade. Expression of cyclin D1 leads to activation of cyclin-dependent kinases (CDK). Cyclin-CDK complexes lead to phosphorylation of Rb. Phosphorylated Rb in turn dissociates from transcription factor E2F, which then initiate transcription of downstream genes required for the progression of the cell cycle into the S phase (Weinberg, 1995). Figure modified from Topacio et al. 2018.

As described above, a small proportion of injury-induced reactive astrocytes can acquire stem cell properties (Buffo et al., 2008, Sirko et al., 2009, Sirko et al., 2013, Gotz et al., 2015, Sirko et al., 2015). Thereby, protein expression levels of Shh correlate with the proliferative response of astrocytes after stab wound and ischemic brain injury (Sirko et al., 2013). After administration of Shh Signaling Agonist (SAG), an activator of the Shh pathway, an increase in proliferative activity as found in the post stab-wound brain could be provoked both *in vivo* and *in vitro*. Notably, this mechanism seems to be influenced by different factors such as aging or neurodegeneration (Sirko et al., 2013, Heimann et al., 2017). In older mice, the extent of reactive gliosis and cell proliferation after stab wound injury was found significantly less pronounced compared to young animals, and even the administration of a Shh agonist could not boost the effect (Heimann et al., 2017). Similarly, in models of Alzheimer's disease, Shh levels showed no increase compared to control animals (Sirko et al., 2013).

Interestingly, the Shh pathway (Fig. 26) also regulates cell proliferation by activation of transcriptional targets via members of the *Gli* family (Ingham, 1998, Rowitch et al., 1999). *Gli* proteins are in turn involved in the activation of proliferative D-type cyclins (Cayuso et al., 2006, Lobjois et al., 2004). This coherence was shown using murine immature cerebellar granule cell cultures which, after exposure to Shh, not only showed increased cyclin D1 levels, but were actively entering the S phase at a higher proportion (Kenney and Rowitch, 2000). Therefore, as GLI1 expression was upregulated in cortical astrocytes 5 days after SCI, we hypothesize that Shh is most likely involved in injury-induced activation of proliferation also within neural stem cell niches, possibly via the cyclin-Rb pathway.

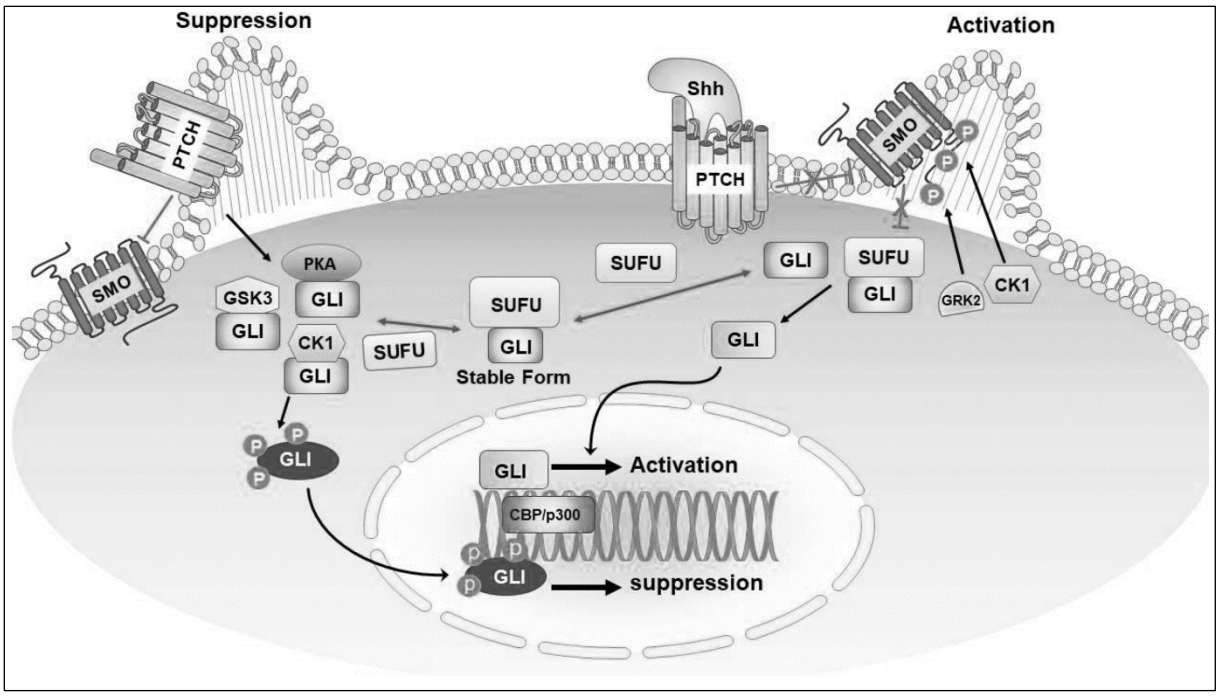

Figure 26. The Shh pathway. In the absence of Shh, Patched (PTCH) inhibits Smoothened (SMO). Shh acts on Ptch, allowing Smo to accumulate. Smo in turn activates the Suppressor of Fused (SUFU)-GLI complex which results in the activation of downstream Gli transcription factors. Gli then enters the nucleus and induces the expression of target genes by binding to promoter areas. Figure modified from Chen et al. 2018.

In line with this, our results suggest that SCI can lead to remote reactive gliosis in the brain by upregulating STAT3 expression, even without anatomical proximity. This can also induce upregulation of Shh expression in reactive astrocytes which in turn become proliferative within adult neural stem cell niches, probably via GLI1 and the Cyclin-Rb axis. Further, STAT3 possibly shifts the differentiation potency of neural progenitors derived from the SEZ and DG towards a more glial lineage.

4.5 Neuroinflammation as a Consequence of Injury with and without Neural Tissue Damage

Generally, CNS injury leads to tissue destruction and necrosis which in turn activates the immune system, resulting in a (non-septic or in open CNS trauma septic) neuroinflammation (Lucas et al., 2006). The involvement of an immune response in the activation of glial cells and manifestation of their proliferative state has already been described in different injury models. It is known that via C-C chemokine receptors (CCR) monocytes from peripheral blood can enter

the injury site with their C-C motif ligands (CCL) (Chu et al., 2014). Interestingly, CCR2 knockout mice presented with increased cell proliferation during the acute post-injury phase, but reduced glial scarring in the long-term, resulting in a more favorable environment for neuronal regeneration (Frik et al., 2018). Further, a genome-wide analysis of reactive astrocytes after stab wound injury at 5dpi revealed that two carbohydrate-binding lectins – Galectins 1 (Gal-1) and 3 (Gal-3) are correlated with increased cell proliferation and induction of stem cell properties in glia (Sirko et al., 2015). Notably, Galectin-3 was also found to be crucial in diffuse brain inflammation in other neurological diseases such as Huntington's disease (Siew et al., 2019) and Alzheimer's disease (Tan et al., 2021).

The neuroinflammatory response following SCI can spread widely beyond the boundary of the localized lesion, even reaching distant brain areas (Dehler et al., 2018, Faden et al., 2016, Wu et al., 2014a, Wu et al., 2014b). This can lead to reactive gliosis and, as this study has shown, the upregulation of STAT3 expression in resident astrocytes, which may contribute to the reduction proliferative activity in a subset of these cells. In a genome and proteome wide interaction analysis following SCI, tumor necrosis factor alpha (TNF-α) and IL-6, two major inflammatory cytokines, were identified as major actors in the posttraumatic inflammatory response (Zhu et al., 2019) (Tab. 2). Here, the JAK/STAT pathway may serve as a regulator of the inflammatory cascade, as pretreatment with a JAK/STAT inhibitor prior to SCI was shown to lead to higher IL-6 levels and worse motor function (Yamauchi et al., 2006). Further, increased levels of TNF-α were found in the SEZ and SGZ shortly after SCI (Felix et al., 2012). Interferon signaling could also play a role. Single cell RNA-sequencing of aNSCs isolated from the SEZ 2 days after induced global brain ischemia revealed an overexpression of IFN-γ targets (Llorens-Bobadilla et al., 2015), which include STAT3 and cluster of differentiation 95 (CD95), also known as Fas receptor (FasR) (Chow et al., 2000). Interestingly, the results of these studies correspond well with the finding that IFN-receptor and CD95-deficient mice did not show an increase of neurogenesis or cell proliferation in general within the DG after SCI (Dehler et al., 2018). Thus, the activation of resident microglia also plays a major role (Faden et al., 2016, Gregoire et al., 2015). The exact transmission pathways are not yet fully understood, but the presence of fenestrated capillaries could be responsible (Falnikar et al., 2018).

1	TNF	Tumor necrosis factor
2	FOS	FBJ murine osteosarcoma viral oncogene homolog
3	IL-6	Interleukin 6
4	PTGS2	Prostaglandin-endoperoxide synthase 2
5	TGFB1	Transforming growth factor beta
6	ICAM 1	Intercellular adhesion molecule 1
7	MMP9	Matrix metallopeptidase 9
8	STAT1	Signal transducer and activator of transcription 1
9	AGT	Angiotensinogen
10	ET1	Endothelin 1

Table 2. Top ten SCI-associated proteins. Table modified from Zhu et al. 2018.

At the same time, our findings in the Sham group, in which the integrity of the spinal cord remained untouched, have shown that no actual CNS lesion is necessary for those changes. This suggests mechanisms that are not locally limited to the affected area or to CNS parenchyma, making a systemic reaction the most likely explanation. Inflammation from lipopolysaccharide (LPS) injection has been shown to alter both *in vivo* and *in vitro* neural precursor cell proliferation in the hippocampus (Melo-Salas et al., 2018). Also in cortical astrocytes, a decrease in process branching and volume as well as impaired Calcium signaling was noted upon LPS-induced neuroinflammation (Diaz-Castro et al., 2021). Interestingly, single-cell RNA sequencing revealed that several of the altered genes were also associated with Alzheimer's disease in humans (Diaz-Castro et al., 2021).

We found two studies that support the idea of systemic inflammation caused by trauma unrelated to any CNS lesion that can lead to CNS-related issues. Dong et al. found increased levels of proinflammatory IL-6 in the hippocampus of adult mice that have undergone abdominal incision and closing. They also showed that by pretreatment of the animals with an IL-6-antibody before surgery, cognitive impairments could be ameliorated. Notably, no deficits were found in mice in which the IL-6-gene was knocked out (Dong et al., 2016). An increased expression of GFAP, CCL2, and CCR2 within the hippocampus as well as the activation of microglia was also observed in rats following open tibial fracture surgery (Xu et al., 2017). These animals further developed impairments of the spatial working memory and learning after surgery that could be averted by preoperative treatment with a CCR2 antagonist, also mirrored by a reduction of immunoreactive changes in histological analysis. In humans, these findings possibly correspond with postoperative cognitive impairment that unrelated to delirium that was particularly observed in elderly patients (Liu, 2000).

4.6 Potential Role of Changes in the Proteomic CSF Profile Following SCI in the Regulation of Cell Reactivity in Distinct Brain Regions

Our findings suggest that traumatic events in the periphery of or even outside the CNS can cause a systemic reaction with diffuse reactive changes throughout the brain, giving rise to the question of how these reactions are transmitted. The CNS is a so-called immune privileged organ, as the blood-brain barrier (BBB) actively regulates molecular exchange and restricts the invasion of peripheral immune cells (Pachter et al., 2003). Therefore, BBB disruption as a consequence of traumatic SCI is associated with the infiltration of immune cells into neural tissue (Krishnamurthy and Laskowitz, 2016). However, in the case of non-invasive surgery without BBB disruption, as for instance following sham surgery in this study, there are likely other mechanisms that contribute to the development of this reactive response. The circulating CSF is one candidate that could induce a blood-borne immune response within the CNS as CSF is 80% plasma-derived and 20% brain-derived (Reiber, 2001). CSF plays a key role in various processes (for review see Zappaterra and Lehtinen, 2012) and Smith et al. have identified 566 unique proteins in the CSF of healthy mice (Smith et al., 2014). The scope of mechanisms that are transmitted via CSF still remains to be unraveled, however, current data already support the idea that CSF acts as a major regulator of glial physiology and pathophysiology.

In the healthy adult mouse brain, it is known that CSF is also involved as a regulator of neurogenesis. aNSCs in the SEZ have direct contact to multiple CSF signaling molecules through their primary processes reaching into the ventricle (Doetsch et al., 1999a, Pastrana et al., 2011). Further, CSF gradients were shown to induce the migration of SEZ-generated neuroblasts to the OB via the RMS (Sawamoto et al., 2006). The identification of responsible molecules still poses challenges, but proteome analysis of avian CSF identified at least 72 proteins that are highly concentrated and related to neurogenic processes (Voukali et al., 2021). More specifically, some proteins, including EGF, Vascular endothelial growth factor (VEGF), Aldh1a2, Dync1h1, Dkk3, Lgals3bp, are involved in regulatory processes of neurogenesis in both the developing and adult mammalian brain (Doetsch et al., 2002, Pelegri et al., 2019, Marei et al., 2012, Laquerriere et al., 2017, Zhu et al., 2014, Fukusumi et al., 2015, Kyrousi et al., 2021, Lugert et al., 2017, Codega et al., 2014).

To date, we know that several neurological conditions are associated with altered CSF characteristics (von Neuhoff et al., 2012, Haines et al., 2015, Burman and Svenningsson, 2016, Marques et al., 2019, Bader et al., 2020, Yang et al., 2021). For instance, CSF likely plays an important role in reorganization processes after brain injury (Walter et al., 1999). When compared to healthy individuals, more than a hundred proteins related to neuroinflammation were found altered in CSF from patients following TBI (Lindblad et al., 2021). Strikingly, BBB disruption in invasive injury showed its unique proteome signature and was associated with worse functional outcome (Lindblad et al., 2021).

Of the 1486 CSF proteins identified in our study, there were marked changes after both SCI and sham surgery compared to naïve controls. Functional analysis revealed that most of the top ten upregulated Reactome Pathways in both experimental groups belonged to immune response, hemostasis, and platelet activation. In agreement, normalized protein expression showed significantly increased levels for members of the complement cascade as well as apolipoproteins, two important groups of molecules transmitting inflammatory signals (Berbee et al., 2005, Markiewski and Lambris, 2007). However, our proteome analysis not only revealed an upregulation of inflammatory proteins. Strikingly, also signaling proteins that are involved in the regulation of neurogenesis and cell proliferation were affected in both experimental groups: for instance, the expression of NSC markers such as Dkk3 (Codega et al., 2014) and regulators of aNSC proliferative activity such as Egfr (Aguirre et al., 2010) were increased after both lesion types. How and to what extent this contributes to reorganization after SCI remains unknown, but after experimental injection of growth factors into the lateral ventricle of mice that suffered TBI, an increase in proliferation within both neurogenic niches was associated with an improvement in functional outcome (Sun et al., 2009). A similar effect could also be demonstrated in models of stroke (Wada et al., 2003, Watanabe et al., 2004). Further, retinoid metabolism was upregulated 5dpi following both hemisection and sham surgery and is known to be crucial for neuronal differentiation in both the embryonic and adult brain (Park et al., 2016, Jacobs et al., 2006). Other proteins with increased expression are essential in neural tube development (Aldh1a2) (Marei et al., 2012) and neuronal migration and positioning (Dync1h1, Lgals3bp) (Kyrousi et al., 2021, Shu et al., 2004).

Of particular interest is the significant enrichment of Galectin-3 binding protein (Lgals3bp), the lectin galactoside-binding soluble 3 binding protein also known as Mac-2 binding protein

(Mac-2BP) or tumor-associated antigen 90K (90K) (Loimaranta V et sl. 2018) that is excreted in extracellular vesicles (Costa et al., 2018, Rana et al., 2021) or nanoparticles (Zhang et al., 2018) and can be found in CSF (Khoonsari et al., 2019, Lecube et al., 2012). Kyrousi et al. found that Lgals3bp is essentially involved in human cortical development and is likely responsible for proper positioning of neurons. As its expression is associated with a variety of neural stem cell markers, it is possible that Lgals3bp also acts as a direct regulator of aNSCs. Overexpression in human cerebral organoids resulted in changes suggestive of premature neuronal differentiation (Kyrousi et al., 2021). Lgals3bp is also linked to various neurological diseases. Patients with mild cognitive impairment showed decreased serum levels (Ijsselstijn et al., 2013) and high serum levels were found in glioma patients (Rana et al., 2021). In brain tissue from deceased Alzheimer's disease patients, an increased expression of Lgals3bp was described (Garranzo-Asensio et al., 2018). Interestingly, elevated CSF levels were found in patients with fibromyalgia (Khoonsari et al., 2019) and high age (Costa et al., 2020). Further, CSF concentration of its binding partner, Galectin-3 (Lgals3), is also increased in some patients with multiple sclerosis (Haines et al., 2015).

However, the question how exactly altered CSF levels of Lgals3bp at 5dpi and 14 dpi after hemisection and to a lesser extent, even 5 days after sham surgery, play a role in pathophysiological processes following SCI demands further research. Assumably, Lgals3bp serves as a link between adult neurogenesis and inflammation as only recently, researchers described an opposing balance between inflammatory and neurogenic potential of aNSCs that is kept by a regulator suppressing several myeloid inflammatory genes including LGALS3 (Shariq et al., 2021). Thereby, an increase in levels of Lgals3 and Lgals3bp were associated with significant reduction of adult neurogenesis both *in vivo* and *in vitro*. In agreement, Lgals3 was also found in proliferating astrocytes of the cortical GM following invasive TBI (Sirko et al., 2015).

Taken together, these findings demonstrate that both SCI and spinal trauma can alter the CSF proteome and open up the possibility that CSF might serve as a signal transmitter of the changes that we observed in distant regions of the brain.

4.7 The Role of Adult Neurogenesis in Brain Physiology and Pathophysiology

In the mammalian brain, proper adult neurogenesis is essential for memory formation, cognitive flexibility, avoidance of memory interference, context-dependent memory, and pattern separation (Goncalves et al., 2016). Abnormal neurogenesis was found in animal models of a broad spectrum of neurological diseases, including Alzheimer's disease, Parkinson's disease, and Huntington's disease (Winner and Winkler, 2015). Psychiatric disorders such as schizophrenia (Duan et al., 2007), depression, and anxiety (for review see Miller and Hen, 2015) are also common. Interestingly, overshooting adult neurogenesis is suspected to contribute to the pathophysiology of mesial temporal lobe epilepsy, as epileptic excitations can increase the formation of aberrant synapses and interregional connectivity, leading to a vicious cycle (Parent et al., 1997).

In this study, we found a significant increase in proliferative activity within both neural stem cell niches after both invasive SCI and non-invasive sham surgery. Current data suggest that a diffuse neuroinflammatory response could be contribute to these changes. There are several animal studies with complying results. Mice that develop a strong inflammatory reaction following SCI more frequently show signs of cognitive impairment, anxiety, and depression-like behavior (Wu et al., 2014b, Diaz-Castro et al., 2021). Both anxiety and depression-like behavior in a rat model of SCI were linked to increased inflammatory signaling molecules such as TNF-α, IL-1α, IL-1β, Granulocyte-macrophage colony-stimulating factor (GM-CSF) (Maldonado-Bouchard et al., 2016). Strikingly, SCI can even lead to a reduction of synapses in ventral hippocampal CA1 pyramidal neurons (Jing et al., 2017), a population that is crucial for storage and processing of social memory (Okuyama et al., 2016) and in the long term, to suppression of forebrain neurogenesis (Das and Basu, 2008, Whitney et al., 2009). It remains unclear whether and if so, how increased proliferation within neural stem cell contributes to structural decline, but these findings suggest that SCI patients could be at risk for permanent neurocognitive deficits (Faden et al., 2016, Ziegler et al., 2018). While further effort is still needed to identify the exact underlying cellular and molecular changes that contribute to SCI-related symptoms such as headaches, cognitive deficits and psychological disorders, our study supports the idea that glial cells including aNSCs in the brain could also play a role.

4.8 Perspectives in Future SCI Therapeutic Strategies

Generally, both preexisting and concomitant infections are a leading cause of death after different types of CNS injury (Meisel et al., 2005) and ever since the discovery of the secondary cascade after SCI, more and more treatment strategies are focusing on its possible target points. These mainly concentrate on controlling the inflammatory response by modulating immune cell interaction, but also manipulation of the extracellular matrix and depletion of extracellular matrix molecules secreted by reactive astrocytes play a role (Orr and Gensel, 2018). However, by simply suppressing the immune system, as by administration of corticosteroids, which is already part of standardized algorithms (Ahuja et al., 2017), the organism may be harmed additionally. Already in 1992, the so-called SCI-induced immune depression syndrome (SCI-IDS) was described that can – as the name suggests – lead to immune cell dysfunction and thus severe infectious complications (Cruse et al., 1992). Still, SCI-IDS only much later shifted into the scientific spotlight and again became subject to more research (Popovich and McTigue, 2009, Riegger et al., 2009). While underlying mechanisms are complex and also involve humoral factors (Brommer et al., 2016, Pruss et al., 2017), the exact signaling pathways still remain incompletely understood. The results of our study suggest that even non-invasive injury can trigger similar cellular and molecular changes as following spinal cord hemisection. Mere immunosuppressants should therefore only be administered with caution regardless the invasiveness of a SCI.

Promising candidates that modulate reactive gliosis and simultaneously reduce the inflammatory response while enhancing neuronal regeneration might be the group of growth factors. Fibroblast growth factor 2 (FGF2) was shown to significantly decrease TNF-α expression at the lesion site in mice that underwent thoracic spinal hemisection, leading to reduced microglial activation and immune cell infiltration while modifying astrocytic morphometric transformation (Goldschmit et al., 2014). These changes possibly favor neurogenesis and axonal sprouting in the course of regeneration. VEGF has also been subject of interest as it is known to induce NSC capacity (Pelegri et al., 2019). When administered intraperitoneally after SCI, VEGF not only increases neuron numbers at the lesion site and promotes the reintegration of those into neuronal networks, but it also inhibits microglial activation and thus neuroinflammation (Li et al., 2017). This finally leads to improved functional outcomes. Intriguingly, a similar effect with a significant reduction in lesion size and

dramatic improvement of motor recovery was found after injecting mice with human IgG (Chio et al., 2019). However, there are also studies suggesting that targeted reduction of reactive gliosis following SCI e.g., through inhibition of the JAK/STAT pathway, can have unfavorable effects, such as impaired motor function recovery (Yamauchi et al., 2006), stressing the complexity of the underlying mechanisms.

Another possible treatment approaches the capacity of endogenous progenitor cells and reactive glial cells to proliferate. Both cell types respond to CNS injury by increasing proliferative activity (Bareyre, 2008, Sirko et al., 2013, Buffo et al., 2008, Gao and Chen, 2013), whereas the latter can even acquire stem cell properties (Gotz et al., 2015, Sirko et al., 2013). When transplanting SEZ-derived neurospheres into the injury site of a thoracic spinal contusion in adult rats, they migrate to the cavity, integrate into local structures, and differentiate into oligodendrocytes, facilitating myelination while decreasing the inflammatory response (Sankavaram et al., 2019). Similarly, transplantation of neural precursor cells decreases macrophage invasion, GFAP upregulation and local apoptosis in cervical SCI, leading to improved behavioral and locomotor recovery (Riemann et al., 2018). There are still only few clinical trials in humans, but preliminary results already show positive effects with little side effects (Curtis et al., 2018, Jin et al., 2019).

While these approaches seem promising, they still remain experimental and require further research to establish standardized and safe treatment protocols. At the same time, there is more and more evidence suggesting that SCI should be considered a condition that involves a multitude of organs, including the brain. Our study suggests that both SCI and spinal trauma lead to reactive changes in glial cells including aNSCs in the brain and that these are likely transmitted via systemic cascades, possibly through CSF. While SCI patients often experience diffuse and unspecific symptoms, making it hard to distinguish the exact pathophysiology, they might be early signs of commencing structural changes due to an adversely adapted body. Thus, future research is needed to understand the organisms' reaction to trauma in order to attain a balance that provides adequate immune cell activation without an overshooting inflammatory response that could cause more damage in remote regions.

4.9 Limitations of this Study

For now, the investigation of cellular and molecular changes in the human CNS is only possible using *post mortem* tissue or specimens resected during neurosurgical procedures. Therefore, preclinical experimental animal models are the widely used research sources providing plethora of relevant insights on how the mammalian CNS reacts to a specific pathological insult.

It is important to discuss the issue of transferability of our results into the human organism. Albeit many structural and molecular similarities, there are also significant differences between the mouse brain and the human brain. In regard to adult neurogenesis, it can indeed be found in the human hippocampus (Boldrini et al., 2018, Spalding et al., 2013, Eriksson et al., 1998). However, there is currently no evidence for the existence of a human SEZ. Still, murine models have served in many ways in different fields of research, and nowadays, the majority of established methods have their origin in basic research with animal models.

Furthermore, it should be mentioned that the number of sacrificed animals in this study were kept at a minimum. As a result, however, statistical analysis can be challenging on experimental groups with sample sizes as small as n=3 as it is difficult to properly perform normality analysis and reach adequate statistical power. Therefore, all data collected in this study provide novel insights and cannot be directly compared to large clinical trials. However, our observations of cellular changes within adult neural stem cell niches and circulating CSF provide a basis for further studies focusing on possible treatment methods targeting pathophysiological processes in the CNS following SCI.

5. Summary

SCI is a common cause for long-term disability, which not only leaves its victims with sudden, greatly impaired functionality. The secondary cascade, a complex sequence of cellular and molecular changes starting already during the acute post-injury phase, has recently caught the attention of researchers, as it is likely responsible for a variety of long-term complications. These are not only limited to pathological processes at the level of the spinal cord, but can even present with symptoms that suggest an involvement of distinct brain regions. However, only little is known about the exact underlying cellular and molecular processes. An increasing body of evidence supports the idea that glial cells may play the most dominant role after trauma, which is why in this present study the reaction to SCI of glial cells and neural stem cell niches in the adult murine brain was investigated. The results of our spatiotemporal analysis revealed that SCI led to an upregulation of cell proliferation in adult neural stem cell niches starting already a few days after the trauma. Most dominantly, an expansion of the neuroblast cell pool could be observed, but also the proliferative activity of aNSCs of the hippocampus was altered. *In vitro* experiments on neurospheres dissected from neurogenic niches showed changes in self-renewing and limited neurogenic (in favor of gliogenic) capacity. Further molecular analyses revealed an upregulation of both reactive and proliferative genes in cortical astrocytes. At the same time, the findings in the sham group suggest that no structural CNS lesion is necessary for those changes, making a reaction that is limited to neural tissue less likely. There is still need for further investigations on the exact underlying mechanisms, but our findings in the context of the most recent data suggest that a systemic inflammatory response affecting resident glial cells of the brain could be responsible. Proteome analysis of CSF revealed marked changes in the expression levels of several proteins involved in NSC regulation and inflammatory processes, providing a possible link in the complex changes following the insult. Animal studies have even shown signs of a diffuse neuroinflammatory response after remote trauma without actual CNS tissue damage, that is linked to altered behavior and neurocognitive impairment. Further effort is needed to identify the role of these changes in human SCI-related comorbidities such as headaches, cognitive deficits, and psychological disorders. Still, SCI should already be considered a multiorgan condition urging researchers to investigate how to optimize the whole organism's reaction to trauma.

6. Zusammenfassung

Rückenmarksverletzungen gehören zu den häufigsten Gründen für langfristige Behinderung. Die Patienten sind jedoch nicht nur mit akuten, verheerenden Funktionseinschränkungen konfrontiert. Die sogenannte sekundäre Kaskade, eine komplexe Abfolge von zellulären und molekularen Veränderungen, die bereits kurzzeitig nach dem Trauma selbst beginnt, ist wahrscheinlich für eine Vielzahl von Langzeitkomplikationen verantwortlich. Hierzu gehören vermutlich auch Symptome, die auf Störungen höherer Hirnfunktionen hinweisen. Bislang ist wenig bekannt über die genauen Mechanismen, aber neuste Erkenntnisse lassen vermuten, dass Gliazellen die wichtigste Rolle hierbei spielen könnten. In der vorliegenden Studie wurde daher die Reaktion von Gliazellen in adulten neuralen Stammzellnischen auf Rückenmarksverletzungen untersucht. Unsere Ergebnisse zeigten, dass bereits wenige Tage posttraumatisch eine Induktion der proliferativen Aktivität in beiden Stammzellnischen mit regional und zeitlich charakteristischem Verlauf erfolgt. Neuroblasten stellen dabei den größten Teil des proliferierenden Zellpools dar, aber auch neurale Stammzellen des Hippocampus werden aktiviert. *In-vitro*-Experimente zeigten zudem eine Veränderung der selbstreplizierenden sowie eine Limitierung der neurogenen zugunsten der gliogenen Fähigkeit von Neurosphären, die aus beiden Nischen gewonnen wurden. Molekularbiologische Analysen zeigten zudem eine Hochregulierung von reaktiven und proliferativen Genen in kortikalen Astrozyten. Dabei deuteten die Ergebnisse in der Scheingruppe darauf hin, dass eine tatsächliche Läsion neuralen Gewebes nicht ausschlaggebend ist und somit eine systemische Reaktion wahrscheinlich verantwortlich ist. Die genauen zugrundeliegenden Mechanismen bedürfen weiterer Untersuchungen, aber die Ergebnisse der vorliegenden Studie im Zusammenhang mit den jüngsten Daten legen nahe, dass eine systemische Entzündungsreaktion mit Auswirkungen auf Gliazellen des Gehirns möglich sein könnte. Tierexperimentelle Studien zeigen bereits Hinweise auf eine diffuse neuroinflammatorische Komponente auch nach Traumata ohne Bezug zum Nervensystem. Während diese mit Beeinträchtigungen in Verhalten und Kognition einhergehen, ist noch unklar, ob hierdurch Komorbiditäten des Menschen wie Kopfschmerzen sowie neurokognitive und psychologische Auffälligkeiten erklärt werden können. Dennoch sollten Rückenmarksverletzungen zunehmend als multisystemische Erkrankung gesehen werden mit Fokus auf eine Optimierung der Reaktion des Gesamtorganismus auf Traumata.

7. References

AASEBO, E., OPSAHL, J. A., BJORLYKKE, Y., MYHR, K. M., KROKSVEEN, A. C. & BERVEN, F. S. 2014. Effects of blood contamination and the rostro-caudal gradient on the human cerebrospinal fluid proteome. *PLoS One,* 9**,** e90429.

AGUIRRE, A., RUBIO, M. E. & GALLO, V. 2010. Notch and EGFR pathway interaction regulates neural stem cell number and self-renewal. *Nature,* 467**,** 323-7.

AHUJA, C. S., MARTIN, A. R. & FEHLINGS, M. 2016. Recent advances in managing a spinal cord injury secondary to trauma. *F1000Res,* 5.

AHUJA, C. S., NORI, S., TETREAULT, L., WILSON, J., KWON, B., HARROP, J., CHOI, D. & FEHLINGS, M. G. 2017. Traumatic Spinal Cord Injury-Repair and Regeneration. *Neurosurgery,* 80**,** S9-S22.

ALIZADEH, A., DYCK, S. M. & KARIMI-ABDOLREZAEE, S. 2019. Traumatic Spinal Cord Injury: An Overview of Pathophysiology, Models and Acute Injury Mechanisms. *Front Neurol,* 10**,** 282.

ALLEN, A. R. 1911. Surgery of experimental lesion of spinal cord equivalent to

crush injury of fracture dislocation of spinal column. *JAMA,* 57**,** 878-880.

ALMAN, J. & DAS, G. D. 1965. Autoradiographic and histological Evidence of Postnatal Hippocampal Neurogenesis in Rats. *The Journal of Comparative Neurology* 124**,** 319-336.

ALTMAN, J. 1962. Are new neurons formed in the brain of adult mammalians? *Science,* 135**,** 1127-1128.

ANDREOTTI, J. P., SILVA, W. N., COSTA, A. C., PICOLI, C. C., BITENCOURT, F. C. O., COIMBRA-CAMPOS, L. M. C., RESENDE, R. R., MAGNO, L. A. V., ROMANO-SILVA, M. A., MINTZ, A. & BIRBRAIR, A. 2019. Neural stem cell niche heterogeneity. *Semin Cell Dev Biol,* 95**,** 42-53.

ANKENY, D. P., GUAN, Z. & POPOVICH, P. G. 2009. B cells produce pathogenic antibodies and impair recovery after spinal cord injury in mice. *J Clin Invest,* 119**,** 2990-9.

BADER, J. M., GEYER, P. E., MULLER, J. B., STRAUSS, M. T., KOCH, M., LEYPOLDT, F., KOERTVELYESSY, P., BITTNER, D., SCHIPKE, C. G., INCESOY, E. I., PETERS, O., DEIGENDESCH, N., SIMONS, M., JENSEN, M. K., ZETTERBERG, H. & MANN, M. 2020. Proteome profiling in cerebrospinal fluid reveals novel biomarkers of Alzheimer's disease. *Mol Syst Biol,* 16**,** e9356.

BARDEHLE, S., KRUGER, M., BUGGENTHIN, F., SCHWAUSCH, J., NINKOVIC, J., CLEVERS, H., SNIPPERT, H. J., THEIS, F. J., MEYER-LUEHMANN, M., BECHMANN, I., DIMOU, L. & GOTZ, M. 2013. Live imaging of astrocyte responses to acute injury reveals selective juxtavascular proliferation. *Nat Neurosci,* 16**,** 580-6.

BAREYRE, F. M. 2008. Neuronal repair and replacement in spinal cord injury. *J Neurol Sci,* 265**,** 63-72.

BARON, R., BINDER, A. & WASNER, G. 2010. Neuropathic pain: diagnosis, pathophysiological mechanisms, and treatment. *Lancet Neurol,* 9**,** 807-19.

BECKERVORDERSANDFORTH, R., TRIPATHI, P., NINKOVIC, J., BAYAM, E., LEPIER, A., STEMPFHUBER, B., KIRCHHOFF, F., HIRRLINGER, J., HASLINGER, A., LIE, D. C., BECKERS, J., YODER, B., IRMLER, M. & GOTZ, M. 2010. In vivo fate mapping and expression analysis reveals molecular hallmarks of prospectively isolated adult neural stem cells. *Cell Stem Cell,* 7**,** 744-58.

BEN HAIM, L., CEYZERIAT, K., CARRILLO-DE SAUVAGE, M. A., AUBRY, F., AUREGAN, G., GUILLERMIER, M., RUIZ, M., PETIT, F., HOUITTE, D., FAIVRE, E., VANDESQUILLE, M., ARON-BADIN, R., DHENAIN, M., DEGLON, N., HANTRAYE, P., BROUILLET, E., BONVENTO, G. & ESCARTIN, C. 2015. The JAK/STAT3 pathway is a common inducer of astrocyte reactivity in Alzheimer's and Huntington's diseases. *J Neurosci,* 35**,** 2817-29.

BERBEE, J. F., HAVEKES, L. M. & RENSEN, P. C. 2005. Apolipoproteins modulate the inflammatory response to lipopolysaccharide. *J Endotoxin Res,* 11**,** 97-103.

BOLDRINI, M., FULMORE, C. A., TARTT, A. N., SIMEON, L. R., PAVLOVA, I., POPOSKA, V., ROSOKLIJA, G. B., STANKOV, A., ARANGO, V., DWORK, A. J., HEN, R. & MANN, J. J. 2018. Human Hippocampal Neurogenesis Persists throughout Aging. *Cell Stem Cell,* 22**,** 589-599 e5.

BRACKEN, M. B., SHEPARD, M. J., COLLINS, W. F., HOLFORD, T. R., YOUNG, W., BASKIN, D. S., EISENBERG, H. M., FLAMM, E., LEO-SUMMERS, L., MAROON, J. & ET AL. 1990. A randomized, controlled trial of methylprednisolone or naloxone in the treatment of acute spinal-cord injury. Results of the Second National Acute Spinal Cord Injury Study. *N Engl J Med,* 322**,** 1405-11.

BREUNIG, J. J., ARELLANO, J. I., MACKLIS, J. D. & RAKIC, P. 2007. Everything that glitters isn't gold: a critical review of postnatal neural precursor analyses. *Cell Stem Cell,* 1**,** 612-27.

BROMMER, B., ENGEL, O., KOPP, M. A., WATZLAWICK, R., MULLER, S., PRUSS, H., CHEN, Y., DEVIVO, M. J., FINKENSTAEDT, F. W., DIRNAGL, U., LIEBSCHER, T., MEISEL, A. & SCHWAB, J. M. 2016. Spinal cord injury-induced immune deficiency syndrome enhances infection susceptibility dependent on lesion level. *Brain,* 139**,** 692-707.

BUFFO, A., RITE, I., TRIPATHI, P., LEPIER, A., COLAK, D., HORN, A. P., MORI, T. & GOTZ, M. 2008. Origin and progeny of reactive gliosis: A source of multipotent cells in the injured brain. *Proc Natl Acad Sci U S A,* 105**,** 3581-6.

BURDA, J. E. & SOFRONIEW, M. V. 2014. Reactive gliosis and the multicellular response to CNS damage and disease. *Neuron,* 81**,** 229-48.

BURMAN, J. & SVENNINGSSON, A. 2016. Cerebrospinal fluid concentration of Galectin-9 is increased in secondary progressive multiple sclerosis. *J Neuroimmunol,* 292**,** 40-4.

CALZOLARI, F., MICHEL, J., BAUMGART, E. V., THEIS, F., GOTZ, M. & NINKOVIC, J. 2015. Fast clonal expansion and limited neural stem cell self-renewal in the adult subependymal zone. *Nat Neurosci,* 18**,** 490-2.

CAMPOS, L. S. 2004. Neurospheres: insights into neural stem cell biology. *J Neurosci Res,* 78**,** 761-9.

CAYUSO, J., ULLOA, F., COX, B., BRISCOE, J. & MARTI, E. 2006. The Sonic hedgehog pathway independently controls the patterning, proliferation and survival of neuroepithelial cells by regulating Gli activity. *Development,* 133**,** 517-28.

CHEN, R., COHEN, L. G. & HALLETT, M. 2002. Nervous system reorganization following injury. *Neuroscience,* 111**,** 761-73.

CHENG, X., YEUNG, P. K. K., ZHONG, K., ZILUNDU, P. L. M., ZHOU, L. & CHUNG, S. K. 2019. Astrocytic endothelin-1 overexpression promotes neural progenitor cells proliferation and differentiation into astrocytes via the Jak2/Stat3 pathway after stroke. *Journal of Neuroinflammation,* 16.

CHIO, J. C. T., WANG, J., BADNER, A., HONG, J., SURENDRAN, V. & FEHLINGS, M. G. 2019. The effects of human immunoglobulin G on enhancing tissue protection and neurobehavioral recovery after traumatic cervical spinal cord injury are mediated through the neurovascular unit. *J Neuroinflammation,* 16**,** 141.

CHOW, W. A., FANG, J. J. & YEE, J. K. 2000. The IFN regulatory factor family participates in regulation of Fas ligand gene expression in T cells. *J Immunol,* 164**,** 3512-8.

CHU, H. X., ARUMUGAM, T. V., GELDERBLOM, M., MAGNUS, T., DRUMMOND, G. R. & SOBEY, C. G. 2014. Role of CCR2 in inflammatory conditions of the central nervous system. *J Cereb Blood Flow Metab,* 34**,** 1425-9.

CODEGA, P., SILVA-VARGAS, V., PAUL, A., MALDONADO-SOTO, A. R., DELEO, A. M., PASTRANA, E. & DOETSCH, F. 2014. Prospective identification and purification of quiescent adult neural stem cells from their in vivo niche. *Neuron,* 82**,** 545-59.

COLAK, D., MORI, T., BRILL, M. S., PFEIFER, A., FALK, S., DENG, C., MONTEIRO, R., MUMMERY, C., SOMMER, L. & GOTZ, M. 2008. Adult neurogenesis requires Smad4-mediated bone morphogenic protein signaling in stem cells. *J Neurosci,* 28**,** 434-46.

COSTA, J., GATERMANN, M., NIMTZ, M., KANDZIA, S., GLATZEL, M. & CONRADT, H. S. 2018. N-Glycosylation of Extracellular Vesicles from HEK-293 and Glioma Cell Lines. *Anal Chem,* 90**,** 7871-7879.

COSTA, J., PRONTO-LABORINHO, A., PINTO, S., GROMICHO, M., BONUCCI, S., TRANFIELD, E., CORREIA, C., ALEXANDRE, B. M. & DE CARVALHO, M. 2020. Investigating LGALS3BP/90 K glycoprotein in the cerebrospinal fluid of patients with neurological diseases. *Sci Rep,* 10**,** 5649.

COUILLARD-DESPRES, S., WINNER, B., SCHAUBECK, S., AIGNER, R., VROEMEN, M., WEIDNER, N., BOGDAHN, U., WINKLER, J., KUHN, H. G. & AIGNER, L. 2005. Doublecortin expression levels in adult brain reflect neurogenesis. *Eur J Neurosci,* 21**,** 1-14.

CRAIG, A., NICHOLSON PERRY, K., GUEST, R., TRAN, Y., DEZARNAULDS, A., HALES, A., EPHRAUMS, C. & MIDDLETON, J. 2015. Prospective study of the occurrence of psychological disorders and comorbidities after spinal cord injury. *Arch Phys Med Rehabil,* 96**,** 1426-34.

CREGG, J. M., CHU, K. A., HAGER, L. E., MAGGARD, R. S. J., STOLTZ, D. R., EDMOND, M., ALILAIN, W. J., PHILIPPIDOU, P., LANDMESSER, L. T. & SILVER, J. 2017. A Latent Propriospinal Network Can Restore Diaphragm Function after High Cervical Spinal Cord Injury. *Cell Rep,* 21**,** 654-665.

CREGG, J. M., DEPAUL, M. A., FILOUS, A. R., LANG, B. T., TRAN, A. & SILVER, J. 2014. Functional regeneration beyond the glial scar. *Exp Neurol,* 253**,** 197-207.

CRUSE, J. M., LEWIS, R. E., BISHOP, G. R., KLIESCH, W. F. & GAITAN, E. 1992. Neuroendocrine-Immune Interactions Assiciociated with Loss and Restoration of Immune System Function in SCI and Stroke Patients. *Immunologic Research,* 11**,** 104-106.

CURTIS, E., MARTIN, J. R., GABEL, B., SIDHU, N., RZESIEWICZ, T. K., MANDEVILLE, R., VAN GORP, S., LEERINK, M., TADOKORO, T., MARSALA, S., JAMIESON, C., MARSALA, M. & CIACCI, J. D. 2018. A First-in-Human, Phase I Study of Neural Stem Cell Transplantation for Chronic Spinal Cord Injury. *Cell Stem Cell,* 22**,** 941-950 e6.

DAS, S. & BASU, A. 2008. Inflammation: a new candidate in modulating adult neurogenesis. *J Neurosci Res,* 86**,** 1199-208.

DAVID, S. & KRONER, A. 2011. Repertoire of microglial and macrophage responses after spinal cord injury. *Nat Rev Neurosci,* 12**,** 388-99.

DEHLER, S., LOU, W. P., GAO, L., SKABKIN, M., DALLENBACH, S., NEUMANN, A. & MARTIN-VILLALBA, A. 2018. An Immune-CNS Axis Activates Remote Hippocampal Stem Cells Following Spinal Transection Injury. *Front Mol Neurosci,* 11**,** 443.

DIAZ-CASTRO, B., BERNSTEIN, A. M., COPPOLA, G., SOFRONIEW, M. V. & KHAKH, B. S. 2021. Molecular and functional properties of cortical astrocytes during peripherally induced neuroinflammation. *Cell Rep,* 36**,** 109508.

DIMOU, L. & GOTZ, M. 2014. Glial cells as progenitors and stem cells: new roles in the healthy and diseased brain. *Physiol Rev,* 94**,** 709-37.

DIZDAROGLU, M., JARUGA, P., BIRINCIOGLU, M. & RODRIGUEZ, H. 2002. Free radical-induced damage to DNA: mechanisms and measurement. *Free Radic Biol Med,* 32**,** 1102-15.

DOETSCH, F., CAILLE, I., LIM, D. A., GARCIA-VERDUGO, J. M. & ALVAREZ-BUYLLA, A. 1999a. Subventricular zone astrocytes are neural stem cells in the adult mammalian brain. *Cell,* 97**,** 703-16.

DOETSCH, F., CAILLE, I., LIM, D. A., GARCIA-VERDUGO, J. M. & ALVAREZ-BUYLLA, A. 1999b. Subventricular Zone Astrocytes Are Neural Stemm Cells in the Adult Mammalian Brain. *Cell,* 76**,** 703-716.

DOETSCH, F., GARCIA-VERDUGO, J. M. & ALVAREZ-BUYLLA, A. 1997. Cellular composition and three-dimensional organization of the subventricular germinal zone in the adult mammalian brain. *J Neurosci,* 17**,** 5046-61.

DOETSCH, F., PETREANU, L., CAILLE, I., GARCIA-VERDUGO, J. M. & ALVAREZ-BUYLLA, A. 2002. EGF converts transit-amplifying neurogenic precursors in the adult brain into multipotent stem cells. *Neuron,* 36**,** 1021-34.

DONG, H., FAZZARO, A., XIANG, C., KORSMEYER, S. J., JACQUIN, M. F. & MCDONALD, J. W. 2003. Enhanced oligodendrocyte survival after spinal cord injury in Bax-deficient mice and mice with delayed Wallerian degeneration. *J Neurosci,* 23**,** 8682-91.

DONG, Y., XU, Z., HUANG, L., ZHANG, Y. & XIE, Z. 2016. Peripheral surgical wounding may induce cognitive impairment through interlukin-6-dependent mechanisms in aged mice. *Med Gas Res,* 6**,** 180-186.

DONNELLY, D. J. & POPOVICH, P. G. 2008. Inflammation and its role in neuroprotection, axonal regeneration and functional recovery after spinal cord injury. *Exp Neurol,* 209**,** 378-88.

DUAN, X., CHANG, J. H., GE, S., FAULKNER, R. L., KIM, J. Y., KITABATAKE, Y., LIU, X. B., YANG, C. H., JORDAN, J. D., MA, D. K., LIU, C. Y., GANESAN, S., CHENG, H. J., MING, G. L., LU, B. & SONG, H. 2007. Disrupted-In-Schizophrenia 1 regulates integration of newly generated neurons in the adult brain. *Cell,* 130**,** 1146-58.

DUMONT, R. J., OKONKWO, D. O., VERMA, S., HURLBERT, R. J., BOULOS, P. T., ELLEGALA, D. B. & DUMONT, A. S. 2001. Acute spinal cord injury, part I: pathophysiologic mechanisms. *Clin Neuropharmacol,* 24**,** 254-64.

DZIENNIS, S. & ALKAYED, N. J. 2008. Role of signal transducer and activator of transcription 3 in neuronal survival and regeneration. *Rev Neurosci,* 19**,** 341-61.

ELLIS, P., FAGAN, B. M., MAGNESS, S. T., HUTTON, S., TARANOVA, O., HAYASHI, S., MCMAHON, A., RAO, M. & PEVNY, L. 2004. SOX2, a persistent marker for multipotential neural stem cells derived from embryonic stem cells, the embryo or the adult. *Dev Neurosci,* 26**,** 148-65.

ENCINAS, J. M., MICHURINA, T. V., PEUNOVA, N., PARK, J. H., TORDO, J., PETERSON, D. A., FISHELL, G., KOULAKOV, A. & ENIKOLOPOV, G. 2011. Division-coupled astrocytic differentiation and age-related depletion of neural stem cells in the adult hippocampus. *Cell Stem Cell,* 8**,** 566-79.

ERIKSSON, P. S., PERFILIEVA, E., BJORK-ERIKSSON, T., ALBORN, A., NORDBORD, C., PETERSON, D. A. & GAGE, F. H. 1998. Neurogenesis in the adult human hippocampus. *Nature Medicine,* 4**,** 1313-1317.

ESCARTIN, C., GALEA, E., LAKATOS, A., O'CALLAGHAN, J. P., PETZOLD, G. C., SERRANO-POZO, A., STEINHAUSER, C., VOLTERRA, A., CARMIGNOTO, G., AGARWAL, A., ALLEN, N. J., ARAQUE, A., BARBEITO, L., BARZILAI, A., BERGLES, D. E., BONVENTO, G., BUTT, A. M., CHEN, W. T., COHEN-SALMON, M., CUNNINGHAM, C., DENEEN, B., DE STROOPER, B., DIAZ-CASTRO, B., FARINA, C., FREEMAN, M., GALLO, V., GOLDMAN, J. E., GOLDMAN, S. A., GOTZ, M., GUTIERREZ, A., HAYDON, P. G., HEILAND, D. H., HOL, E. M., HOLT, M. G., IINO, M., KASTANENKA, K. V., KETTENMANN, H., KHAKH, B. S., KOIZUMI, S., LEE, C. J., LIDDELOW, S. A., MACVICAR, B. A., MAGISTRETTI, P., MESSING, A., MISHRA, A., MOLOFSKY, A. V., MURAI, K. K., NORRIS, C. M., OKADA, S., OLIET, S. H. R., OLIVEIRA, J. F., PANATIER, A., PARPURA, V., PEKNA, M., PEKNY, M., PELLERIN, L., PEREA, G., PEREZ-NIEVAS, B. G., PFRIEGER, F. W., POSKANZER, K. E., QUINTANA, F. J., RANSOHOFF, R. M., RIQUELME-PEREZ, M., ROBEL, S., ROSE, C. R., ROTHSTEIN, J. D., ROUACH, N., ROWITCH, D. H., SEMYANOV, A., SIRKO, S., SONTHEIMER, H., SWANSON, R. A., VITORICA, J., WANNER, I. B., WOOD, L. B., WU, J., ZHENG, B., ZIMMER, E. R., ZOREC, R., SOFRONIEW, M. V. & VERKHRATSKY, A. 2021. Reactive astrocyte nomenclature, definitions, and future directions. *Nat Neurosci,* 24**,** 312-325.

ESCARTIN, C., GUILLEMAUD, O. & CARRILLO-DE SAUVAGE, M. A. 2019. Questions and (some) answers on reactive astrocytes. *Glia,* 67**,** 2221-2247.

FADEN, A. I., WU, J., STOICA, B. A. & LOANE, D. J. 2016. Progressive inflammation-mediated neurodegeneration after traumatic brain or spinal cord injury. *Br J Pharmacol,* 173**,** 681-91.

FALNIKAR, A., STRATTON, J., LIN, R., ANDREWS, C. E., TYBURSKI, A., TROVILLION, V. A., GOTTSCHALK, C., GHOSH, B., IACOVITTI, L., ELLIOTT, M. B. & LEPORE, A. C. 2018. Differential Response in Novel Stem Cell Niches of the Brain after Cervical Spinal Cord Injury and Traumatic Brain Injury. *J Neurotrauma,* 35**,** 2195-2207.

FEHLINGS, M. G., VACCARO, A. R., BOAKYE, M., ROSSIGNOL, S., DITUNNO, J. J. F. & BURNS, A. S. 2013. *Essentials of Spinal Cord Injury - Basic Research to Clinical Practice,* New York, NY, USA, Thieme Publishers

FEHLINGS, M. G., WILSON, J. R., TETREAULT, L. A., AARABI, B., ANDERSON, P., ARNOLD, P. M., BRODKE, D. S., BURNS, A. S., CHIBA, K., DETTORI, J. R., FURLAN, J. C., HAWRYLUK, G., HOLLY, L. T., HOWLEY, S., JEJI, T., KALSI-RYAN, S., KOTTER, M., KURPAD, S., KWON, B. K., MARINO, R. J., MARTIN, A. R., MASSICOTTE, E., MERLI, G., MIDDLETON, J. W., NAKASHIMA, H., NAGOSHI, N., PALMIERI, K., SKELLY, A. C., SINGH, A., TSAI, E. C., VACCARO, A., YEE, A. & HARROP, J. S. 2017. A Clinical Practice Guideline for the Management of Patients With Acute Spinal Cord Injury: Recommendations on the Use of Methylprednisolone Sodium Succinate. *Global Spine J,* 7**,** 203S-211S.

FELIX, M. S., POPA, N., DJELLOUL, M., BOUCRAUT, J., GAUTHIER, P., BAUER, S. & MATARAZZO, V. A. 2012. Alteration of forebrain neurogenesis after cervical spinal cord injury in the adult rat. *Front Neurosci,* 6**,** 45.

FILIPPOV, V., KRONENBERG, G., PIVNEVA, T., REUTER, K., STEINER, B., WANG, L. P., YAMAGUCHI, M., KETTENMANN, H. & KEMPERMANN, G. 2003. Subpopulation of nestin-expressing progenitor cells in the adult murine hippocampus shows electrophysiological and morphological characteristics of astrocytes. *Mol Cell Neurosci,* 23**,** 373-82.

FISCHER, J., BECKERVORDERSANDFORTH, R., TRIPATHI, P., STEINER-MEZZADRI, A., NINKOVIC, J. & GOTZ, M. 2011. Prospective isolation of adult neural stem cells from the mouse subependymal zone. *Nat Protoc,* 6**,** 1981-9.

FRANZ, S., CIATIPIS, M., PFEIFER, K., KIERDORF, B., SANDNER, B., BOGDAHN, U., BLESCH, A., WINNER, B. & WEIDNER, N. 2014. Thoracic rat spinal cord contusion injury induces remote spinal gliogenesis but not neurogenesis or gliogenesis in the brain. *PLoS One,* 9**,** e102896.

FREUND, P., WEISKOPF, N., ASHBURNER, J., WOLF, K., SUTTER, R., ALTMANN, D. R., FRISTON, K., THOMPSON, A. & CURT, A. 2013. MRI investigation of the sensorimotor cortex and the corticospinal tract after acute spinal cord injury: a prospective longitudinal study. *Lancet Neurol,* 12**,** 873-881.

FRIK, J., MERL-PHAM, J., PLESNILA, N., MATTUGINI, N., KJELL, J., KRASKA, J., GOMEZ, R. M., HAUCK, S. M., SIRKO, S. & GOTZ, M. 2018. Cross-talk between monocyte invasion and astrocyte proliferation regulates scarring in brain injury. *EMBO Rep,* 19.

FUKUSUMI, Y., MEIER, F., GOTZ, S., MATHEUS, F., IRMLER, M., BECKERVORDERSANDFORTH, R., FAUS-KESSLER, T., MININA, E., RAUSER, B., ZHANG, J., ARENAS, E., ANDERSSON, E., NIEHRS, C., BECKERS, J., SIMEONE, A., WURST, W. & PRAKASH, N. 2015. Dickkopf 3 Promotes the Differentiation of a Rostrolateral Midbrain Dopaminergic Neuronal Subset In Vivo and from Pluripotent Stem Cells In Vitro in the Mouse. *J Neurosci,* 35**,** 13385-401.

GAO, X. & CHEN, J. 2013. Moderate traumatic brain injury promotes neural precursor proliferation without increasing neurogenesis in the adult hippocampus. *Exp Neurol,* 239**,** 38-48.

GARRANZO-ASENSIO, M., SAN SEGUNDO-ACOSTA, P., MARTINEZ-USEROS, J., MONTERO-CALLE, A., FERNANDEZ-ACENERO, M. J., HAGGMARK-MANBERG, A., PELAEZ-GARCIA, A., VILLALBA, M., RABANO, A., NILSSON, P. & BARDERAS, R. 2018. Identification of prefrontal cortex protein alterations in Alzheimer's disease. *Oncotarget,* 9**,** 10847-10867.

GENSEL, J. C., KOPPER, T. J., ZHANG, B., ORR, M. B. & BAILEY, W. M. 2017. Predictive screening of M1 and M2 macrophages reveals the immunomodulatory effectiveness of post spinal cord injury azithromycin treatment. *Sci Rep,* 7**,** 40144.

GERDES, J., LEMKE, H., BAISCH, H., WACKER, H. H., SCHWAB, U. & STEIN, H. 1984. Cell cycle analysis of a cell proliferation-associated human nuclear antigen defined by the monoclonal antibody Ki-67. *J Immunol,* 133**,** 1710-5.

GERDES, J., SCHWAB, U., LEMKE, H. & STEIN, H. 1983. Production of a mouse monoclonal antibody reactive with a human nuclear antigen associated with cell proliferation. *Int J Cancer,* 31**,** 13-20.

GOLDSCHMIT, Y., FRISCA, F., PINTO, A. R., PÉBAY, A., TANG, J. K. Y., SIEGEL, A. L., KASLIN, J. & CURRIE, P. D. 2014. Fgf2 improves functional recovery - decreasing gliosis

and increasing radial glia and neural progenitor cells

after spinal cord injury. *Brain Behav,* 4**,** 187-200.

GONCALVES, J. T., SCHAFER, S. T. & GAGE, F. H. 2016. Adult Neurogenesis in the Hippocampus: From Stem Cells to Behavior. *Cell,* 167**,** 897-914.

GOTZ, M. & BARDE, Y. A. 2005. Radial glial cells defined and major intermediates between embryonic stem cells and CNS neurons. *Neuron,* 46**,** 369-72.

GOTZ, M., NAKAFUKU, M. & PETRIK, D. 2016. Neurogenesis in the Developing and Adult Brain-Similarities and Key Differences. *Cold Spring Harb Perspect Biol,* 8.

GOTZ, M., SIRKO, S., BECKERS, J. & IRMLER, M. 2015. Reactive astrocytes as neural stem or progenitor cells: In vivo lineage, In vitro potential, and Genome-wide expression analysis. *Glia,* 63**,** 1452-68.

GREGOIRE, C. A., GOLDENSTEIN, B. L., FLORIDDIA, E. M., BARNABE-HEIDER, F. & FERNANDES, K. J. 2015. Endogenous neural stem cell responses to stroke and spinal cord injury. *Glia,* 63**,** 1469-82.

HACHEM, L. D., AHUJA, C. S. & FEHLINGS, M. G. 2017. Assessment and management of acute spinal cord injury: From point of injury to rehabilitation. *J Spinal Cord Med,* 40**,** 665-675.

HAINES, J. D., VIDAURRE, O. G., ZHANG, F., RIFFO-CAMPOS, A. L., CASTILLO, J., CASANOVA, B., CASACCIA, P. & LOPEZ-RODAS, G. 2015. Multiple sclerosis patient-derived CSF induces transcriptional changes in proliferating oligodendrocyte progenitors. *Mult Scler,* 21**,** 1655-69.

HAUCK, S. M., DIETTER, J., KRAMER, R. L., HOFMAIER, F., ZIPPLIES, J. K., AMANN, B., FEUCHTINGER, A., DEEG, C. A. & UEFFING, M. 2010. Deciphering membrane-associated molecular processes in target tissue of autoimmune uveitis by label-free quantitative mass spectrometry. *Mol Cell Proteomics,* 9**,** 2292-305.

HEIMANN, G., CANHOS, L. L., FRIK, J., JAGER, G., LEPKO, T., NINKOVIC, J., GOTZ, M. & SIRKO, S. 2017. Changes in the Proliferative Program Limit Astrocyte Homeostasis in the Aged Post-Traumatic Murine Cerebral Cortex. *Cereb Cortex,* 27**,** 4213-4228.

HELLAWELL, D. J., TAYLOR, R. T. & PENTLAND, B. 1999. Cognitive and psychosocial outcome following moderate or severe traumatic brain injury. *Brain Inj,* 13**,** 489-504.

HERRMANN, J. E., IMURA, T., SONG, B., QI, J., AO, Y., NGUYEN, T. K., KORSAK, R. A., TAKEDA, K., AKIRA, S. & SOFRONIEW, M. V. 2008. STAT3 is a critical regulator of astrogliosis and scar formation after spinal cord injury. *J Neurosci,* 28**,** 7231-43.

HUGHES, E. G., KANG, S. H., FUKAYA, M. & BERGLES, D. E. 2013. Oligodendrocyte progenitors balance growth with self-repulsion to achieve homeostasis in the adult brain. *Nat Neurosci,* 16**,** 668-76.

HUMANES-VALERA, D., FOFFANI, G., ALONSO-CALVIÑO, E., FERNÁNDEZ-LÓPEZ, E. & AGUILAR, J. 2016. Dual Cortical Plasticity After Spinal Cord Injury. *Cerebral Cortex*.

IJSSELSTIJN, L., PAPMA, J. M., DEKKER, L. J., CALAME, W., STINGL, C., KOUDSTAAL, P. J., PRINS, N. D., SILLEVIS SMITT, P. A. & LUIDER, T. M. 2013. Serum proteomics in amnestic mild cognitive impairment. *Proteomics,* 13**,** 2526-33.

INGHAM, P. W. 1998. Transducing Hedgehog: the story so far. *EMBO J,* 17**,** 3505-11.

IRVINE, K. A. & CLARK, J. D. 2018. Chronic Pain After Traumatic Brain Injury: Pathophysiology and Pain Mechanisms. *Pain Med,* 19**,** 1315-1333.

JACOBS, S., LIE, D. C., DECICCO, K. L., SHI, Y., DELUCA, L. M., GAGE, F. H. & EVANS, R. M. 2006. Retinoic acid is required early during adult neurogenesis in the dentate gyrus. *Proc Natl Acad Sci U S A,* 103**,** 3902-7.

JESSEN, K. R. 2004. Glial cells. *Int J Biochem Cell Biol,* 36**,** 1861-7.

JIN, M. C., MEDRESS, Z. A., AZAD, T. D., DOULAMES, V. M. & VEERAVAGU, A. 2019. Stem cell therapies for acute spinal cord injury in humans: a review. *Neurosurg Focus,* 46**,** E10.

JING, Y., BAI, F., CHEN, H. & DONG, H. 2017. Acute spinal cord injury diminishes silent synapses in the rat hippocampus. *Neuroreport,* 28**,** 1139-1143.

JURE, I., PIETRANERA, L., DE NICOLA, A. F. & LABOMBARDA, F. 2017. Spinal Cord Injury Impairs Neurogenesis and Induces Glial Reactivity in the Hippocampus. *Neurochem Res,* 42**,** 2178-2190.

JUTZELER, C. R., FREUND, P., HUBER, E., CURT, A. & KRAMER, J. L. K. 2015. Neuropathic Pain and Functional Reorganization in the Primary Sensorimotor Cortex After Spinal Cord Injury. *J Pain,* 16**,** 1256-1267.

KAPLAN, M. S. & HINDS, J. W. 1977. Neurogenesis in the adult rat: electron microscopic analysis of light radioautographs. *Science,* 197**,** 1092-4.

KARSY, M. & HAWRYLUK, G. 2019. Modern Medical Management of Spinal Cord Injury. *Curr Neurol Neurosci Rep,* 19**,** 65.

KATO, J., MATSUSHIME, H., HIEBERT, S. W., EWEN, M. E. & SHERR, C. J. 1993. Direct binding of cyclin D to the retinoblastoma gene product (pRb) and pRb phosphorylation by the cyclin D-dependent kinase CDK4. *Genes Dev,* 7**,** 331-42.

KEMPERMANN, G., SONG, H. & GAGE, F. H. 2015. Neurogenesis in the Adult Hippocampus. *Cold Spring Harb Perspect Biol,* 7**,** a018812.

KENNEY, A. M. & ROWITCH, D. H. 2000. Sonic hedgehog promotes G1 cyclin expression and sustained cell cycle progression in mammalian neuronal precursors. *Molecular and cellular biology* 20**,** 9055-9067.

KHOONSARI, P. E., MUSUNRI, S., HERMAN, S., SVENSSON, C. I., TANUM, L., GORDH, T. & KULTIMA, K. 2019. Systematic analysis of the cerebrospinal fluid proteome of fibromyalgia patients. *J Proteomics,* 190**,** 35-43.

KISSELEVA, T., BHATTACHARYA, S., BRAUNSTEIN, J. & SCHINDLER, C. W. 2002. Signaling through the JAK/STAT pathway, recent advances and future challenges. *Gene,* 285**,** 1-24.

KNOLLER, N., AUERBACH, G., FULGA, V., ZELIG, G., ATTIAS, J., BAKIMER, R., MARDER, J. B., YOLES, E., BELKIN, M., SCHWARTZ, M. & HADANI, M. 2005. Clinical experience using incubated autologous macrophages as a treatment for complete spinal cord injury: phase I study results. *J Neurosurg Spine,* 3**,** 173-81.

KRIEGSTEIN, A. & ALVAREZ-BUYLLA, A. 2009. The glial nature of embryonic and adult neural stem cells. *Annu Rev Neurosci,* 32**,** 149-84.

KRISHNAMURTHY, K. & LASKOWITZ, D. T. 2016. Cellular and Molecular Mechanisms of Secondary Neuronal Injury following Traumatic Brain Injury. *In:* LASKOWITZ, D. & GRANT, G. (eds.) *Translational Research in Traumatic Brain Injury.* Boca Raton (FL).

KUAN, C. Y., SCHLOEMER, A. J., LU, A., BURNS, K. A., WENG, W. L., WILLIAMS, M. T., STRAUSS, K. I., VORHEES, C. V., FLAVELL, R. A., DAVIS, R. J., SHARP, F. R. & RAKIC, P. 2004. Hypoxia-ischemia induces DNA synthesis without cell proliferation in dying neurons in adult rodent brain. *J Neurosci,* 24**,** 10763-72.

KYROUSI, C., O'NEILL, A. C., BRAZOVSKAJA, A., HE, Z., KIELKOWSKI, P., COQUAND, L., DI GIAIMO, R., P, D. A., BELKA, A., FORERO ECHEVERRY, A., MEI, D., LENGE, M., CRUCEANU, C., BUCHSBAUM, I. Y., KHATTAK, S., FABIEN, G., BINDER, E., ELMSLIE, F., GUERRINI, R., BAFFET, A. D., SIEBER, S. A., TREUTLEIN, B., ROBERTSON, S. P. & CAPPELLO, S. 2021. Extracellular LGALS3BP regulates neural progenitor position and relates to human cortical complexity. *Nat Commun,* 12**,** 6298.

LANG, C., GUO, X., KERSCHENSTEINER, M. & BAREYRE, F. M. 2012. Single collateral reconstructions reveal distinct phases of corticospinal remodeling after spinal cord injury. *PLoS One,* 7**,** e30461.

LANGE CANHOS, L., CHEN, M., FALK, S., POPPER, B., STRAUB, T., GOTZ, M. & SIRKO, S. 2021. Repetitive injury and absence of monocytes promote astrocyte self-renewal and neurological recovery. *Glia,* 69**,** 165-181.

LAQUERRIERE, A., MAILLARD, C., CAVALLIN, M., CHAPON, F., MARGUET, F., MOLIN, A., SIGAUDY, S., BLOUET, M., BENOIST, G., FERNANDEZ, C., POIRIER, K., CHELLY, J., THOMAS, S. & BAHI-BUISSON, N. 2017. Neuropathological Hallmarks of Brain Malformations in Extreme Phenotypes Related to DYNC1H1 Mutations. *J Neuropathol Exp Neurol,* 76**,** 195-205.

LECOMTE, M. D., SHIMADA, I. S., SHERWIN, C. & SPEES, J. L. 2015. Notch1-STAT3-ETBR signaling axis controls reactive astrocyte proliferation after brain injury. *Proc Natl Acad Sci U S A,* 112**,** 8726-31.

LECUBE, A., POCA, M. A., COLOME, N., BECH-SERRA, J. J., HERNANDEZ, C., GARCIA-RAMIREZ, M., GANDARA, D., CANALS, F. & SIMO, R. 2012. Proteomic analysis of cerebrospinal fluid from obese women with idiopathic intracranial hypertension: a new approach for identifying new candidates in the pathogenesis of obesity. *J Neuroendocrinol,* 24**,** 944-52.

LESLIE, K., LANG, C., DEVGAN, G., AZARE, J., BERISHAJ, M., GERALD, W., KIM, Y. B., PAZ, K., DARNELL, J. E., ALBANESE, C., SAKAMAKI, T., PESTELL, R. & BROMBERG, J. 2006. Cyclin D1 is transcriptionally regulated by and required for transformation by activated signal transducer and activator of transcription 3. *Cancer Res,* 66**,** 2544-52.

LI, J., CHEN, S., ZHAO, Z., LUO, Y., HOU, Y., LI, H., HE, L., ZHOU, L. & WU, W. 2017. Effect of VEGF on Inflammatory Regulation, Neural Survival, and Functional Improvement in Rats following a Complete Spinal Cord Transection. *Front Cell Neurosci,* 11**,** 381.

LI, M. & SIRKO, S. 2018. Traumatic Brain Injury: At the Crossroads of Neuropathology and Common Metabolic Endocrinopathies. *J Clin Med,* 7.

LI, S. & STYS, P. K. 2000. Mechanisms of ionotropic glutamate receptor-mediated excitotoxicity in isolated spinal cord white matter. *J Neurosci,* 20**,** 1190-8.

LINDBLAD, C., PIN, E., JUST, D., AL NIMER, F., NILSSON, P., BELLANDER, B. M., SVENSSON, M., PIEHL, F. & THELIN, E. P. 2021. Fluid proteomics of CSF and serum reveal important

neuroinflammatory proteins in blood-brain barrier disruption and outcome prediction following severe traumatic brain injury: a prospective, observational study. *Crit Care,* 25**,** 103.

LIU, L. L. L., J. M. 2000. Predicting adverse postoperative outcomes in patients aged 80 years or older. *Journal of the American Geriatrics Society,* 48**,** 405-412.

LIVAK, K. J. & SCHMITTGEN, T. D. 2001. Analysis of relative gene expression data using real-time quantitative PCR and the 2(-Delta Delta C(T)) Method. *Methods,* 25**,** 402-8.

LLORENS-BOBADILLA, E., ZHAO, S., BASER, A., SAIZ-CASTRO, G., ZWADLO, K. & MARTIN-VILLALBA, A. 2015. Single-Cell Transcriptomics Reveals a Population of Dormant Neural Stem Cells that Become Activated upon Brain Injury. *Cell Stem Cell,* 17**,** 329-40.

LOBJOIS, V., BENAZERAF, B., BERTRAND, N., MEDEVIELLE, F. & PITUELLO, F. 2004. Specific regulation of cyclins D1 and D2 by FGF and Shh signaling coordinates cell cycle progression, patterning, and differentiation during early steps of spinal cord development. *Dev Biol,* 273**,** 195-209.

LUCAS, S. M., ROTHWELL, N. J. & GIBSON, R. M. 2006. The role of inflammation in CNS injury and disease. *Br J Pharmacol,* 147 Suppl 1**,** S232-40.

LUGERT, S., KREMER, T., JAGASIA, R., HERRMANN, A., AIGNER, S., GIACHINO, C., MENDEZ-DAVID, I., GARDIER, A. M., CARRALOT, J. P., MEISTERMANN, H., AUGUSTIN, A., SAXE, M. D., LAMERZ, J., DURAN-PACHECO, G., DUCRET, A., TAYLOR, V., DAVID, D. J. & CZECH, C. 2017. Glypican-2 levels in cerebrospinal fluid predict the status of adult hippocampal neurogenesis. *Sci Rep,* 7**,** 46543.

MALDONADO-BOUCHARD, S., PETERS, K., WOLLER, S. A., MADAHIAN, B., FAGHIHI, U., PATEL, S., BAKE, S. & HOOK, M. A. 2016. Inflammation is increased with anxiety- and depression-like signs in a rat model of spinal cord injury. *Brain Behav Immun,* 51**,** 176-95.

MAREI, H. E., AHMED, A. E., MICHETTI, F., PESCATORI, M., PALLINI, R., CASALBORE, P., CENCIARELLI, C. & ELHADIDY, M. 2012. Gene expression profile of adult human olfactory bulb and embryonic neural stem cell suggests distinct signaling pathways and epigenetic control. *PLoS One,* 7**,** e33542.

MARKIEWSKI, M. M. & LAMBRIS, J. D. 2007. The role of complement in inflammatory diseases from behind the scenes into the spotlight. *Am J Pathol,* 171**,** 715-27.

MARQUES, T. M., VAN RUMUND, A., BRUINSMA, I. B., WESSELS, H., GLOERICH, J., ESSELINK, R. A. J., BLOEM, B. R., KUIPERIJ, H. B. & VERBEEK, M. M. 2019. Cerebrospinal Fluid Galectin-1 Levels Discriminate Patients with Parkinsonism from Controls. *Mol Neurobiol,* 56**,** 5067-5074.

MEISEL, C., SCHWAB, J. M., PRASS, K., MEISEL, A. & DIRNAGL, U. 2005. Central nervous system injury-induced immune deficiency syndrome. *Nat Rev Neurosci,* 6**,** 775-86.

MELO-SALAS, M. S., PEREZ-DOMINGUEZ, M. & ZEPEDA, A. 2018. Systemic Inflammation Impairs Proliferation of Hippocampal Type 2 Intermediate Precursor Cells. *Cell Mol Neurobiol,* 38**,** 1517-1528.

MILLER, B. R. & HEN, R. 2015. The current state of the neurogenic theory of depression and anxiety. *Curr Opin Neurobiol,* 30**,** 51-8.

MILLER, M. W. & NOWAKOWSKI, R. S. 1988. Use of bromodeoxyuridine-immunohistochemistry to examine the proliferation, migration and time of origin of cells in the central nervous system. *Brain Res,* 457**,** 44-52.

MIRZADEH, Z., MERKLE, F. T., SORIANO-NAVARRO, M., GARCIA-VERDUGO, J. M. & ALVAREZ-BUYLLA, A. 2008. Neural stem cells confer unique pinwheel architecture to the ventricular surface in neurogenic regions of the adult brain. *Cell Stem Cell,* 3**,** 265-78.

NAKAMURA, M., HOUGHTLING, R. A., MACARTHUR, L., BAYER, B. M. & BREGMAN, B. S. 2003. Differences in cytokine gene expression profile between acute and secondary injury in adult rat spinal cord. *Exp Neurol,* 184**,** 313-25.

NAKAMURA, M. & OKANO, H. 2013. Cell transplantation therapies for spinal cord injury focusing on induced pluripotent stem cells. *Cell Res,* 23**,** 70-80.

NARDONE, R., HÖLLER, Y., BRIGO, F., SEIDL, M., CHRISTOVA, M., BERGMANN, J., GOLASZEWSKI, S. & TRINKA, E. 2013. Functional brain reorganization after spinal cord injury: Systematic review of animal and human studies. *Brain Research,* 1504**,** 58-73.

NARDONE, R., HOLLER, Y., SEBASTIANELLI, L., VERSACE, V., SALTUARI, L., BRIGO, F., LOCHNER, P. & TRINKA, E. 2018. Cortical morphometric changes after spinal cord injury. *Brain Res Bull,* 137**,** 107-119.

NIMMERJAHN, A., KIRCHHOFF, F. & HELMCHEN, F. 2005. Resting microglial cells are highly dynamic surveillants of brain parenchyma in vivo. *Science,* 308**,** 1314-8.

NORENBERG, M. D., SMITH, J. & MARCILLO, A. 2004. The Pathology of Human Spinal Cord Injury: Defining the Problems. *Journal of Neurotrauma,* 21**,** 420-440.

NSCISC, N. S. C. I. S. C. 2019. Spinal Cord Injury - Facts and Figures at a glance Birmingham, AL.

O'CALLAGHAN, J. P., KELLY, K. A., VANGILDER, R. L., SOFRONIEW, M. V. & MILLER, D. B. 2014. Early activation of STAT3 regulates reactive astrogliosis induced by diverse forms of neurotoxicity. *PLoS One,* 9**,** e102003.

OKADA, S., NAKAMURA, M., KATOH, H., MIYAO, T., SHIMAZAKI, T., ISHII, K., YAMANE, J., YOSHIMURA, A., IWAMOTO, Y., TOYAMA, Y. & OKANO, H. 2006. Conditional ablation of Stat3 or Socs3 discloses a dual role for reactive astrocytes after spinal cord injury. *Nat Med,* 12**,** 829-34.

OKUYAMA, T., KITAMURA, T., ROY, D. S., ITOHARA, S. & TONEGAWA, S. 2016. Ventral CA1 neurons store social memory. *Science,* 353**,** 1536-1541.

ORR, M. B. & GENSEL, J. C. 2018. Spinal Cord Injury Scarring and Inflammation: Therapies Targeting Glial and Inflammatory Responses. *Neurotherapeutics,* 15**,** 541-553.

PACHTER, J. S., DE VRIES, H. E. & FABRY, Z. 2003. The blood-brain barrier and its role in immune privilege in the central nervous system. *J Neuropathol Exp Neurol,* 62**,** 593-604.

PARENT, J. M., YU, T. W., LEIBOWITZ, R. T., GESCHWIND, D. H., SLOVITER, R. S. & LOWENSTEIN, D. H. 1997. Dentate granule cell neurogenesis is increased by seizures and contributes to aberrant network reorganization in the adult rat hippocampus. *J Neurosci,* 17**,** 3727-38.

PARK, J. C., JEONG, W. J., KIM, M. Y., MIN, D. & CHOI, K. Y. 2016. Retinoic-acid-mediated HRas stabilization induces neuronal differentiation of neural stem cells during brain development. *J Cell Sci,* 129**,** 2997-3007.

PASTRANA, E., SILVA-VARGAS, V. & DOETSCH, F. 2011. Eyes wide open: a critical review of sphere-formation as an assay for stem cells. *Cell Stem Cell,* 8**,** 486-98.

PEKNY, M., WILHELMSSON, U. & PEKNA, M. 2014. The dual role of astrocyte activation and reactive gliosis. *Neurosci Lett,* 565**,** 30-8.

PELEGRI, N. G., GORRIE, C. A. & SANTOS, J. 2019. Rat Hippocampal Neural Stem Cell Modulation Using PDGF, VEGF, PDGF/VEGF, and BDNF. *Stem Cells Int,* 2019**,** 4978917.

PEREIRA, I. M., MAROTE, A., SALGADO, A. J. & SILVA, N. A. 2019. Filling the Gap: Neural Stem Cells as A Promising Therapy for Spinal Cord Injury. *Pharmaceuticals (Basel),* 12.

PINEAU, I., SUN, L., BASTIEN, D. & LACROIX, S. 2010. Astrocytes initiate inflammation in the injured mouse spinal cord by promoting the entry of neutrophils and inflammatory monocytes in an IL-1 receptor/MyD88-dependent fashion. *Brain Behav Immun,* 24**,** 540-53.

POPOVICH, P. & MCTIGUE, D. 2009. Damage control in the nervous system: beware the immune system in spinal cord injury. *Nature Medicine,* 15**,** 736-737.

PRUSS, H., TEDESCHI, A., THIRIOT, A., LYNCH, L., LOUGHHEAD, S. M., STUTTE, S., MAZO, I. B., KOPP, M. A., BROMMER, B., BLEX, C., GEURTZ, L. C., LIEBSCHER, T., NIEDEGGEN, A., DIRNAGL, U., BRADKE, F., VOLZ, M. S., DEVIVO, M. J., CHEN, Y., VON ANDRIAN, U. H. & SCHWAB, J. M. 2017. Spinal cord injury-induced immunodeficiency is mediated by a sympathetic-neuroendocrine adrenal reflex. *Nat Neurosci,* 20**,** 1549-1559.

RANA, R., CHAUHAN, K., GAUTAM, P., KULKARNI, M., BANARJEE, R., CHUGH, P., CHHABRA, S. S., ACHARYA, R., KALRA, S. K., GUPTA, A., JAIN, S. & GANGULY, N. K. 2021. Plasma-Derived Extracellular Vesicles Reveal Galectin-3 Binding Protein as Potential Biomarker for Early Detection of Glioma. *Front Oncol,* 11**,** 778754.

REIBER, H. 2001. Dynamics of brain-derived proteins in cerebrospinal fluid. *Clin Chim Acta,* 310**,** 173-86.

REICHENBACH, N., DELEKATE, A., PLESCHER, M., SCHMITT, F., KRAUSS, S., BLANK, N., HALLE, A. & PETZOLD, G. C. 2019. Inhibition of Stat3-mediated astrogliosis ameliorates pathology in an Alzheimer's disease model. *EMBO Mol Med,* 11.

REYNOLDS, B. A. & WEISS, S. 1992. Generation of Neurons and Astrocytes from Isolated Cells of the Adult Mammalian CNS. *Science,* 255**,** 1707-1710.

RICHARDS, L. J., KILPATRICK, T. J. & BARTLETT, P. F. 1992. De novo generation of neuronal cells from the adult mouse brain. *Proc Natl Acad Sci U S A,* 89**,** 8591-8595.

RIEGGER, T., CONRAD, S., SCHLUESENER, H. J., KAPS, H. P., BADKE, A., BARON, C., GERSTEIN, J., DIETZ, K., ABDIZAHDEH, M. & SCHWAB, J. M. 2009. Immune depression syndrome following human spinal cord injury (SCI): a pilot study. *Neuroscience,* 158**,** 1194-9.

RIEMANN, L., YOUNSI, A., SCHERER, M., ZHENG, G., SKUTELLA, T., UNTERBERG, A. W. & ZWECKBERGER, K. 2018. Transplantation of Neural Precursor Cells Attenuates Chronic Immune Environment in Cervical Spinal Cord Injury. *Front Neurol,* 9**,** 428.

ROBEL, S., BERNINGER, B. & GOTZ, M. 2011. The stem cell potential of glia: lessons from reactive gliosis. *Nat Rev Neurosci,* 12**,** 88-104.

ROWITCH, D. H., B, S. J., LEE, S. M., FLAX, J. D., SNYDER, E. Y. & MCMAHON, A. P. 1999. Sonic hedgehog regulates proliferation and inhibits differentiation of CNS precursor cells. *J Neurosci,* 19**,** 8954-65.

SABRE, L., RUGO, M., ASSER, T., KORV, J. & BRASCHINSKY, M. 2016. Headaches after traumatic spinal cord injury in Estonia. *Cephalalgia,* 36**,** 403-12.

SACHDEVA, R., GAO, F., CHAN, C. C. H. & KRASSIOUKOV, A. V. 2018. Cognitive function after spinal cord injury: A systematic review. *Neurology*.

SANDROW-FEINBERG, H. R. & HOULE, J. D. 2015. Exercise after spinal cord injury as an agent for neuroprotection, regeneration and rehabilitation. *Brain Res,* 1619**,** 12-21.

SANKAVARAM, S. R., HAKIM, R., COVACU, R., FROSTELL, A., NEUMANN, S., SVENSSON, M. & BRUNDIN, L. 2019. Adult Neural Progenitor Cells Transplanted into Spinal Cord Injury Differentiate into Oligodendrocytes, Enhance Myelination, and Contribute to Recovery. *Stem Cell Reports,* 12**,** 950-966.

SAWAMOTO, K., WICHTERLE, H., GONZALEZ-PEREZ, O., CHOLFIN, J. A., YAMADA, M., SPASSKY, N., MURCIA, N. S., GARCIA-VERDUGO, J. M., MARIN, O., RUBENSTEIN, J. L., TESSIER-LAVIGNE, M., OKANO, H. & ALVAREZ-BUYLLA, A. 2006. New neurons follow the flow of cerebrospinal fluid in the adult brain. *Science,* 311**,** 629-32.

SCHINDLER, C. & STREHLOW, I. 2000. Cytokines and STAT signaling. *Adv Pharmacol,* 47**,** 113-74.

SCHOLZEN, T. & GERDES, J. 2000. The Ki-67 protein: from the known and the unknown. *J Cell Physiol,* 182**,** 311-22.

SEIF, M., CURT, A., THOMPSON, A. J., GRABHER, P., WEISKOPF, N. & FREUND, P. 2018. Quantitative MRI of rostral spinal cord and brain regions is predictive of functional recovery in acute spinal cord injury. *Neuroimage Clin,* 20**,** 556-563.

SHARIQ, M., SAHASRABUDDHE, V., KRISHNA, S., RADHA, S., NRUTHYATHI, BELLAMPALLI, R., DWIVEDI, A., CHERAMANGALAM, R., REIZIS, B., HEBERT, J. & GHOSH, H. S. 2021. Adult neural stem cells have latent inflammatory potential that is kept suppressed by Tcf4 to facilitate adult neurogenesis. *Sci Adv,* 7.

SHU, T., AYALA, R., NGUYEN, M. D., XIE, Z., GLEESON, J. G. & TSAI, L. H. 2004. Ndel1 operates in a common pathway with LIS1 and cytoplasmic dynein to regulate cortical neuronal positioning. *Neuron,* 44**,** 263-77.

SIEW, J. J., CHEN, H. M., CHEN, H. Y., CHEN, H. L., CHEN, C. M., SOONG, B. W., WU, Y. R., CHANG, C. P., CHAN, Y. C., LIN, C. H., LIU, F. T. & CHERN, Y. 2019. Galectin-3 is required for the microglia-mediated brain inflammation in a model of Huntington's disease. *Nat Commun,* 10**,** 3473.

SIRKO, S., BEHRENDT, G., JOHANSSON, P. A., TRIPATHI, P., COSTA, M., BEK, S., HEINRICH, C., TIEDT, S., COLAK, D., DICHGANS, M., FISCHER, I. R., PLESNILA, N., STAUFENBIEL, M., HAASS, C., SNAPYAN, M., SAGHATELYAN, A., TSAI, L. H., FISCHER, A., GROBE, K., DIMOU, L. & GOTZ, M. 2013. Reactive glia in the injured brain acquire stem cell properties in response to sonic hedgehog. [corrected]. *Cell Stem Cell,* 12**,** 426-39.

SIRKO, S., IRMLER, M., GASCON, S., BEK, S., SCHNEIDER, S., DIMOU, L., OBERMANN, J., DE SOUZA PAIVA, D., POIRIER, F., BECKERS, J., HAUCK, S. M., BARDE, Y. A. & GOTZ, M. 2015. Astrocyte reactivity after brain injury-: The role of galectins 1 and 3. *Glia,* 63**,** 2340-61.

SIRKO, S., NEITZ, A., MITTMANN, T., HORVAT-BROCKER, A., VON HOLST, A., EYSEL, U. T. & FAISSNER, A. 2009. Focal laser-lesions activate an endogenous population of neural stem/progenitor cells in the adult visual cortex. *Brain,* 132**,** 2252-64.

SIRKO, S., VON HOLST, A., WIZENMANN, A., GOTZ, M. & FAISSNER, A. 2007. Chondroitin sulfate glycosaminoglycans control proliferation, radial glia cell differentiation and neurogenesis in neural stem/progenitor cells. *Development,* 134**,** 2727-38.

SMITH, J. S., ANGEL, T. E., CHAVKIN, C., ORTON, D. J., MOORE, R. J. & SMITH, R. D. 2014. Characterization of individual mouse cerebrospinal fluid proteomes. *Proteomics,* 14**,** 1102-6.

SOFRONIEW, M. V. 2005. Reactive astrocytes in neural repair and protection. *Neuroscientist,* 11**,** 400-7.

SOFRONIEW, M. V. 2009. Molecular dissection of reactive astrogliosis and glial scar formation. *Trends Neurosci,* 32**,** 638-47.

SOLSTRAND DAHLBERG, L., BECERRA, L., BORSOOK, D. & LINNMAN, C. 2018. Brain changes after spinal cord injury, a quantitative meta-analysis and review. *Neuroscience & Biobehavioral Reviews,* 90**,** 272-293.

SPALDING, K. L., BERGMANN, O., ALKASS, K., BERNARD, S., SALEHPOUR, M., HUTTNER, H. B., BOSTROM, E., WESTERLUND, I., VIAL, C., BUCHHOLZ, B. A., POSSNERT, G., MASH, D. C., DRUID, H. & FRISEN, J. 2013. Dynamics of hippocampal neurogenesis in adult humans. *Cell,* 153**,** 1219-1227.

SROGA, J. M., JONES, T. B., KIGERL, K. A., MCGAUGHY, V. M. & POPOVICH, P. G. 2003. Rats and mice exhibit distinct inflammatory reactions after spinal cord injury. *J Comp Neurol,* 462**,** 223-40.

STIRLING, D. P., LIU, S., KUBES, P. & YONG, V. W. 2009. Depletion of Ly6G/Gr-1 leukocytes after spinal cord injury in mice alters wound healing and worsens neurological outcome. *J Neurosci,* 29**,** 753-64.

STOOP, M. P., COULIER, L., ROSENLING, T., SHI, S., SMOLINSKA, A. M., BUYDENS, L., AMPT, K., STINGL, C., DANE, A., MUILWIJK, B., LUITWIELER, R. L., SILLEVIS SMITT, P. A., HINTZEN, R. Q., BISCHOFF, R., WIJMENGA, S. S., HANKEMEIER, T., VAN GOOL, A. J. & LUIDER, T. M. 2010. Quantitative proteomics and metabolomics analysis of normal human cerebrospinal fluid samples. *Mol Cell Proteomics,* 9**,** 2063-75.

SUN, D., BULLOCK, M. R., MCGINN, M. J., ZHOU, Z., ALTEMEMI, N., HAGOOD, S., HAMM, R. & COLELLO, R. J. 2009. Basic fibroblast growth factor-enhanced neurogenesis contributes to cognitive recovery in rats following traumatic brain injury. *Exp Neurol,* 216**,** 56-65.

TAN, Y., ZHENG, Y., XU, D., SUN, Z., YANG, H. & YIN, Q. 2021. Galectin-3: a key player in microglia-mediated neuroinflammation and Alzheimer's disease. *Cell Biosci,* 11**,** 78.

TAVERNA, E., GOTZ, M. & HUTTNER, W. B. 2014. The cell biology of neurogenesis: toward an understanding of the development and evolution of the neocortex. *Annu Rev Cell Dev Biol,* 30**,** 465-502.

TEMPLE, S. 1999. CNS development: The obscure origins of adult stem cells. *Curr Biol,* 9**,** R397-9.

VAN PRAAG, H., KEMPERMANN, G. & GAGE, F. H. 1999. Running increases cell proliferation and neurogenesis in the adult mouse dentate gyrus. *Nat Neurosci,* 2**,** 266-70.

VAN PRAAG, H., KEMPERMANN, G. & GAGE, F. H. 2000. Neural consequences of environmental enrichment. *Nat Rev Neurosci,* 1**,** 191-8.

VOIGT, T. 1989. Development of glial cells in the cerebral wall of ferrets: direct tracing of their transformation from radial glia into astrocytes. *J Comp Neurol,* 289**,** 74-88.

VON NEUHOFF, N., OUMERACI, T., WOLF, T., KOLLEWE, K., BEWERUNGE, P., NEUMANN, B., BRORS, B., BUFLER, J., WURSTER, U., SCHLEGELBERGER, B., DENGLER, R., ZAPATKA, M. & PETRI, S. 2012. Monitoring CSF proteome alterations in amyotrophic lateral sclerosis: obstacles and perspectives in translating a novel marker panel to the clinic. *PLoS One,* 7**,** e44401.

VOSKUHL, R. R., PETERSON, R. S., SONG, B., AO, Y., MORALES, L. B., TIWARI-WOODRUFF, S. & SOFRONIEW, M. V. 2009. Reactive astrocytes form scar-like perivascular barriers to leukocytes during adaptive immune inflammation of the CNS. *J Neurosci,* 29**,** 11511-22.

VOUKALI, E., VEETIL, N. K., NEMEC, P., STOPKA, P. & VINKLER, M. 2021. Comparison of plasma and cerebrospinal fluid proteomes identifies gene products guiding adult neurogenesis and neural differentiation in birds. *Sci Rep,* 11**,** 5312.

WADA, K., SUGIMORI, H., BHIDE, P. G., MOSKOWITZ, M. A. & FINKLESTEIN, S. P. 2003. Effect of basic fibroblast growth factor treatment on brain progenitor cells after permanent focal ischemia in rats. *Stroke,* 34**,** 2722-8.

WALTER, H. J., BERRY, M., HILL, D. J., CWYFAN-HUGHES, S., HOLLY, J. M. & LOGAN, A. 1999. Distinct sites of insulin-like growth factor (IGF)-II expression and localization in lesioned rat brain: possible roles of IGF binding proteins (IGFBPs) in the mediation of IGF-II activity. *Endocrinology,* 140**,** 520-32.

WANG, X., SEEKAEW, P., GAO, X. & CHEN, J. 2016. Traumatic Brain Injury Stimulates Neural Stem Cell Proliferation via Mammalian Target of Rapamycin Signaling Pathway Activation. *eNeuro,* 3.

WANNER, I. B., ANDERSON, M. A., SONG, B., LEVINE, J., FERNANDEZ, A., GRAY-THOMPSON, Z., AO, Y. & SOFRONIEW, M. V. 2013. Glial scar borders are formed by newly proliferated, elongated astrocytes that interact to corral inflammatory and fibrotic cells via STAT3-dependent mechanisms after spinal cord injury. *J Neurosci,* 33**,** 12870-86.

WARNER, F. M., CRAGG, J. J., WEISSKOPF, M. G. & KRAMER, J. K. 2015. Spinal Cord Injury and Migraine Headache: A Population-Based Study. *PLoS One,* 10**,** e0135550.

WATANABE, T., OKUDA, Y., NONOGUCHI, N., ZHAO, M. Z., KAJIMOTO, Y., FURUTAMA, D., YUKAWA, H., SHIBATA, M. A., OTSUKI, Y., KUROIWA, T. & MIYATAKE, S. 2004. Postischemic intraventricular administration of FGF-2 expressing adenoviral vectors improves neurologic outcome and reduces infarct volume after transient focal cerebral ischemia in rats. *J Cereb Blood Flow Metab,* 24**,** 1205-13.

WATERS, R. L., YAKURA, J. S., ADKINS, R. H. & SIE, I. 1992. Recovery following complete paraplegia. *Arch Phys Med Rehabil,* 73**,** 784-9.

WECHT, J. M. & BAUMAN, W. A. 2013. Decentralized cardiovascular autonomic control and cognitive deficits in persons with spinal cord injury. *J Spinal Cord Med,* 36**,** 74-81.

WEINBERG, R. A. 1995 The Retinoblastoma protein and cell cycle control. *Cell,* 81**,** 323-330.

WHITNEY, N. P., EIDEM, T. M., PENG, H., HUANG, Y. & ZHENG, J. C. 2009. Inflammation mediates varying effects in neurogenesis: relevance to the pathogenesis of brain injury and neurodegenerative disorders. *J Neurochem,* 108**,** 1343-59.

WILSON, J. R., TETREAULT, L. A., KWON, B. K., ARNOLD, P. M., MROZ, T. E., SHAFFREY, C., HARROP, J. S., CHAPMAN, J. R., CASHA, S., SKELLY, A. C., HOLMER, H. K., BRODT, E. D. & FEHLINGS, M. G. 2017. Timing of Decompression in Patients With Acute Spinal Cord Injury: A Systematic Review. *Global Spine J,* 7**,** 95S-115S.

WINNER, B. & WINKLER, J. 2015. Adult neurogenesis in neurodegenerative diseases. *Cold Spring Harb Perspect Biol,* 7**,** a021287.

WU, J., STOICA, B. A., LUO, T., SABIRZHANOV, B., ZHAO, Z., GUANCIALE, K., NAYAR, S. K., FOSS, C. A., POMPER, M. G. & FADEN, A. I. 2014a. Isolated spinal cord contusion in rats induces chronic brain neuroinflammation, neurodegeneration, and cognitive impairment. Involvement of cell cycle activation. *Cell Cycle,* 13**,** 2446-58.

WU, J., ZHAO, Z., SABIRZHANOV, B., STOICA, B. A., KUMAR, A., LUO, T., SKOVIRA, J. & FADEN, A. I. 2014b. Spinal cord injury causes brain inflammation associated with cognitive and affective changes: role of cell cycle pathways. *J Neurosci,* 34**,** 10989-1006.

WU, Y., XU, J., XU, J., ZHENG, W., CHEN, Q. & JIAO, D. 2018. Study on the mechanism of JAK2/STAT3 signaling pathway-mediated inflammatory reaction after cerebral ischemia. *Mol Med Rep,* 17**,** 5007-5012.

XIONG, Y., CONNOLLY, T., FUTCHER, B. & BEACH, D. 1991. Human D-type cyclin. *Cell,* 65**,** 691-9.

XU, J., DONG, H., QIAN, Q., ZHANG, X., WANG, Y., JIN, W. & QIAN, Y. 2017. Astrocyte-derived CCL2 participates in surgery-induced cognitive dysfunction and neuroinflammation via evoking microglia activation. *Behav Brain Res,* 332**,** 145-153.

YAMAUCHI, K., OSUKA, K., TAKAYASU, M., USUDA, N., NAKAZAWA, A., NAKAHARA, N., YOSHIDA, M., AOSHIMA, C., HARA, M. & YOSHIDA, J. 2006. Activation of JAK/STAT signalling in neurons following spinal cord injury in mice. *J Neurochem,* 96**,** 1060-70.

YANAGISAWA, M., KURIHARA, H., KIMURA, S., GOTO, K. & MASAKI, T. 1988. A novel peptide vasoconstrictor, endothelin, is produced by vascular endothelium and modulates smooth muscle Ca2+ channels. *J Hypertens Suppl,* 6**,** S188-91.

YANG, C., FARIAS, F. H. G., IBANEZ, L., SUHY, A., SADLER, B., FERNANDEZ, M. V., WANG, F., BRADLEY, J. L., EIFFERT, B., BAHENA, J. A., BUDDE, J. P., LI, Z., DUBE, U., SUNG, Y. J., MIHINDUKULASURIYA, K. A., MORRIS, J. C., FAGAN, A. M., PERRIN, R. J., BENITEZ, B. A., RHINN, H., HARARI, O. & CRUCHAGA, C. 2021. Genomic atlas of the proteome from brain, CSF and plasma prioritizes proteins implicated in neurological disorders. *Nat Neurosci,* 24**,** 1302-1312.

YOU, J. S., GELFANOVA, V., KNIERMAN, M. D., WITZMANN, F. A., WANG, M. & HALE, J. E. 2005. The impact of blood contamination on the proteome of cerebrospinal fluid. *Proteomics,* 5**,** 290-6.

YUAN, Y. M. & HE, C. 2013. The glial scar in spinal cord injury and repair. *Neurosci Bull,* 29**,** 421-35.

ZAPPATERRA, M. W. & LEHTINEN, M. K. 2012. The cerebrospinal fluid: regulator of neurogenesis, behavior, and beyond. *Cell Mol Life Sci,* 69**,** 2863-78.

ZHANG, B., BAILEY, W. M., KOPPER, T. J., ORR, M. B., FEOLA, D. J. & GENSEL, J. C. 2015. Azithromycin drives alternative macrophage activation and improves recovery and tissue sparing in contusion spinal cord injury. *J Neuroinflammation,* 12**,** 218.

ZHANG, H., FREITAS, D., KIM, H. S., FABIJANIC, K., LI, Z., CHEN, H., MARK, M. T., MOLINA, H., MARTIN, A. B., BOJMAR, L., FANG, J., RAMPERSAUD, S., HOSHINO, A., MATEI, I., KENIFIC, C. M., NAKAJIMA, M., MUTVEI, A. P., SANSONE, P., BUEHRING, W., WANG, H., JIMENEZ, J. P., COHEN-GOULD, L., PAKNEJAD, N., BRENDEL, M., MANOVA-TODOROVA, K., MAGALHAES, A., FERREIRA, J. A., OSORIO, H., SILVA, A. M., MASSEY, A., CUBILLOS-RUIZ, J. R., GALLETTI, G., GIANNAKAKOU, P., CUERVO, A. M., BLENIS, J., SCHWARTZ, R., BRADY, M. S., PEINADO, H., BROMBERG, J., MATSUI, H., REIS, C. A. & LYDEN, D. 2018. Identification of distinct

nanoparticles and subsets of extracellular vesicles by asymmetric flow field-flow fractionation. *Nat Cell Biol,* 20**,** 332-343.

ZHANG, J. & JIAO, J. 2015. Molecular Biomarkers for Embryonic and Adult Neural Stem Cell and Neurogenesis. *Biomed Res Int,* 2015**,** 727542.

ZHOU, Y. & DANBOLT, N. C. 2013. GABA and Glutamate Transporters in Brain. *Front Endocrinol (Lausanne),* 4**,** 165.

ZHU, W., CHEN, X., NING, L. & JIN, K. 2019. Network Analysis Reveals TNF as a Major Hub of Reactive Inflammation Following Spinal Cord Injury. *Sci Rep,* 9**,** 928.

ZHU, Y., DEMIDOV, O. N., GOH, A. M., VIRSHUP, D. M., LANE, D. P. & BULAVIN, D. V. 2014. Phosphatase WIP1 regulates adult neurogenesis and WNT signaling during aging. *J Clin Invest,* 124**,** 3263-73.

ZIEGLER, G., GRABHER, P., THOMPSON, A., ALTMANN, D., HUPP, M., ASHBURNER, J., FRISTON, K., WEISKOPF, N., CURT, A. & FREUND, P. 2018. Progressive neurodegeneration following spinal cord injury: Implications for clinical trials. *Neurology,* 90**,** e1257-e1266.

8. List of Abbreviations

+	plus/positive
-	minus/negative
±	plus minus
°C	degrees Celsius
µg	microgram(s)
µl	microliter(s)
µm	micrometer(s)
Aldh1a2	Aldehyde dehydrogenase 1 family member A2
aNSC	Adult neural stem cell
Apoc3	Apolipoprotein C3
Apoe	Apolipoprotein E
BBB	Blood-brain barrier
BDNF	Brain-derived neurotrophic factor
BrdU	5-Bromo-2'-Deoxyuridine
BSA	Bovine serum albumine
C1qa	Complement C1q subcomponent A
C1qb	Complement C1q subcomponent B
C3	Complement C3
CA	Cornu ammonis layer
$CaCl_2$	Calcium chloride
CCL	C-C motif ligand
CCND1	Cyclin D1 (gene)
CCR	C-C motif chemokine receptor
CD	Cluster of differentiation
CDK	Cyclin-dependent kinase
cDNA	Complementary DNA
CN	Caudate nucleus
CNS	Central nervous system
Cy3	Indocarbocyanine
CSF	Cerebrospinal fluid
DAPI	4,6-Diamidino-2-Phenylindoledilactate
DCX	Doublecortin
dest.	Destilled
DG	Dentate gyrus
Dkk3	Dickkopf 3
DMEM	Dulbecco's modified Eagle medium
DNA	Deoxyribonucleic acid
dpi	Day(s) post injury
Dync1h1	Dynein cytoplasmic 1 heavy chain 1
e.g.	exempli gratia
EAAT1	Excitatory amino acid transporter 1
EDTA	Ethylenediaminetetraacetic acid
EGF	Epidermal growth factor
Egfr	Epidermal growth factor receptor
et al.	and others

ET-1	Endothelin-1
ETBR	Endothelin receptor type B
FasR	Fas receptor
FCS	Fetal calf serum
FDR	False discovery rate
FGF	Fibroblast growth factor
Fig.	Figure
g	gram(s)
Gal	Galectin
GCL	Granular cell layer
GFAP	Glial fibrillary acidic protein
GLAST	Glutamate aspartate transporter
GLI1	GLI family zinc finger 1 (gene)
GM	Grey matter
GM-CSF	Granulocyte-macrophage colony-stimulating factor
Gpc2	Glypican-2
h	hour(s)
H_2O	Water
Hb	Hemoglobin
HBA	Hemoglobin A
HBB1	Hemoglobin B1
HC	Hippocampus
HCl	Hydrochloric acid
Hemi	Hemisection
HEPES	4-(2-hydroxyethyl)-1-piperazineethanesulfonic acid
HPRT1	Hypoxanthine phosphoribosyltransferase 1 (gene)
Iba 1	Ionized calcium binding adaptor molecule 1
IFN	Interferon
IGF	Insulin-like Growth Factor
IGFBP	Insulin-like Growth Factor binding protein
IgG	Immunoglobulin G
IgM	Immunoglobulin M
IL	Interleukin
JAK	Janus kinase
KCl	Potassium chloride
KH_2PO_4	Monopotassium phosphate
KRH	Krebs-Ringer-Hepes solution
l	liter(s)
Lgals3bp	Galectin-3 binding protein
Log	logarithm
LV	Lateral ventricle
M	molar
Mac-2BP	Mac-2 binding protein
MACS	Magnetic-activated cell sorting
mg	milligram(s)
MgSO4	Magnesium sulfate
min	minute(s)
MKI67	Marker of proliferation Ki-67 (gene)

ML	Molecular layer
ml	milliliter(s)
mm	millimeter(s)
mm^3	cubic millimeter(s)
MMF	Midazolam/Medetomidine/Fentanyl
mmol	millimole
mRNA	Messenger RNA
n	number of biological replicates per experiment
NaCl	Sodium chloride
NaOH	Sodium hydroxide
NB	Neuroblast
ng	nanogram(s)
NG2	Neuron-glial antigen 2
NGS	Normal goat serum
nm	nanometer(s)
NO	Nitric oxide
NSC	Neural stem cell
O_2	Oxygen
OB	Olfactory bulb
OPC	Oligodendrocyte progenitor cell
p	p-value
PBS	Phosphate buffer saline
PDGF	Platelet derived growth factor
PDL	Poly-D-Lysine
PFA	Paraformaldehyde
pH	pH-value
PLO	Poly-L-Ornithine
PO_4	Phosphate
PTCH	Patched
qNSC	Quiescent neural stem cell
Rb	Retinoblastoma protein
RG	Radial glia
RMS	Rostral migratory stream
RNA	Ribonucleic acid
ROS	Reactive oxygen species
rpm	Revolutions per minute
RT-qPCR	Real-time quantitative polymerase chain reaction
s	second(s)
S100β	S100 Calcium binding protein β
SAG	Shh Signaling Agonist
SCI	Spinal cord injury
SCI-IDS	SCI-induced immune depression syndrome
SEM	Standard error of the mean
SEZ	Subependymal zone
SGZ	Subgranular zone
Sh/Sham	Sham surgery
SHH	Sonic Hedgehog
SMO	Smoothened

Sox2	Sex determining region Y-box 2
STAT3	Signal transducer and activator of transcription 3
SUFU	Suppressor of Fused
SVZ	Subventricular zone
SWI	Stab wound injury
Tab.	Table
TAP	Transit amplifying progenitor
TBI	Traumatic brain injury
TGF	Transforming growth factor
TNF	Tumor necrosis factor
U	unit(s)
Tx	Triton X-100
VEGF	Vascular endothelial growth factor
WM	White matter
WT	Wild type

9. List of Figures

10. List of Tables

11. Danksagungen

Ich möchte diese Gelegenheit nutzen, um meiner Doktormutter und Betreuerin Dr. Swetlana Sirko meinen besonderen Dank auszusprechen. Ohne Ihren Enthusiasmus für das Thema, ihre ungezügelte Begeisterung für die Neurowissenschaften und ihr Durchhaltevermögen sowie ihren Pragmatismus in jeder noch so schwierigen Situation wäre eine Arbeit in diesem Umfang nicht möglich gewesen. Nicht zuletzt bin ich dankbar für eine Mentorin auch außerhalb der Wissenschaft, die ich für immer dazugewonnen habe.

Großer Dank gebührt außerdem dem ganzen Team der Physiologischen Genomik der LMU und insbesondere der Direktorin, Prof. Dr. Magdalena Götz, die es mir ermöglicht hat, in einem so renommierten und internationalen Labor zu arbeiten. All die wertvollen Erfahrungen und Freundschaften aus meiner Zeit im Labor und auf Kongressen habe ich ihnen zu verdanken. Hier möchte ich Dr. Giacomo Masserdotti, Dr. Judith Fischer-Sternjak, Tatiana Simon-Ebert, Gabi Jäger und Manja Thorwirth hervorheben, die maßgeblich zur Entstehung meiner Ergebnisse beigetragen haben durch ihre methodische und fachliche Expertise. Nicht zu vergessen sind ihre täglichen Aufmunterungen, wenn nichts zu funktionieren schien.

Ich möchte auch Dr. Kristina Loy und Dr. Florence Bayrere aus dem Institut für Neuroimmunologie der LMU, ebenso wie Dr. Fabian Metzger und Dr. Stefanie Hauck der Research Unit Protein Science des Helmholtz Instituts München für ihre tolle Zusammenarbeit bei den Tierexperimenten beziehungsweise der Proteomanalyse danken. Mein Beileid gilt allen, die Fabian als Kollegen, Freund oder Familienangehörigen verloren haben.

Danke auch an meine gewissenhaften Korrekturleser, Dr. Markus Lauerer, Dr. Johannes Melms und Dr. Giacomo Masserdotti für den nötigen Feinschliff. Danke außerdem an Florian Hollunder, Markus Lauerer und Jonas Kraska, die mich nie alleine gelassen haben mit den Schwierigkeiten, die man speziell als MedizinstudentIn ohne bedeutende Laborerfahrung bei einem solchen Projekt konfrontieren muss.

Zuallerletzt gilt aber mein größter Dank meiner Familie und meinem Freund. Ohne deren Rückhalt und Motivation, die jede meiner Launen überstanden und jeden Moment der Überforderung abgefedert haben, wäre ich heute nicht hier, wo ich bin und vor allem nicht die Person, die ich heute bin. Eine einfache Widmung dieser Arbeit wird dem Dank ihnen gegenüber nicht annähernd gerecht.

12. Eidesstattliche Versicherung

Eidesstattliche Versicherung

Li, Melanie

Ich erkläre hiermit an Eides statt, dass ich die vorliegende Dissertation mit dem Thema

Adaptive Cellular Response within
Neural Stem Cell Niches in the Adult Murine Brain
Following Spinal Cord Injury

selbständig verfasst, mich außer der angegebenen keiner weiteren Hilfsmittel bedient und alle Erkenntnisse, die aus dem Schrifttum ganz oder annähernd übernommen sind, als solche kenntlich gemacht und nach ihrer Herkunft unter Bezeichnung der Fundstelle einzeln nachgewiesen habe. Ich erkläre des Weiteren, dass die hier vorgelegte Dissertation nicht in gleicher oder in ähnlicher Form bei einer anderen Stelle zur Erlangung eines akademischen Grades eingereicht wurde.

Melanie Li

New York, den 27.02.2023